

## Appendix B

Time series variations of atmospheric  $^{137}\text{Cs}$  concentrations observed at 99 SPM sampling sites listed in Table 1 are shown in this Appendix B. Original numerical data sets are available from Appendix A. Although  $^{134}\text{Cs}$  activity was measured along with  $^{137}\text{Cs}$  activity, its variations are not shown because its time series variations are essentially the same as those for  $^{137}\text{Cs}$ , as implied by the nearly constant activity ratios (approximately 1) of  $^{134}\text{Cs}/^{137}\text{Cs}$  for most SPM samples analyzed. In the figures, a detection limit is expressed by symbol "-", and an error bar expresses the one originated in only gamma-ray counting statistics ( $1\sigma$ ).

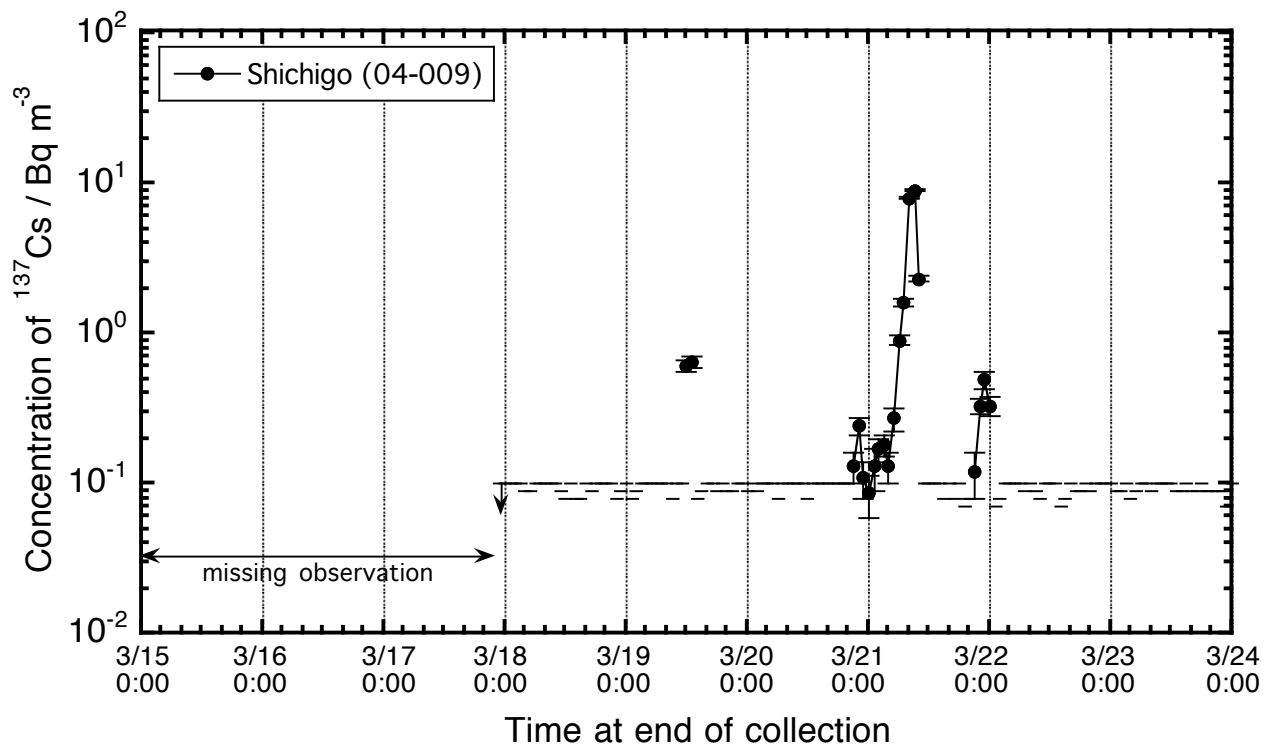


Figure B1. Time series variation of atmospheric  $^{137}\text{Cs}$  concentration observed at Shichigo station (04-009) in Sendai-shi, Miyagi.

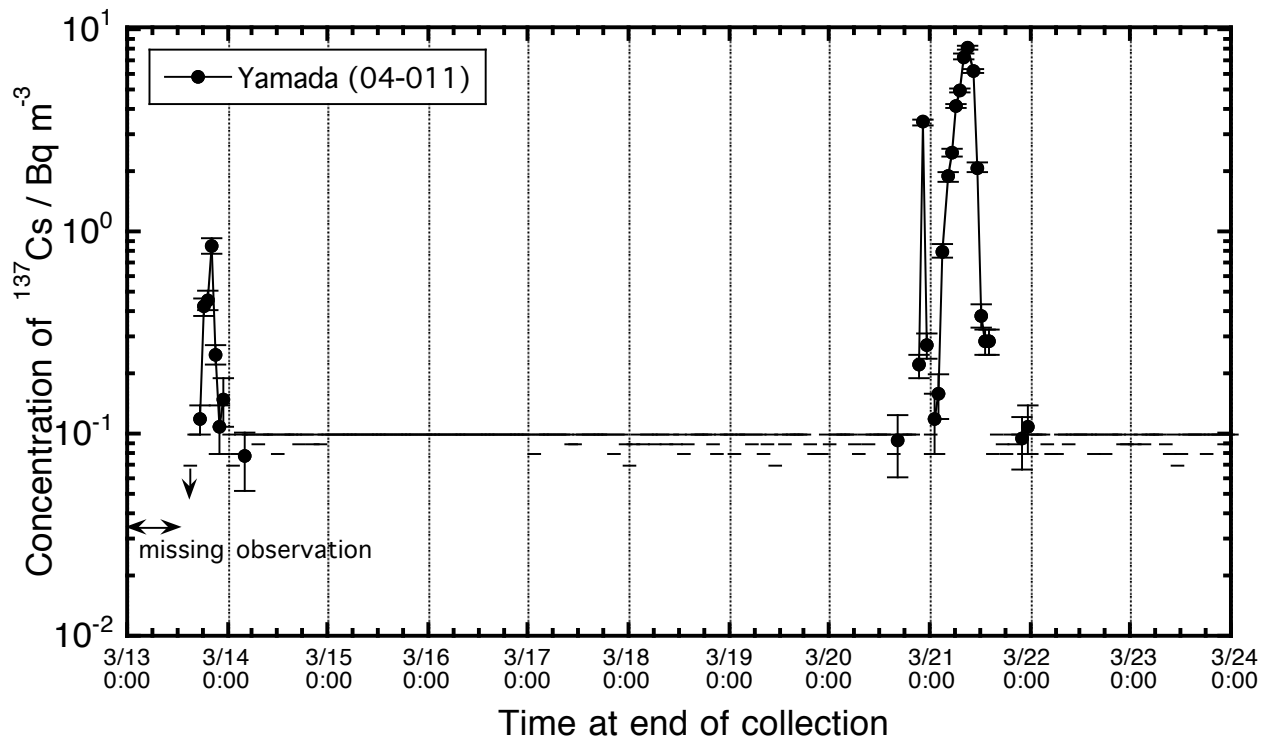


Figure B2. Time series variation of atmospheric  $^{137}\text{Cs}$  concentration observed at Yamada station (04-011) in Sendai-shi, Miyagi.

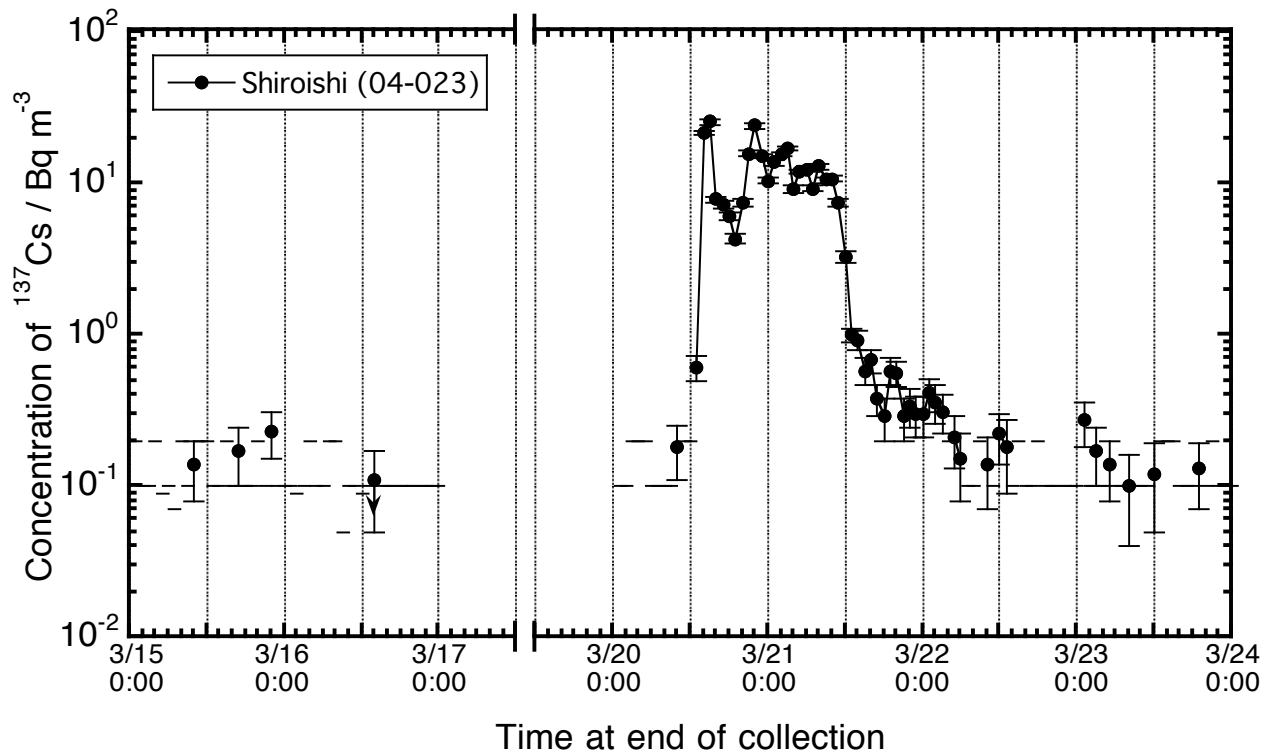


Figure B3. Time series variation of atmospheric  $^{137}\text{Cs}$  concentration observed at Shiroishi station (04-023) in Shiroishi-shi, Miyagi.

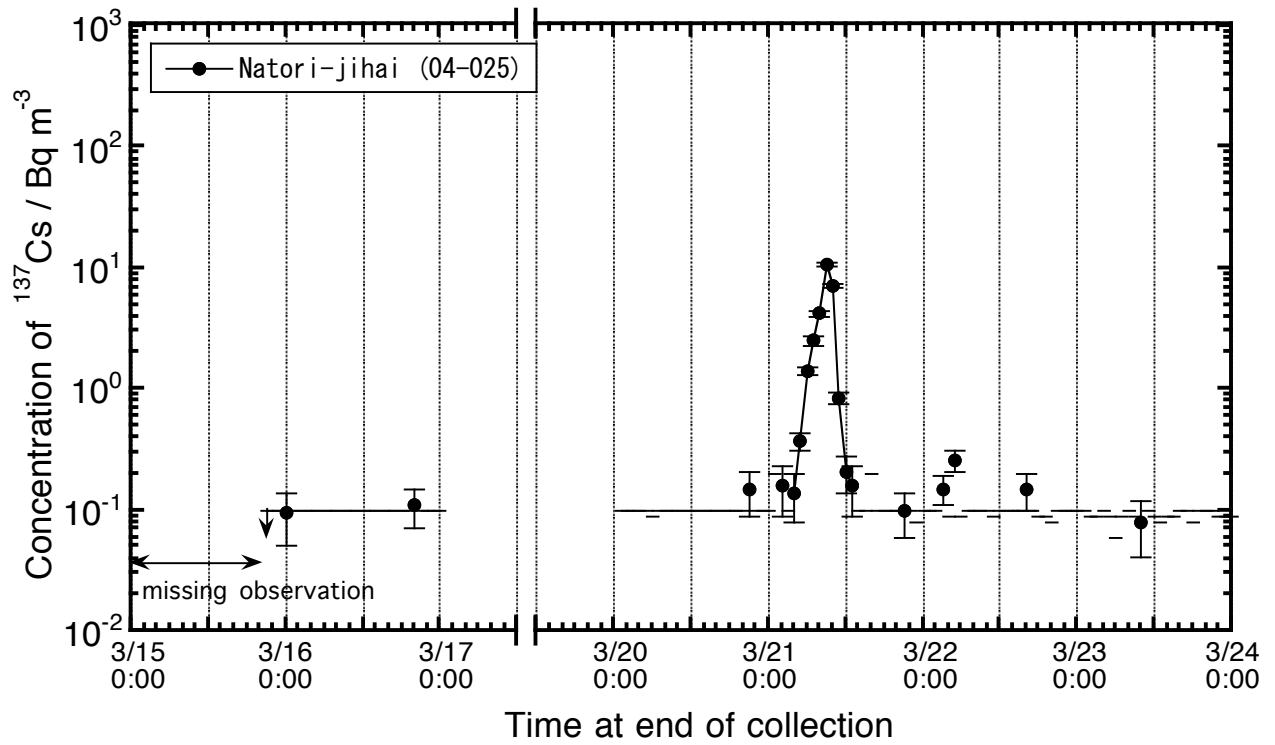


Figure B4. Time series variation of atmospheric  $^{137}\text{Cs}$  concentration observed at Natori-jihai station (04-025) in Natori-shi, Miyagi.

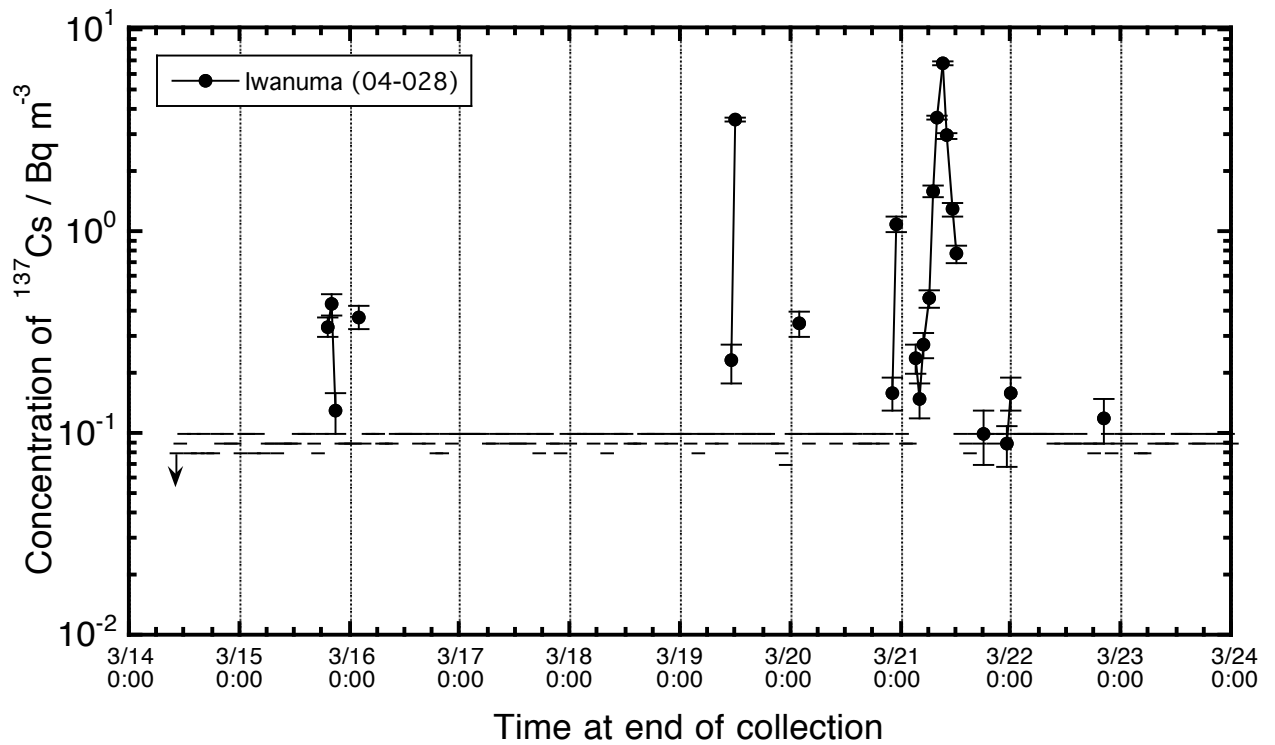


Figure B5. Time series variation of atmospheric  $^{137}\text{Cs}$  concentration observed at Iwanuma station (04-028) in Iwanuma-shi, Miyagi.

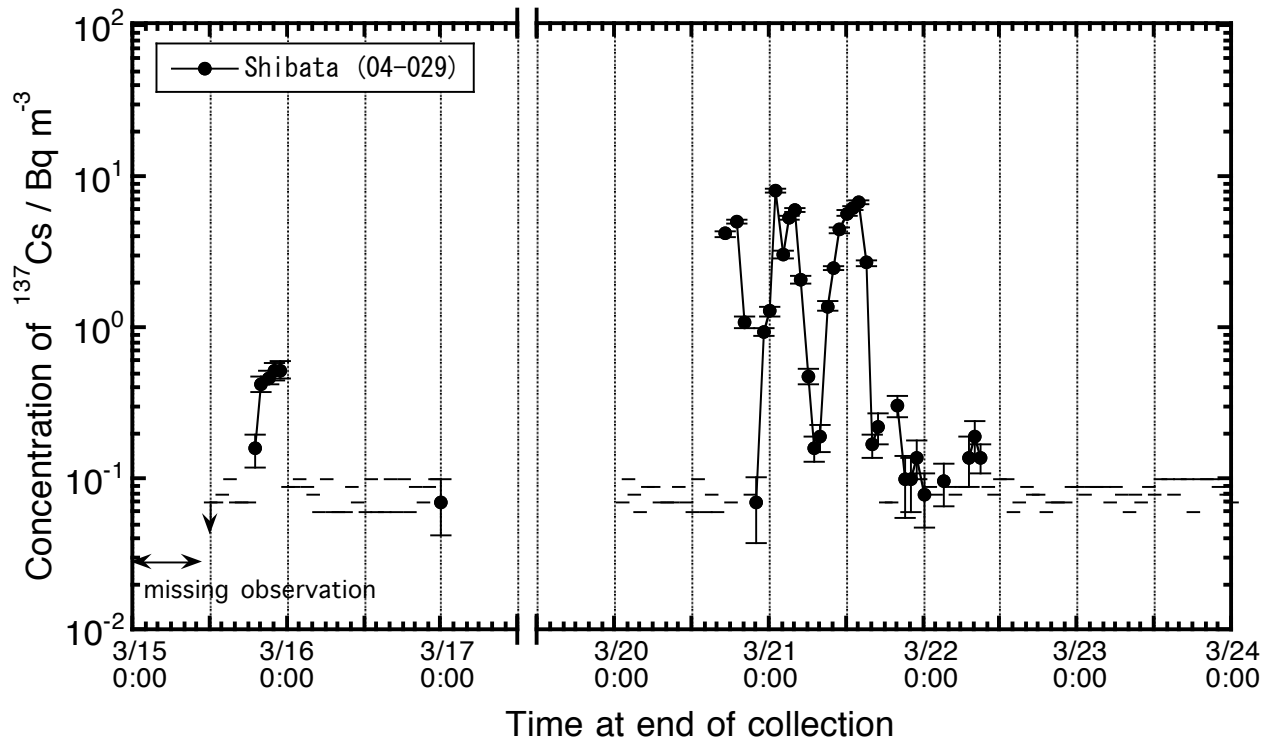


Figure B6. Time series variation of atmospheric  $^{137}\text{Cs}$  concentration observed at Shibata station (04-029) in Shibata-machi, Miyagi.

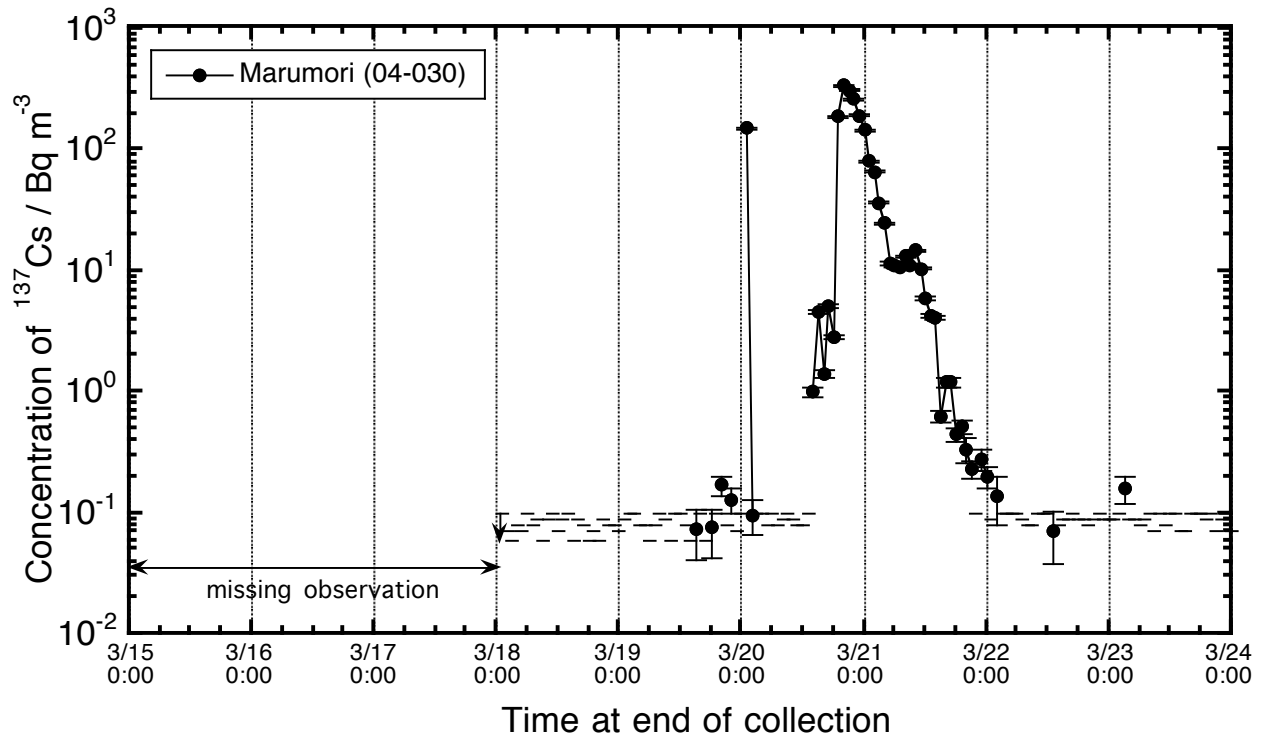


Figure B7. Time series variation of atmospheric  $^{137}\text{Cs}$  concentration observed at Marumori station (04-030) in Marumori-machi, Miyagi.

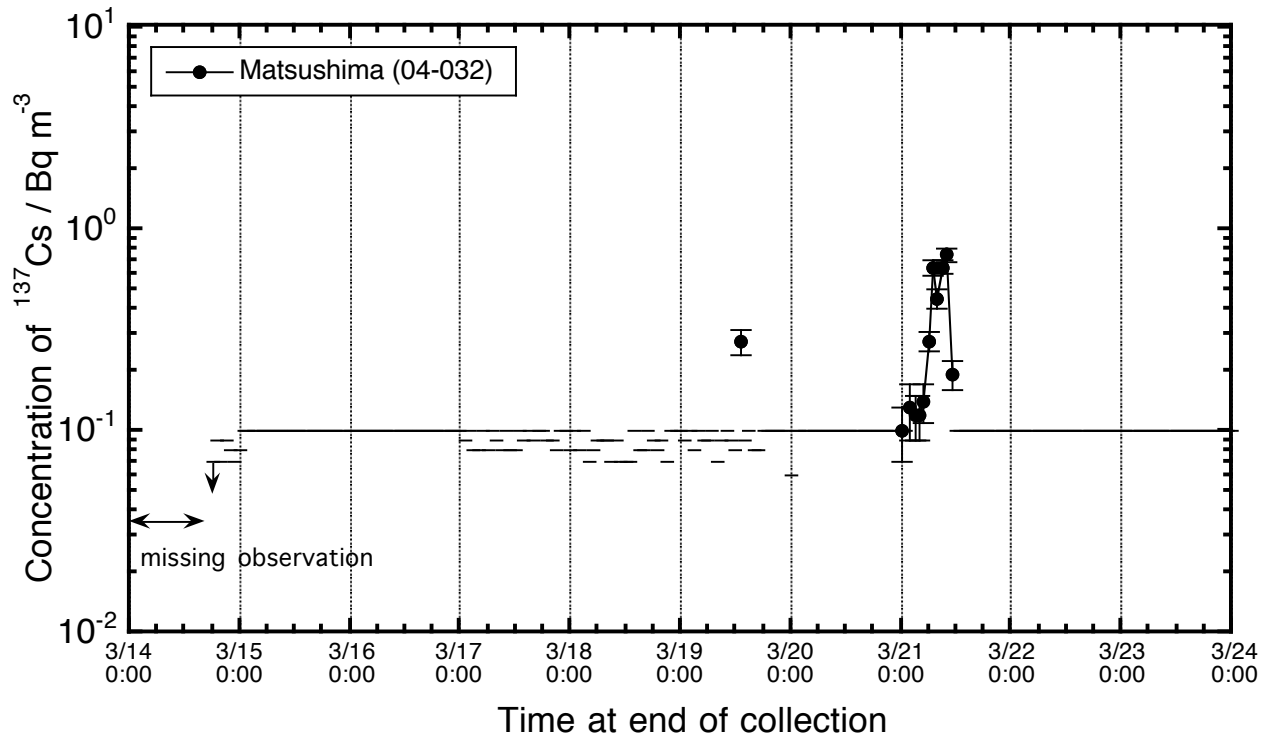


Figure B8. Time series variation of atmospheric  $^{137}\text{Cs}$  concentration observed at Matsushima station (04-032) in Matsushima-machi, Miyagi.

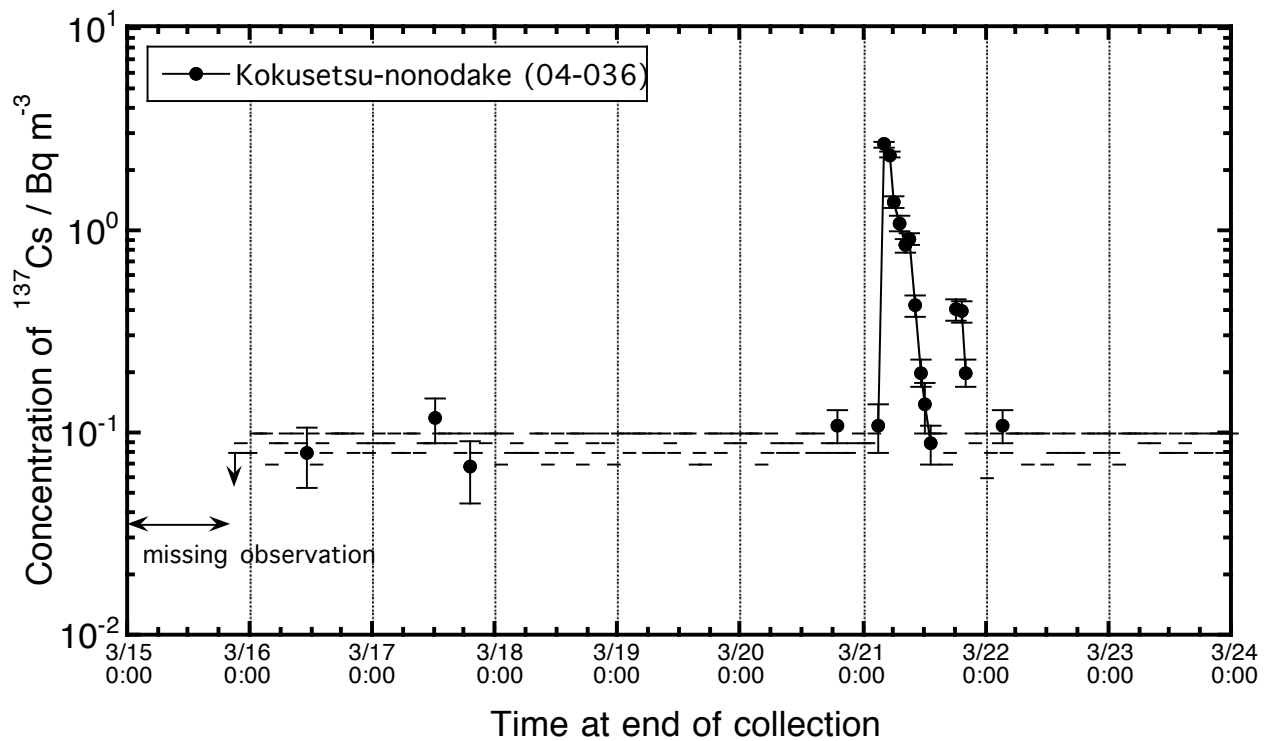


Figure B9. Time series variation of atmospheric  $^{137}\text{Cs}$  concentration observed at Kokusetsu-nonodake station (04-036) in Wakutani-machi, Miyagi.

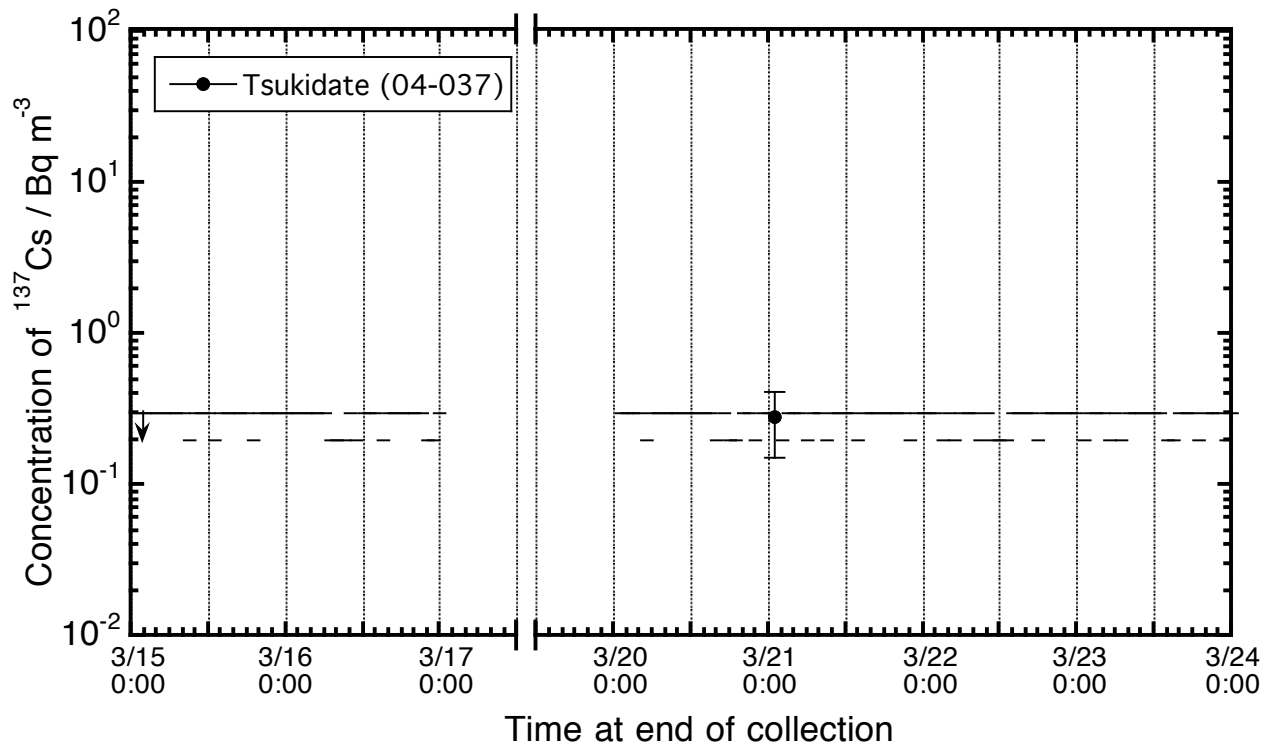


Figure B10. Time series variation of atmospheric  $^{137}\text{Cs}$  concentration observed at Tsukidate station (04-037) in Kurihara-shi, Miyagi.

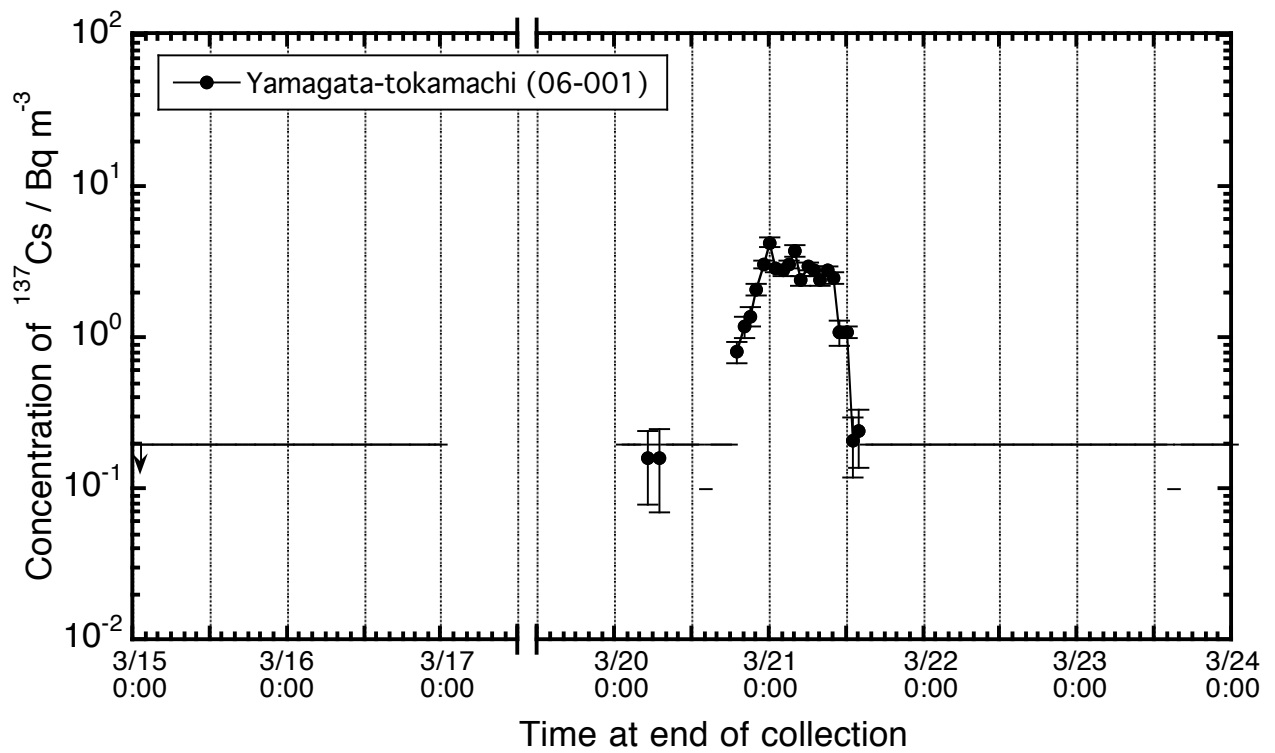


Figure B11. Time series variation of atmospheric  $^{137}\text{Cs}$  concentration observed at Yamagata-tokamachi station (06-001) in Yamagata-shi, Yamagata.

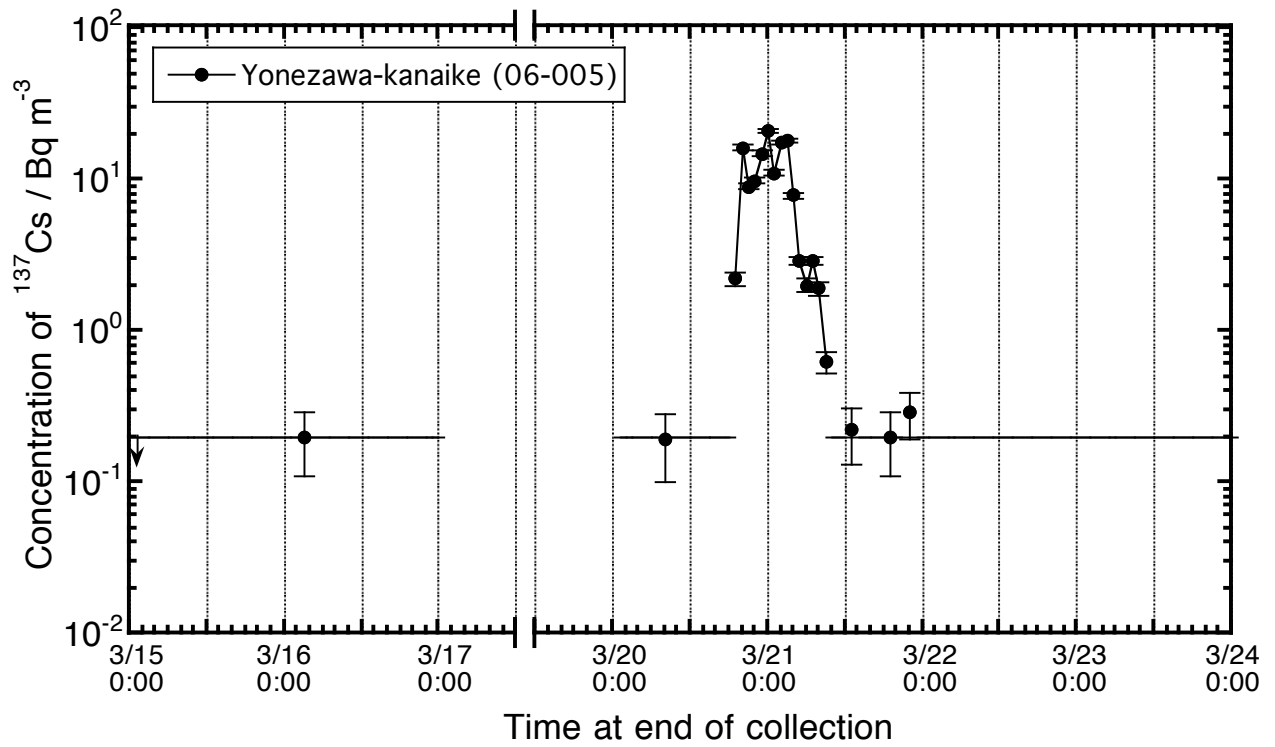


Figure B12. Time series variation of atmospheric  $^{137}\text{Cs}$  concentration observed at Yonezawa-Kanaike station (06-005) in Yonezawa-shi, Yamagata.

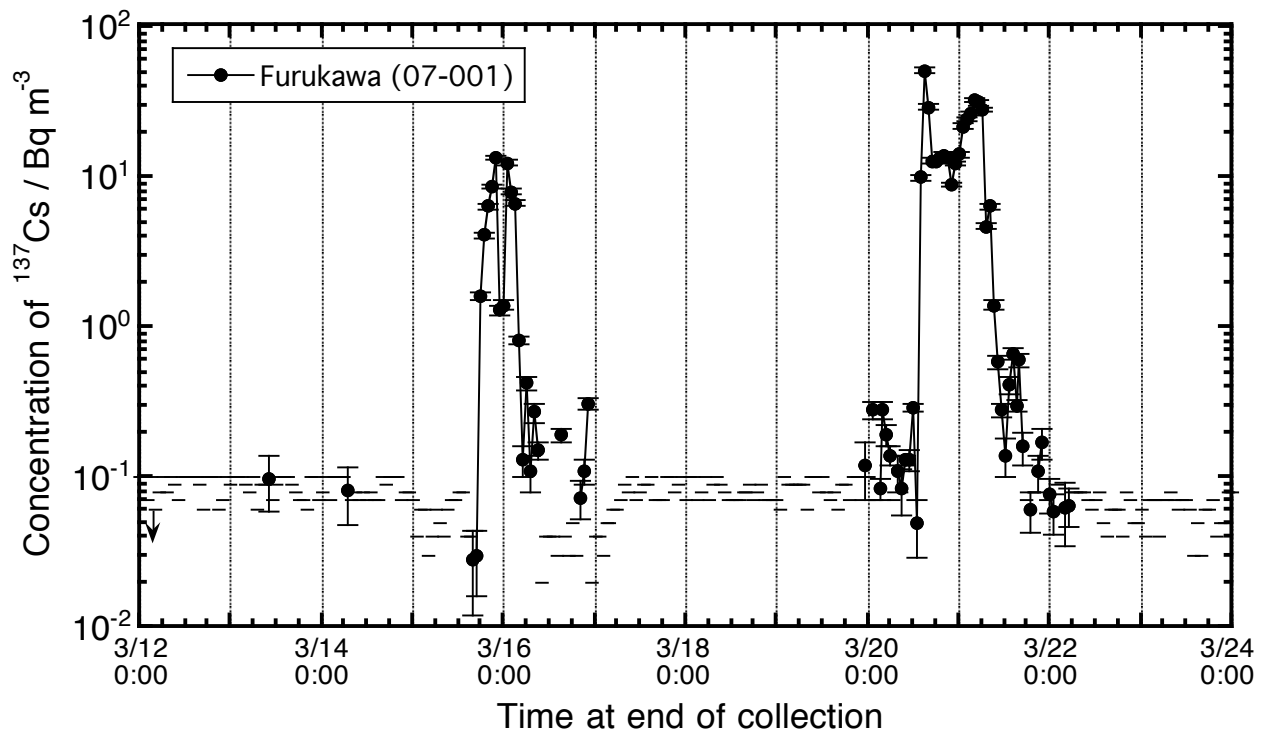


Figure B13. Time series variation of atmospheric  $^{137}\text{Cs}$  concentration observed at Furukawa station (07-001) in Fukushima-shi, Fukushima.

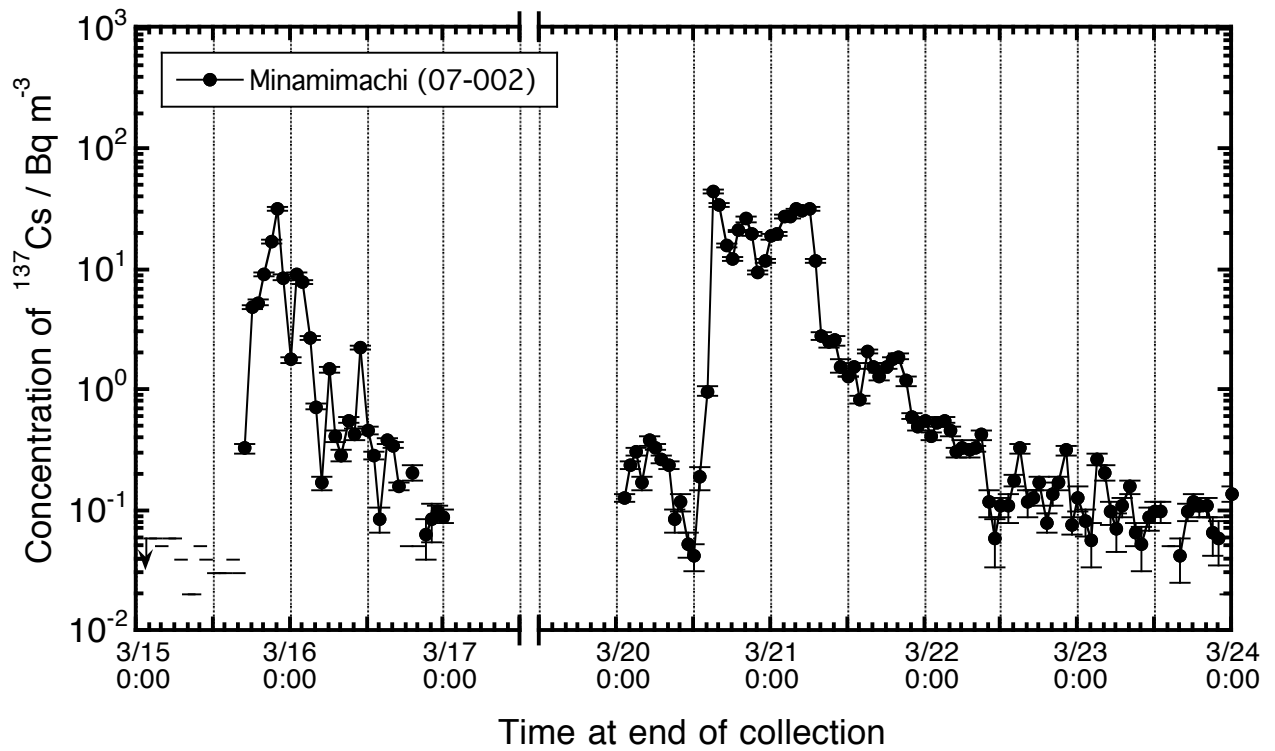


Figure B14. Time series variation of atmospheric  $^{137}\text{Cs}$  concentration observed at Minamimachi station (07-002) in Fukushima-shi, Fukushima.

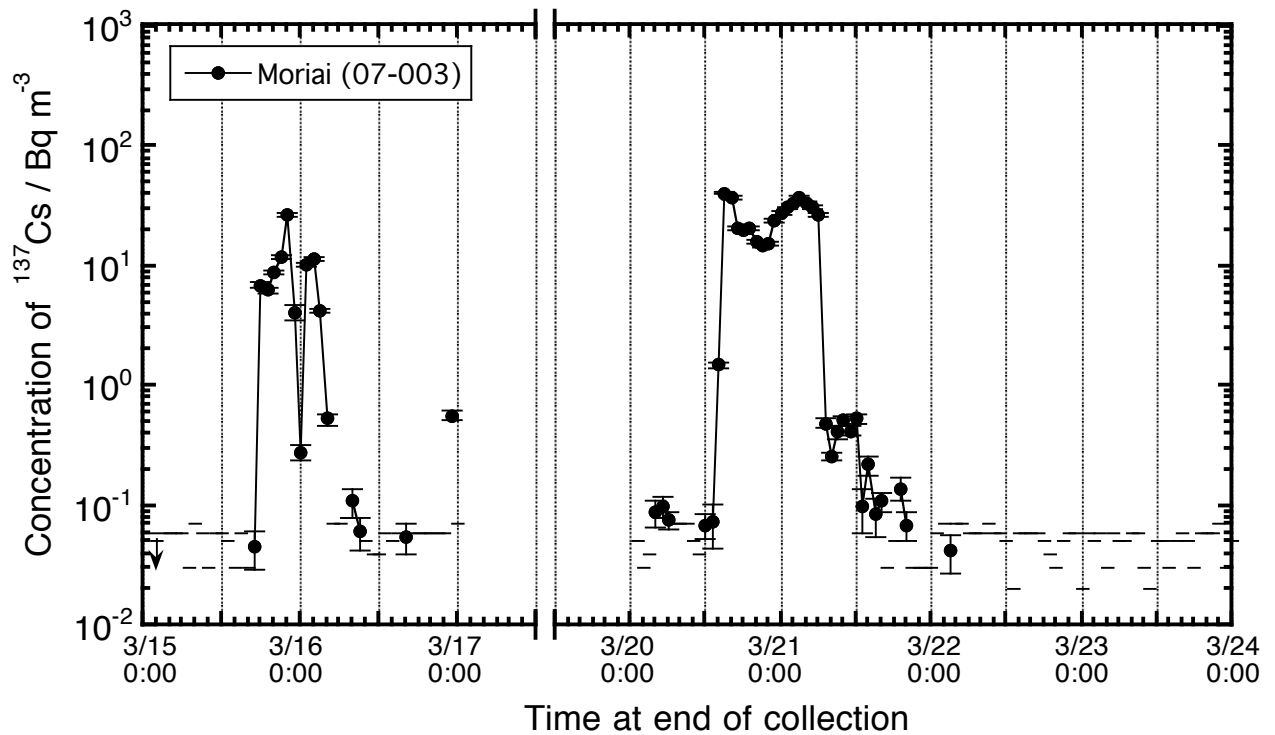


Figure B15. Time series variation of atmospheric  $^{137}\text{Cs}$  concentration observed at Moriai station (07-003) in Fukushima-shi, Fukushima.



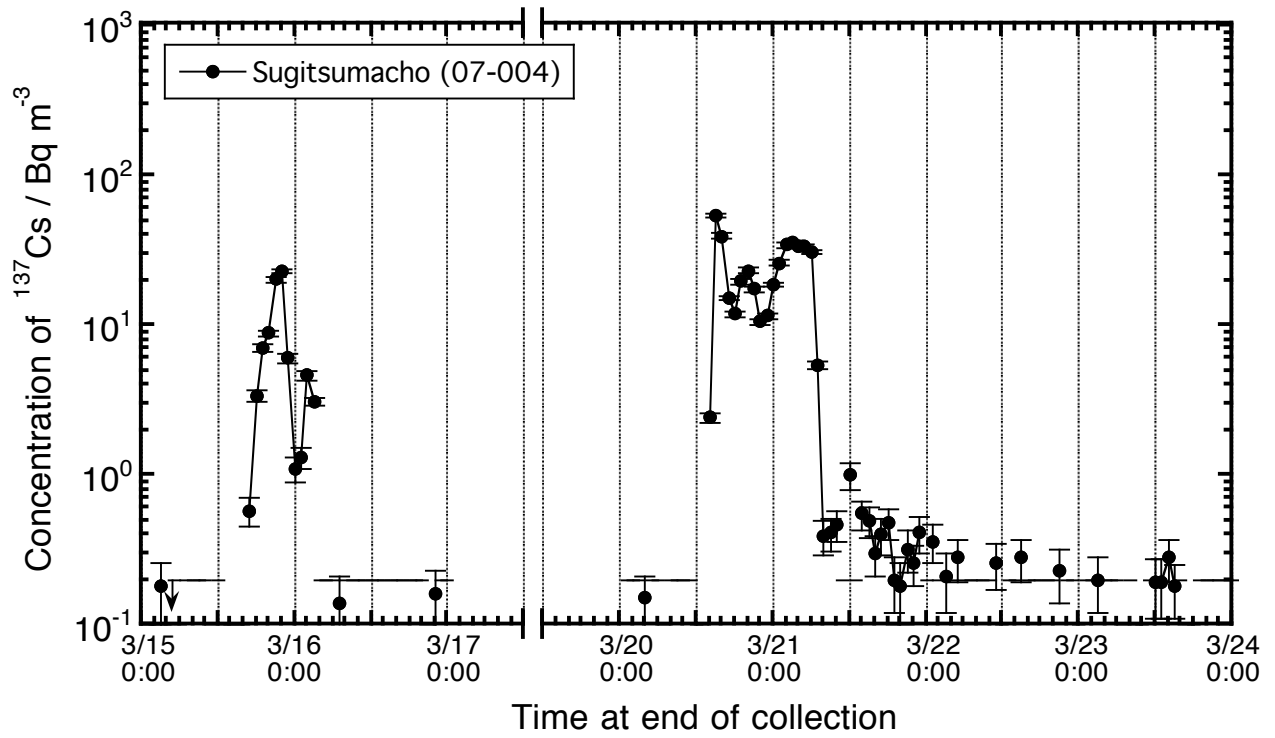


Figure B16. Time series variation of atmospheric  $^{137}\text{Cs}$  concentration observed at Sugitsumacho station (07-004) in Fukushima-shi, Fukushima.

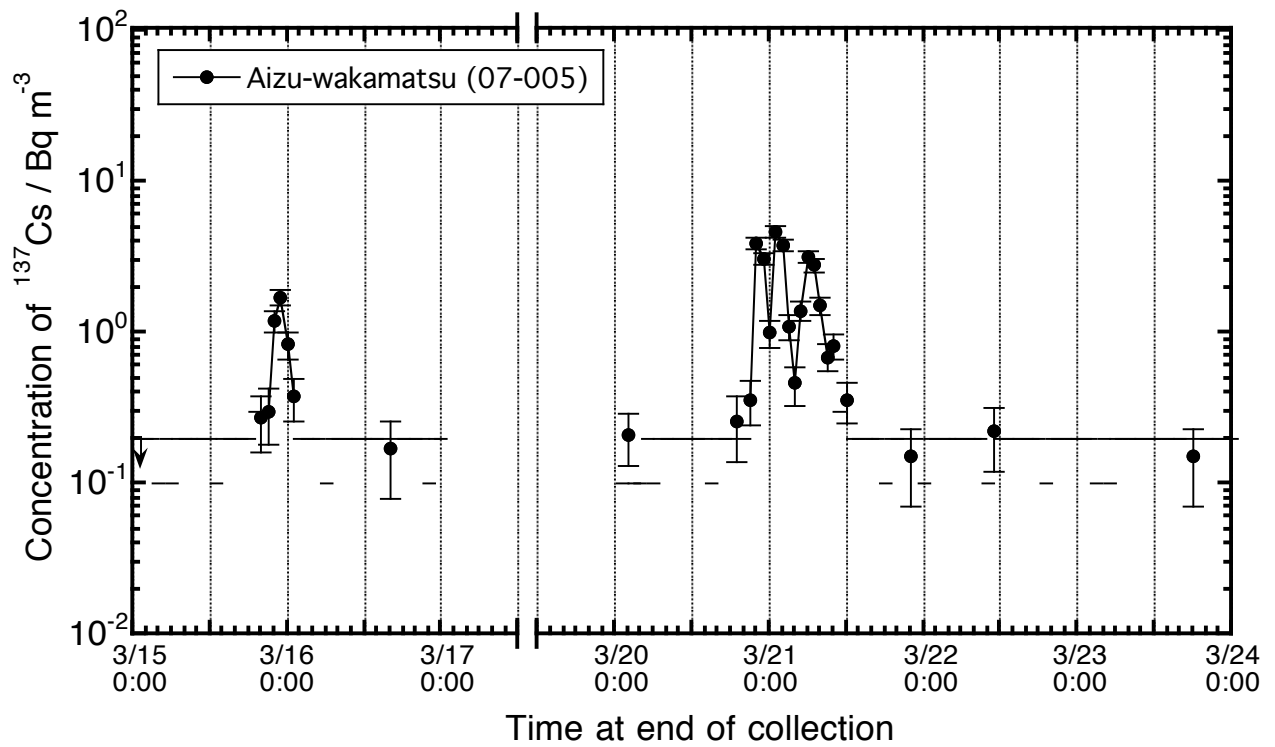


Figure B17. Time series variation of atmospheric  $^{137}\text{Cs}$  concentration observed at Aizuwakamatsu station (07-005) in Aizuwakamatsu-shi, Fukushima.

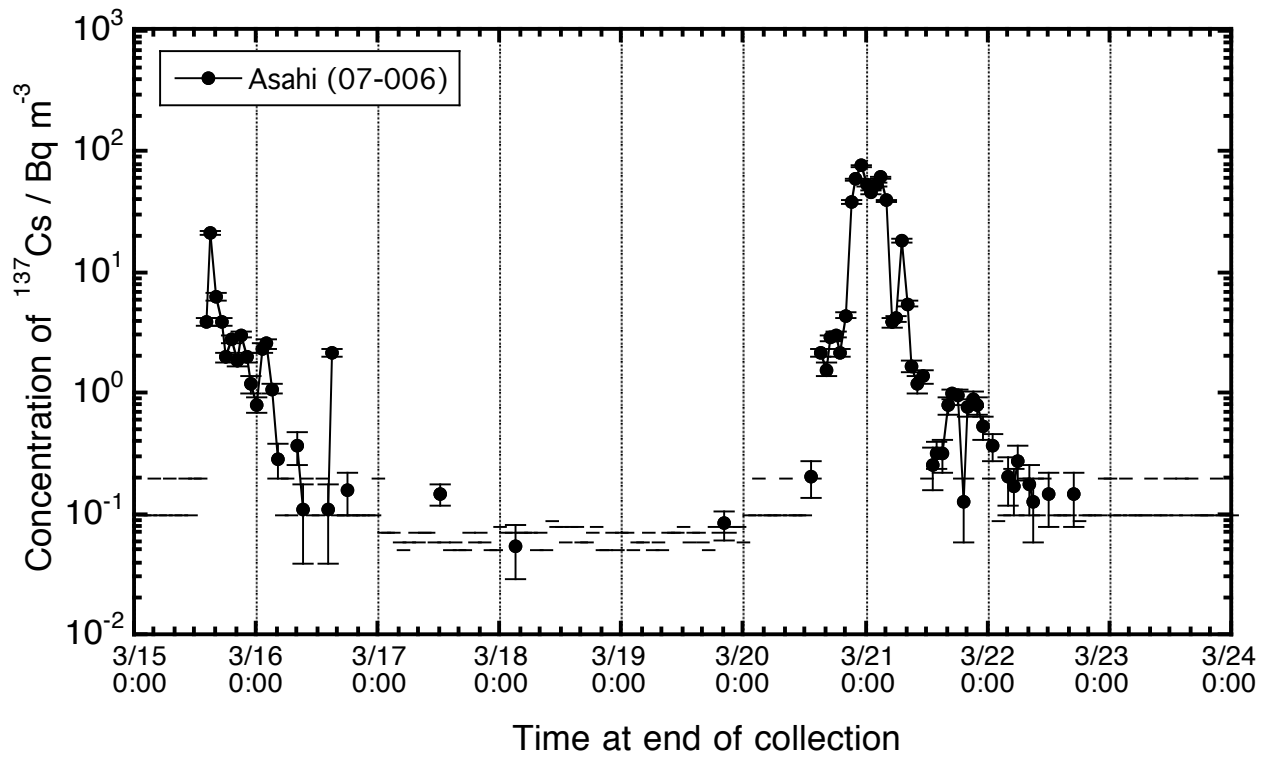


Figure B18. Time series variation of atmospheric  $^{137}\text{Cs}$  concentration observed at Asahi station (07-006) in Koriyama-shi, Fukushima.

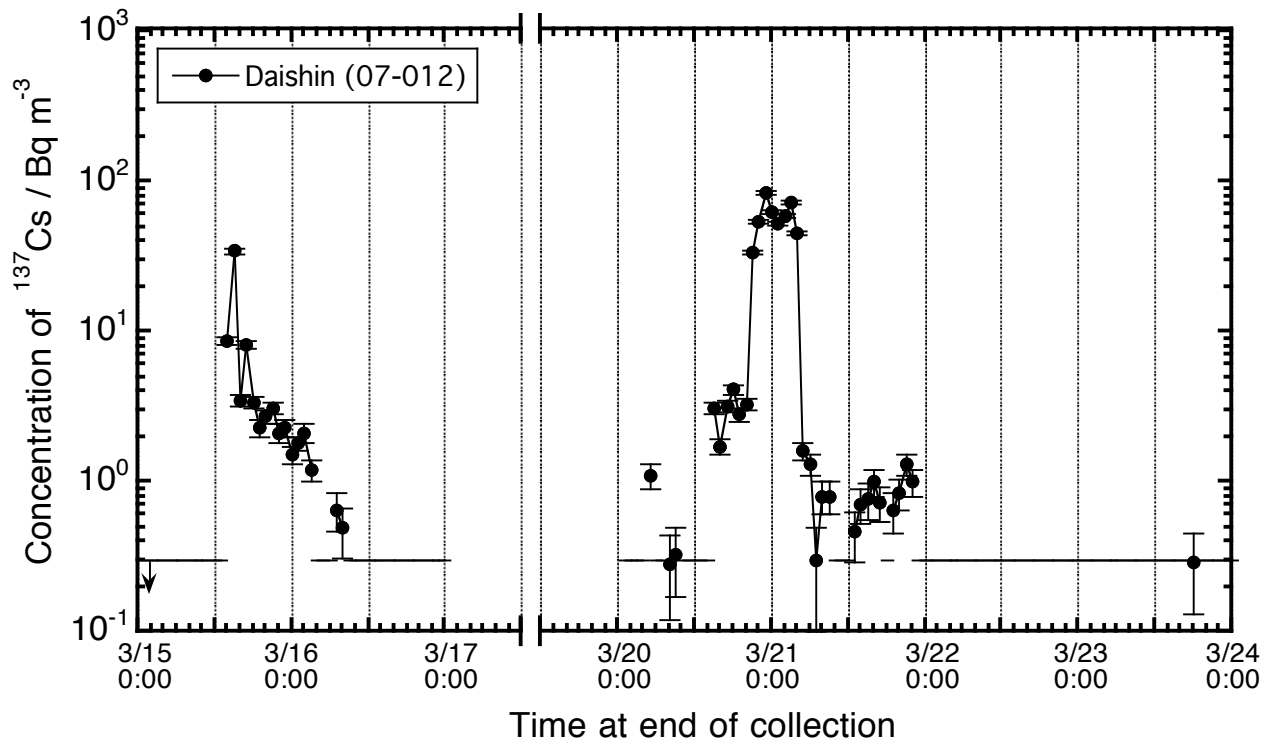


Figure B19. Time series variation of atmospheric  $^{137}\text{Cs}$  concentration observed at Daishin station (07-012) in Koriyama-shi, Fukushima.

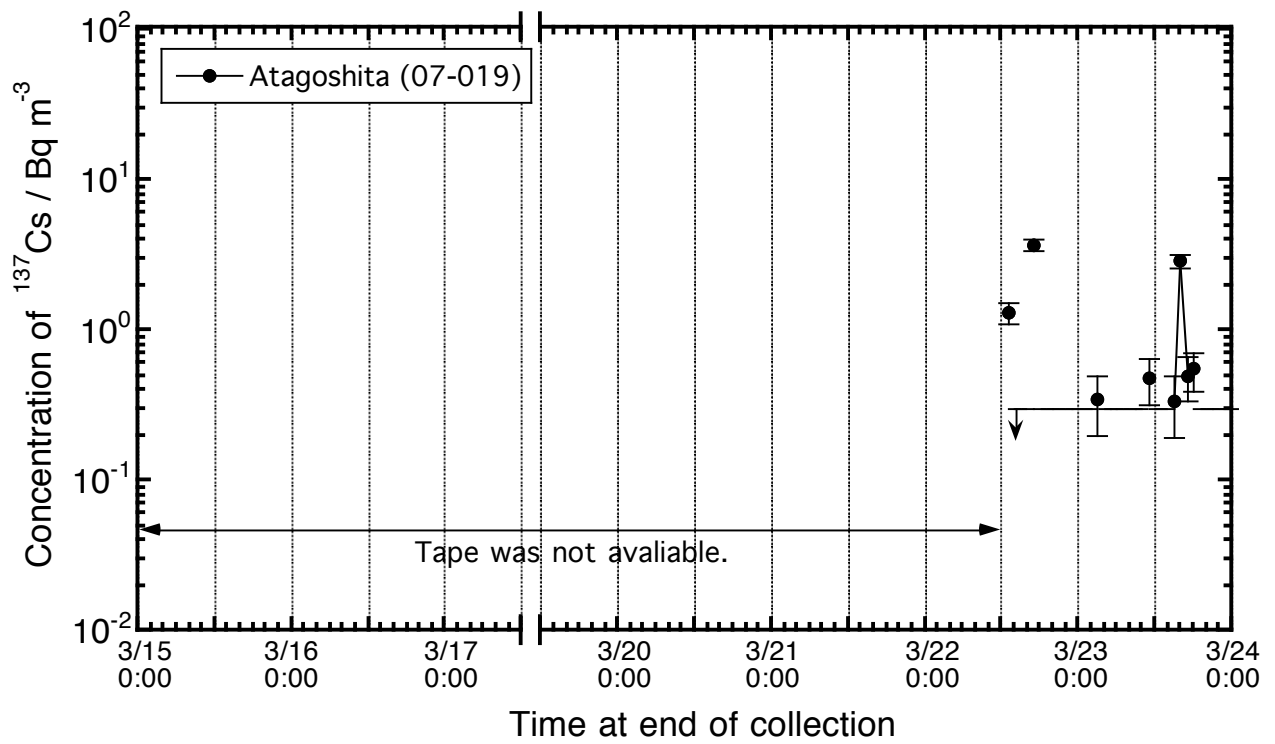


Figure B20. Time series variation of atmospheric  $^{137}\text{Cs}$  concentration observed at Atagoshita station (07-019) in Iwaki-shi, Fukushima.

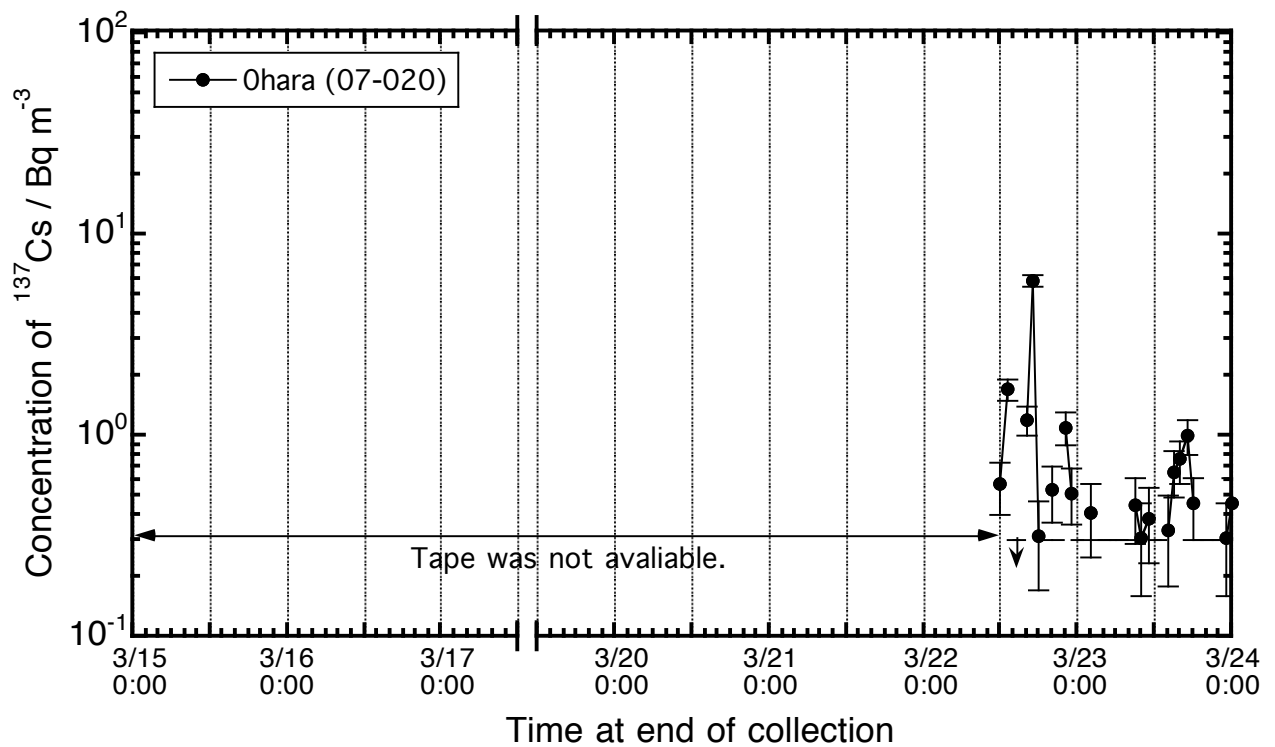


Figure B21. Time series variation of atmospheric  $^{137}\text{Cs}$  concentration observed at Ohara station (07-020) in Iwaki-shi, Fukushima.

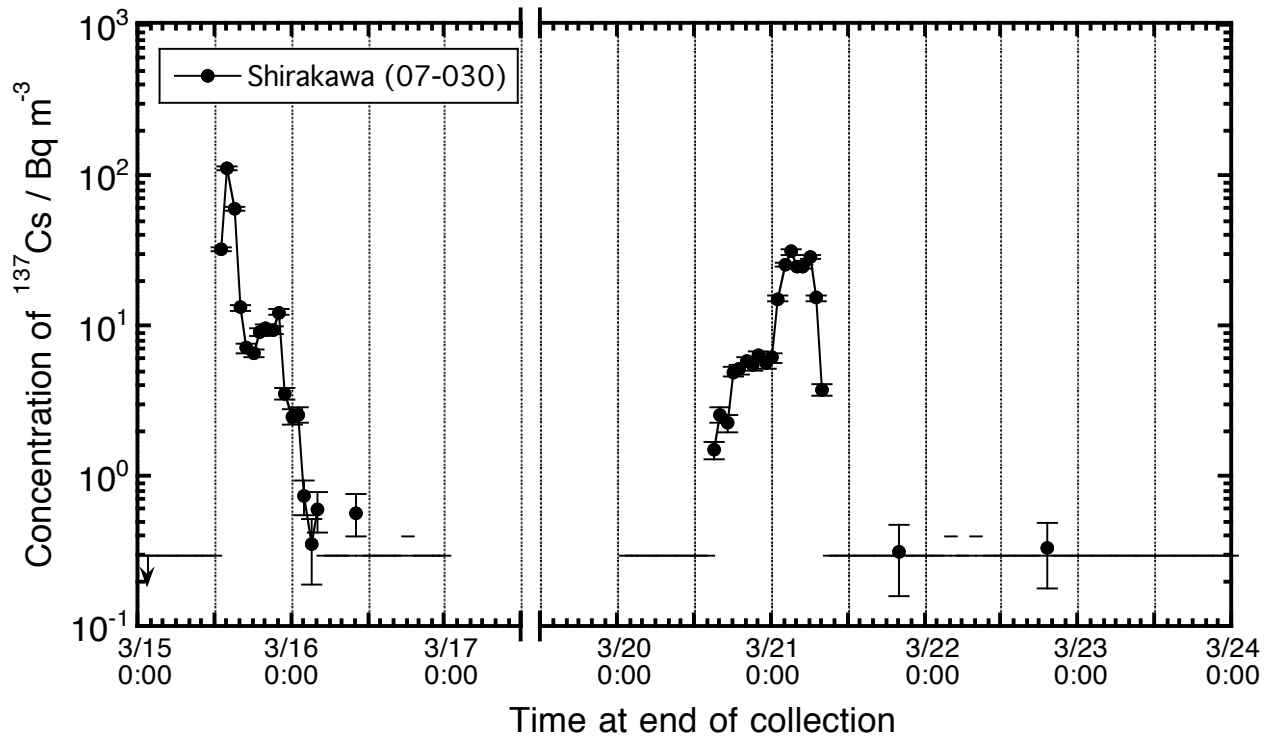


Figure B22. Time series variation of atmospheric  $^{137}\text{Cs}$  concentration observed at Shirakawa station (07-030) in Shirakawa-shi, Fukushima.

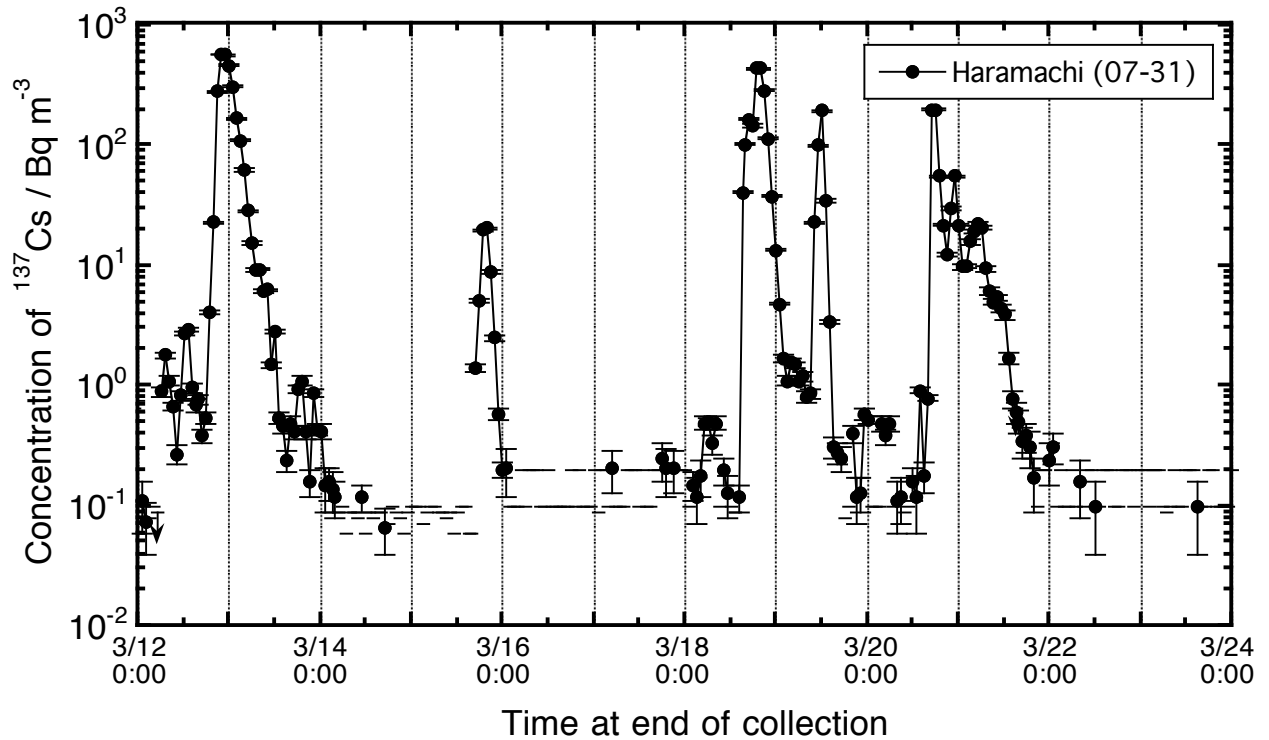


Figure B23. Time series variation of atmospheric  $^{137}\text{Cs}$  concentration observed at Haramachi station (07-031) in Minamisoma-shi, Fukushima.

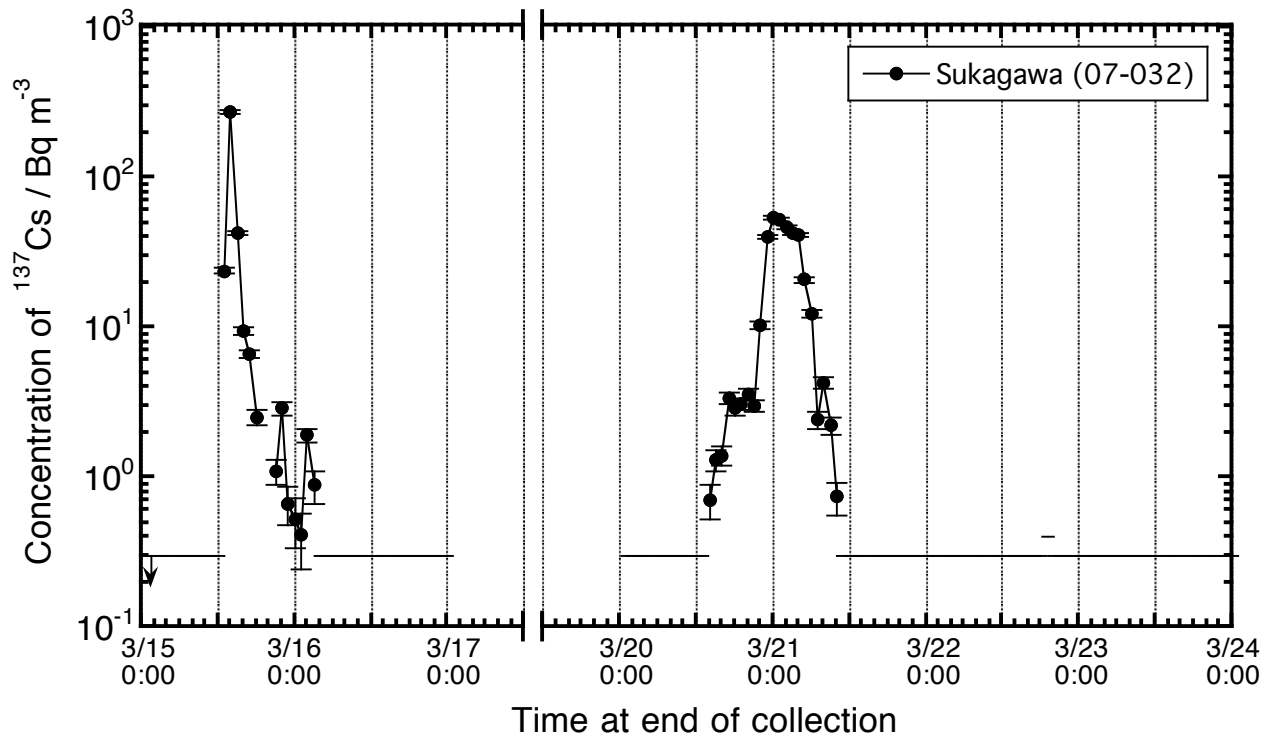


Figure B24. Time series variation of atmospheric  $^{137}\text{Cs}$  concentration observed at Sukagawa station (07-032) in Sukagawa-shi, Fukushima.

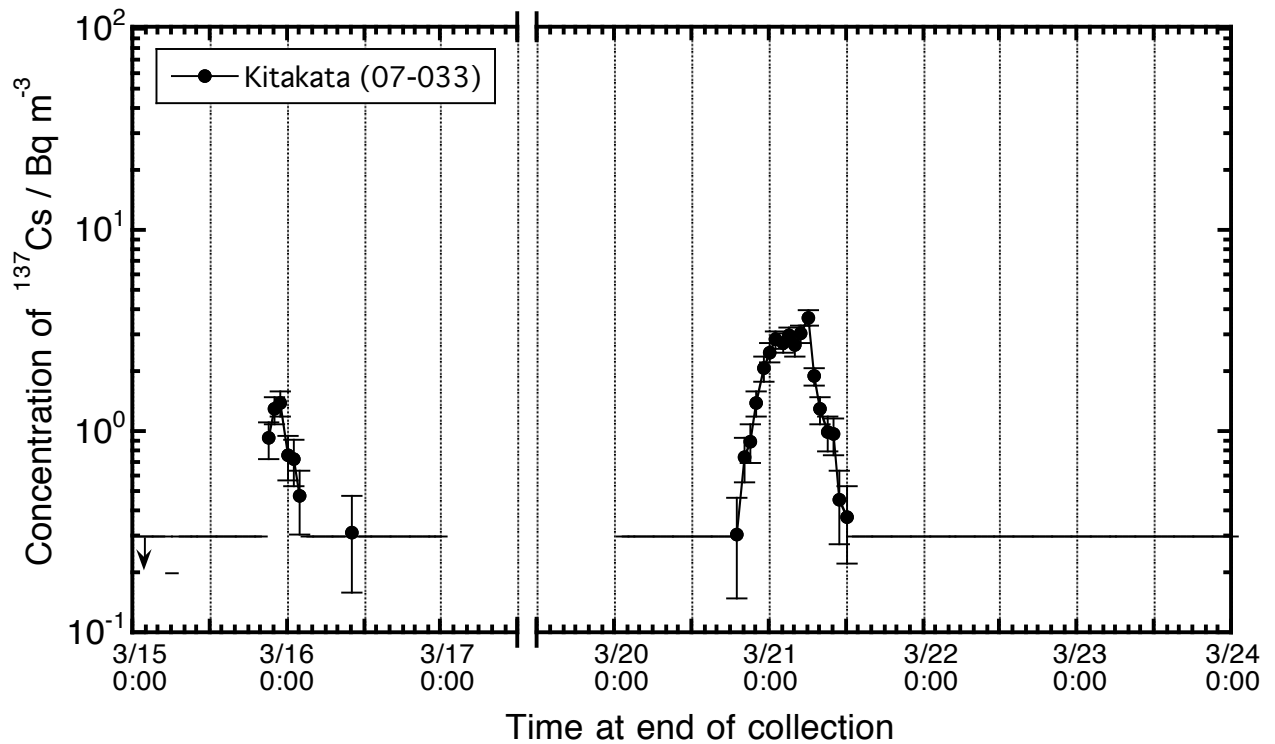


Figure B25. Time series variation of atmospheric  $^{137}\text{Cs}$  concentration observed at Kitakata station (07-033) in Kitakata-shi, Fukushima.

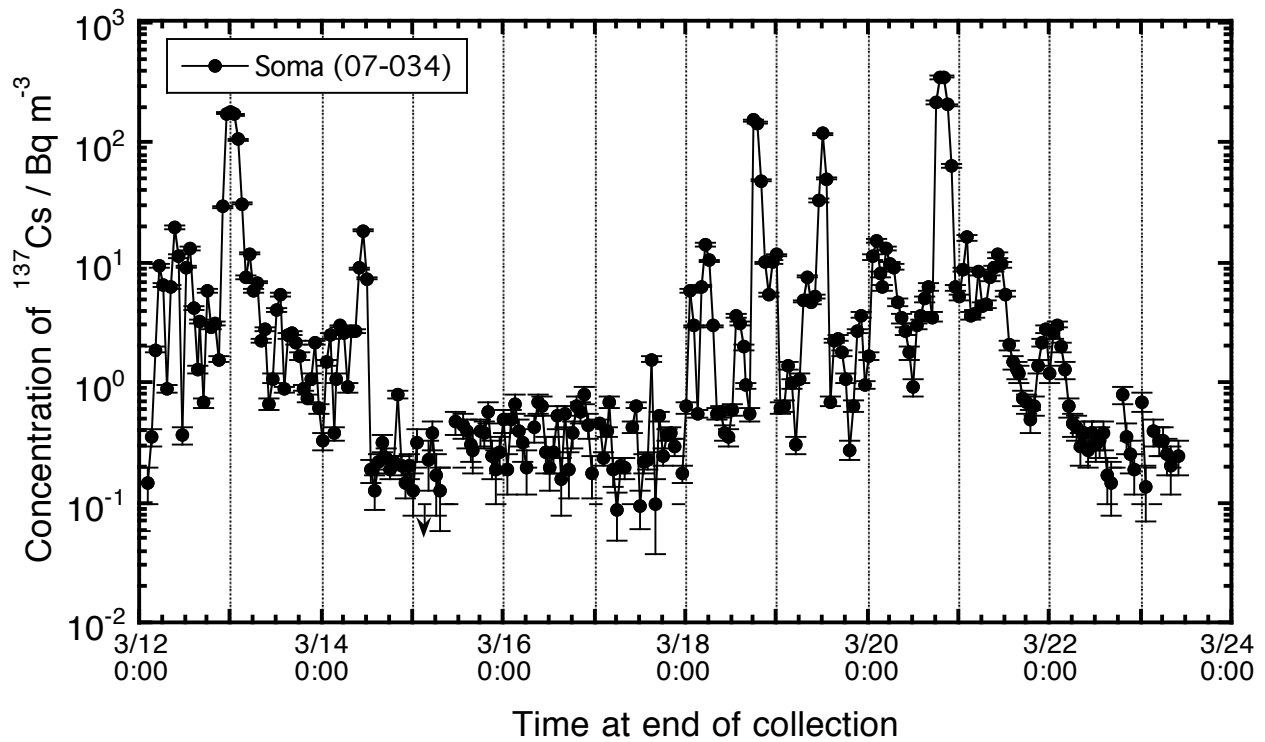


Figure B26. Time series variation of atmospheric  $^{137}\text{Cs}$  concentration observed at Soma station (07-034) in Soma-shi, Fukushima.

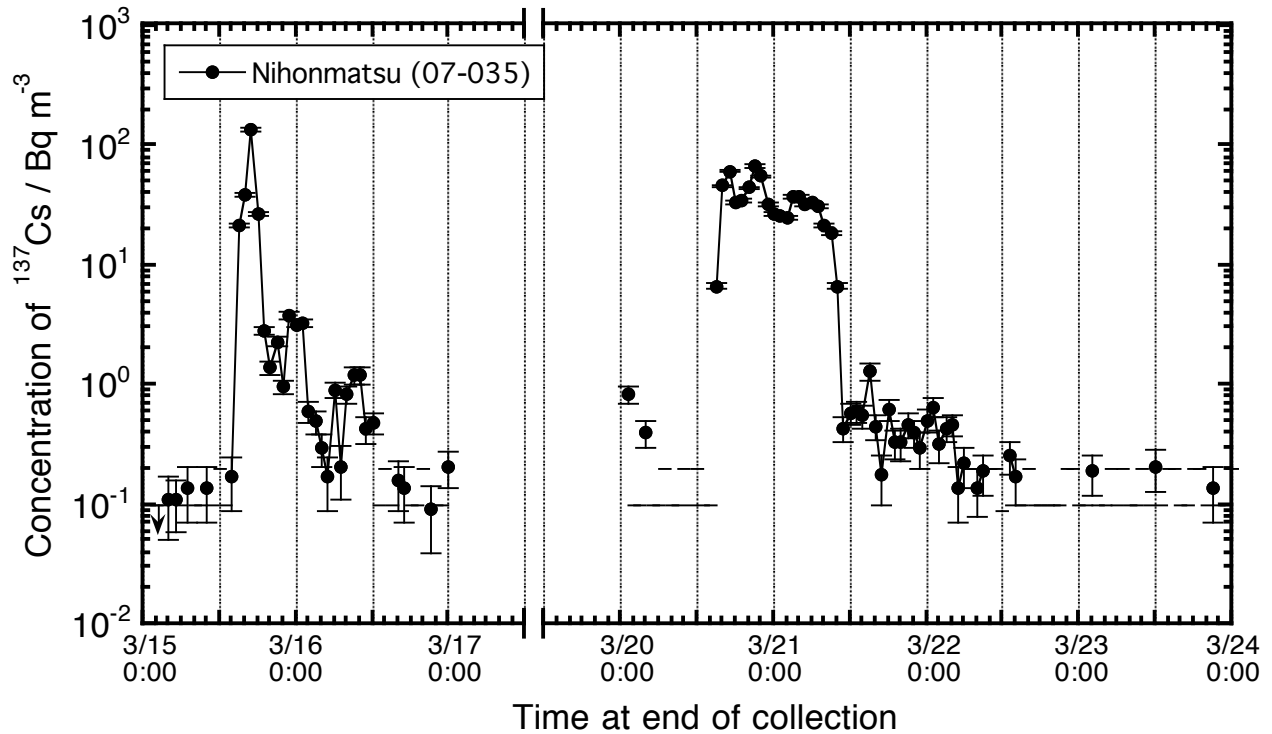


Figure B27. Time series variation of atmospheric  $^{137}\text{Cs}$  concentration observed at Nihonmatsu station (07-035) in Nihonmatsu-shi, Fukushima.

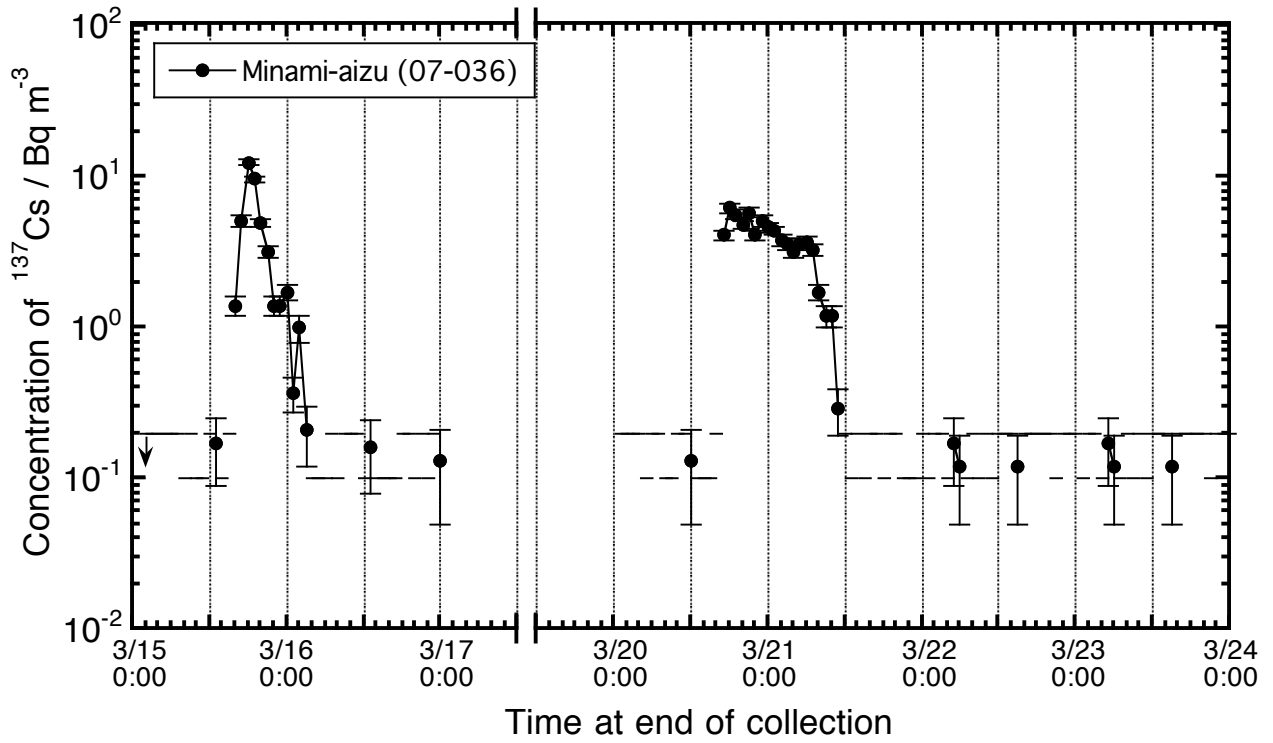


Figure B28. Time series variation of atmospheric  $^{137}\text{Cs}$  concentration observed at Minami-aizu station (07-036) in Minamiaizu-machi, Fukushima.

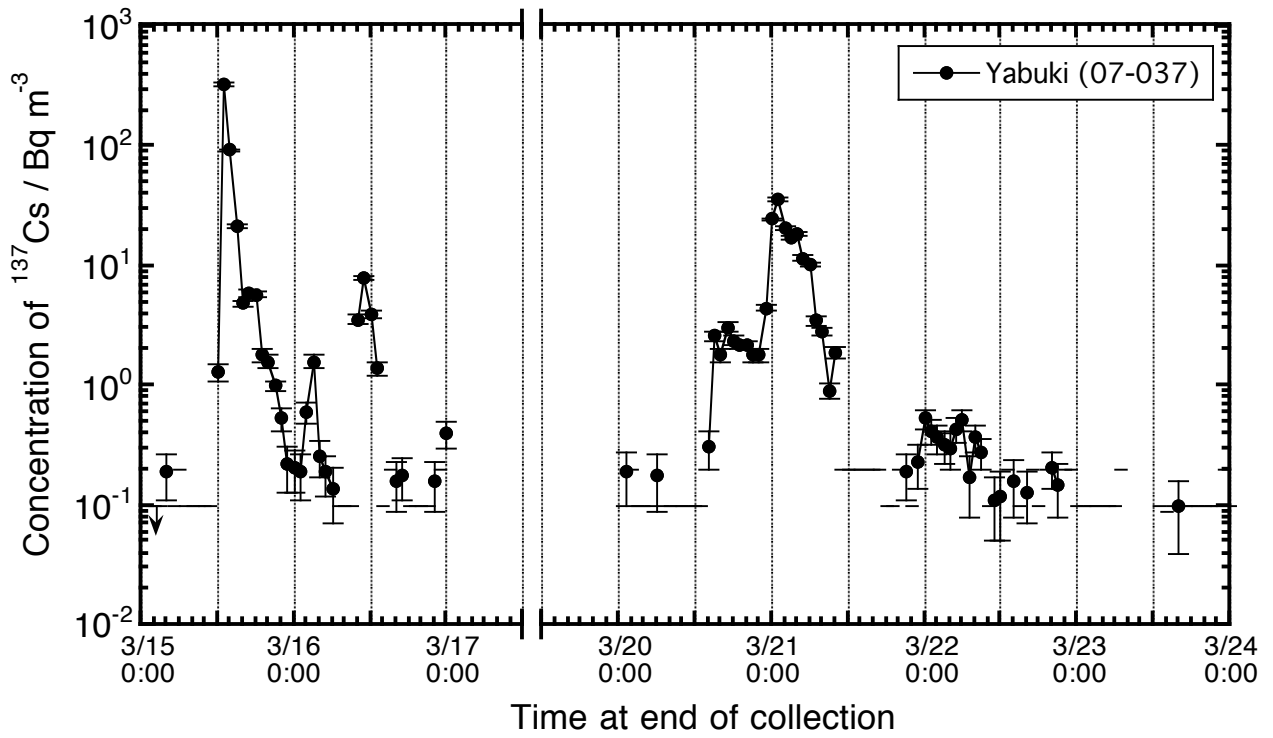


Figure B29. Time series variation of atmospheric  $^{137}\text{Cs}$  concentration observed at Yabuki station (07-037) in Yabuki-machi, Fukushima.

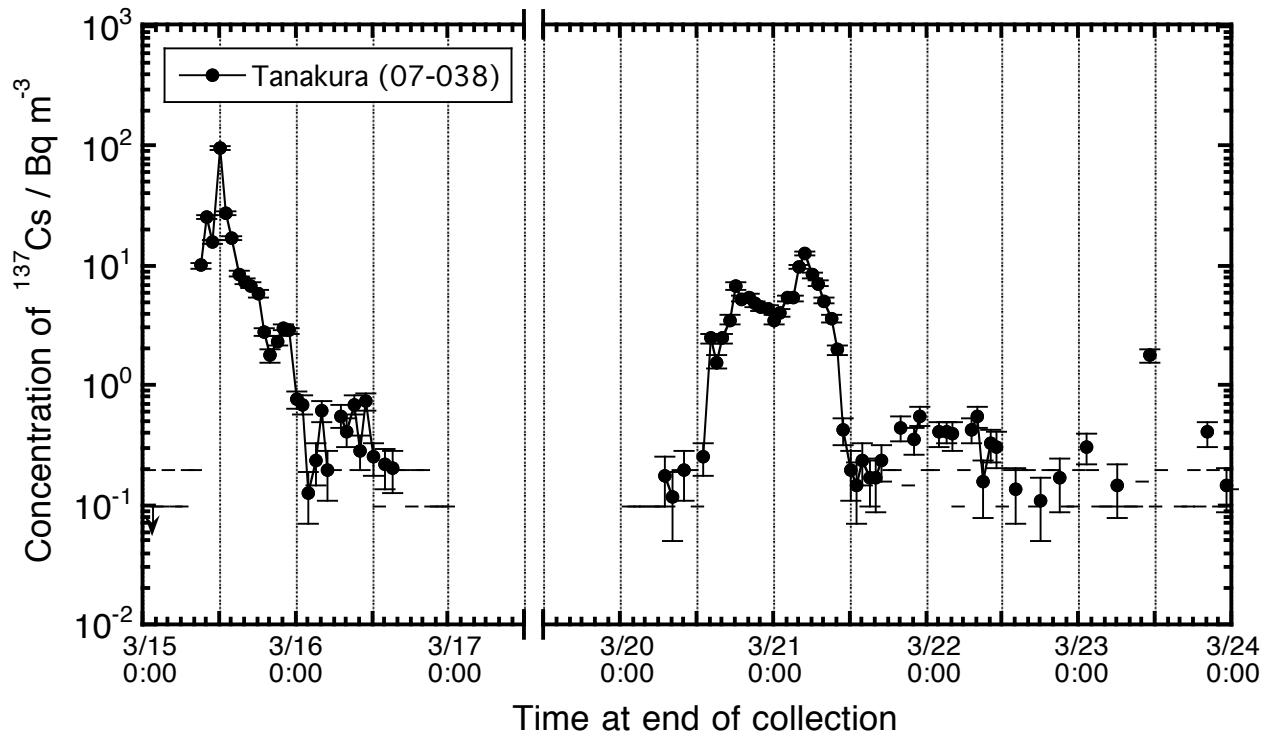


Figure B30. Time series variation of atmospheric  $^{137}\text{Cs}$  concentration observed at Tanakura station (07-038) in Tanakura-machi, Fukushima.

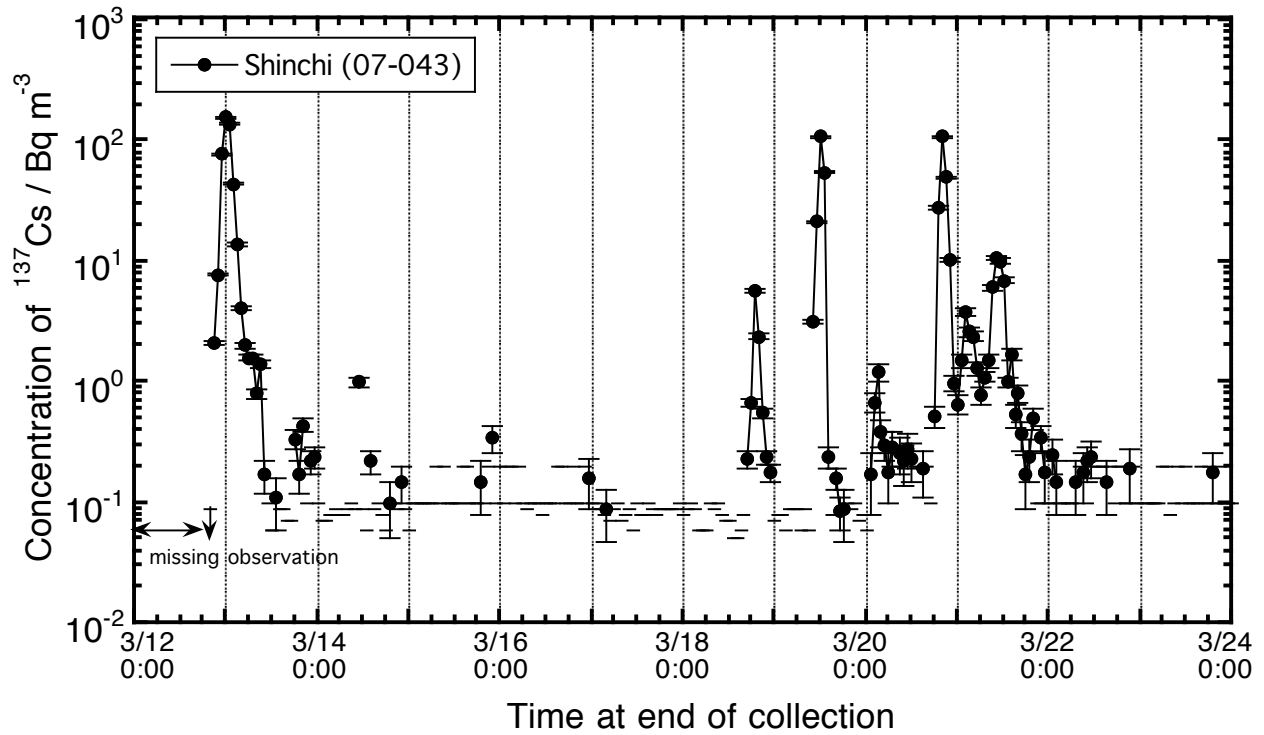


Figure B31. Time series variation of atmospheric  $^{137}\text{Cs}$  concentration observed at Shinchi station (07-043) in Shinchi-machi, Fukushima. The collection time of March 23 is tentatively identified because the day has only 23 spots.



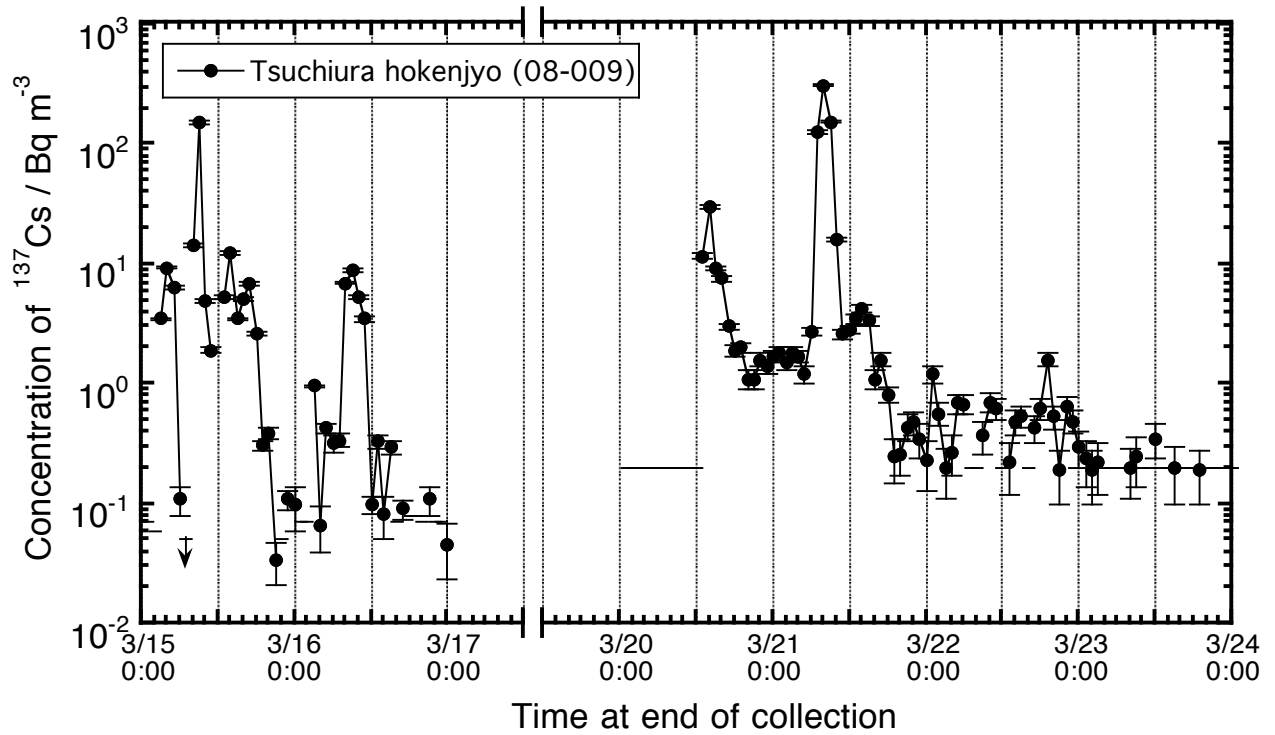


Figure B32. Time series variation of atmospheric  $^{137}\text{Cs}$  concentration observed at Tsuchiura hokenjyo station (08-009) in Tsuchiura-shi, Ibaraki.

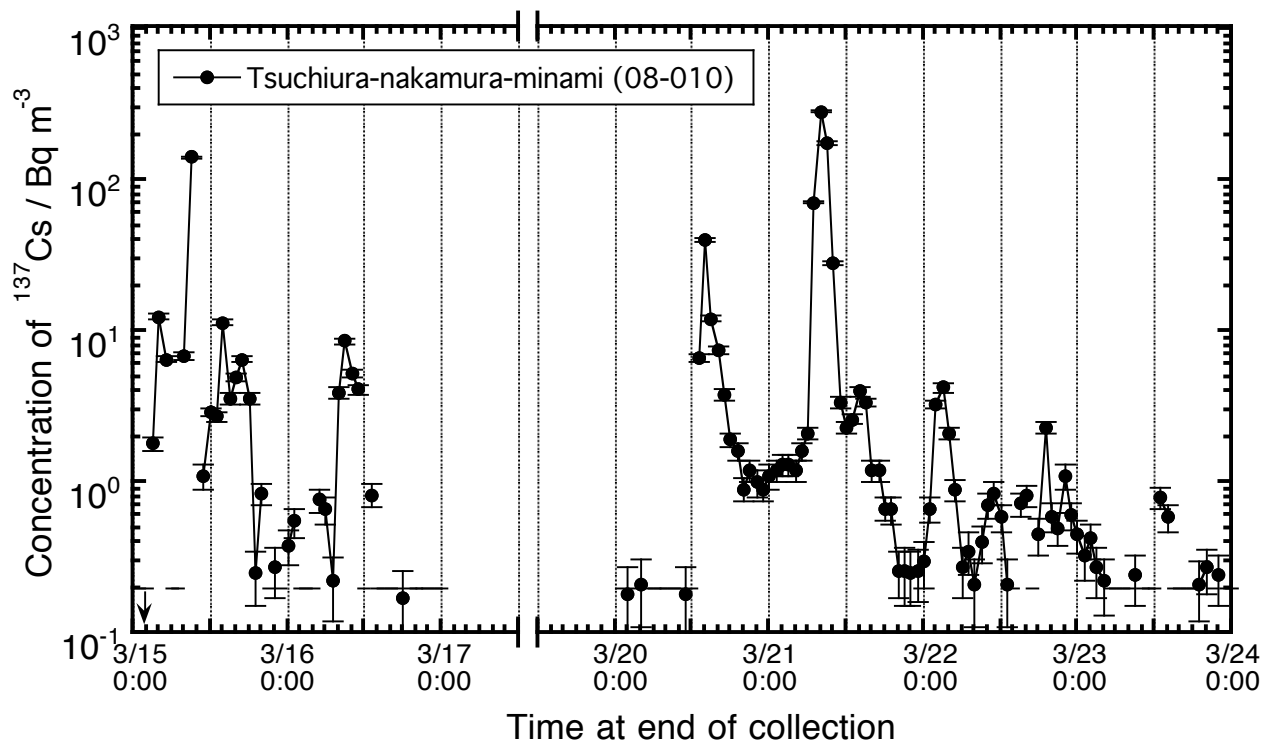


Figure B33. Time series variation of atmospheric  $^{137}\text{Cs}$  concentration observed at Tsuchiura-nakamura-minami station (08-010) in Tsuchiura-shi, Ibaraki.

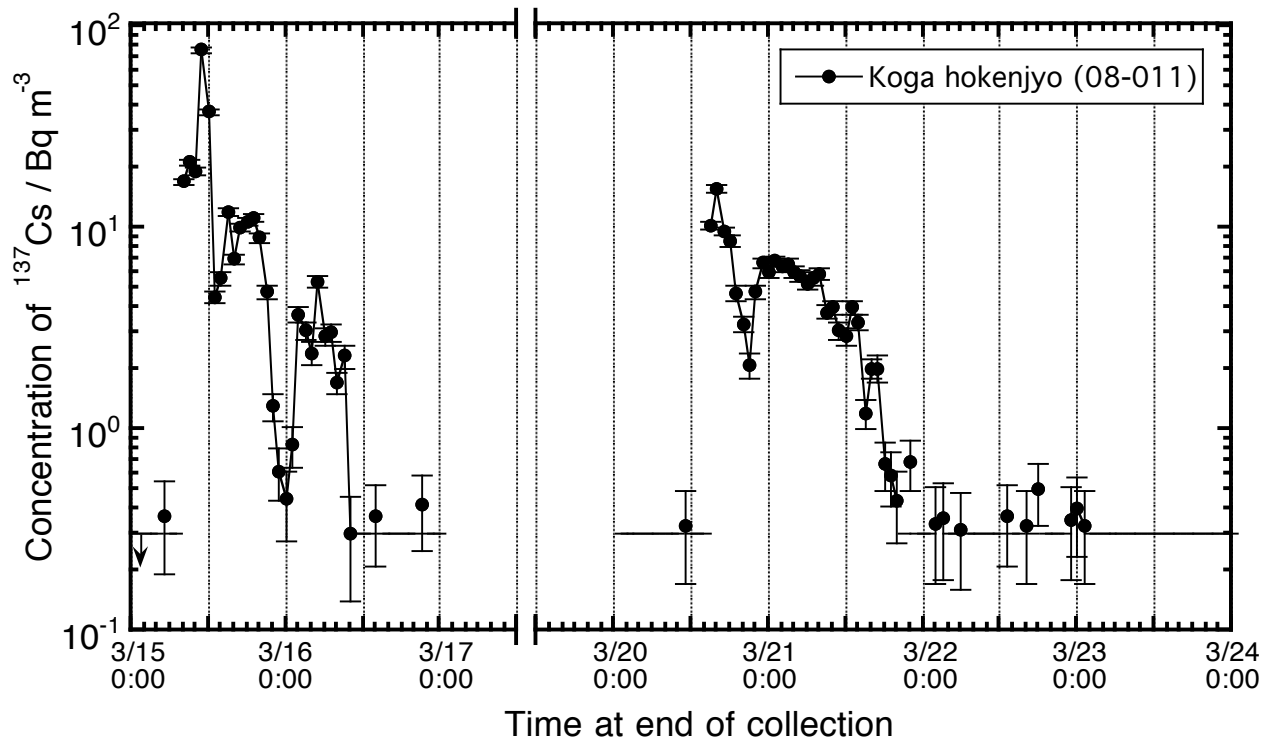


Figure B34. Time series variation of atmospheric  $^{137}\text{Cs}$  concentration observed at Koga hokenjyo station (08-011) in Koga-shi, Ibaraki.

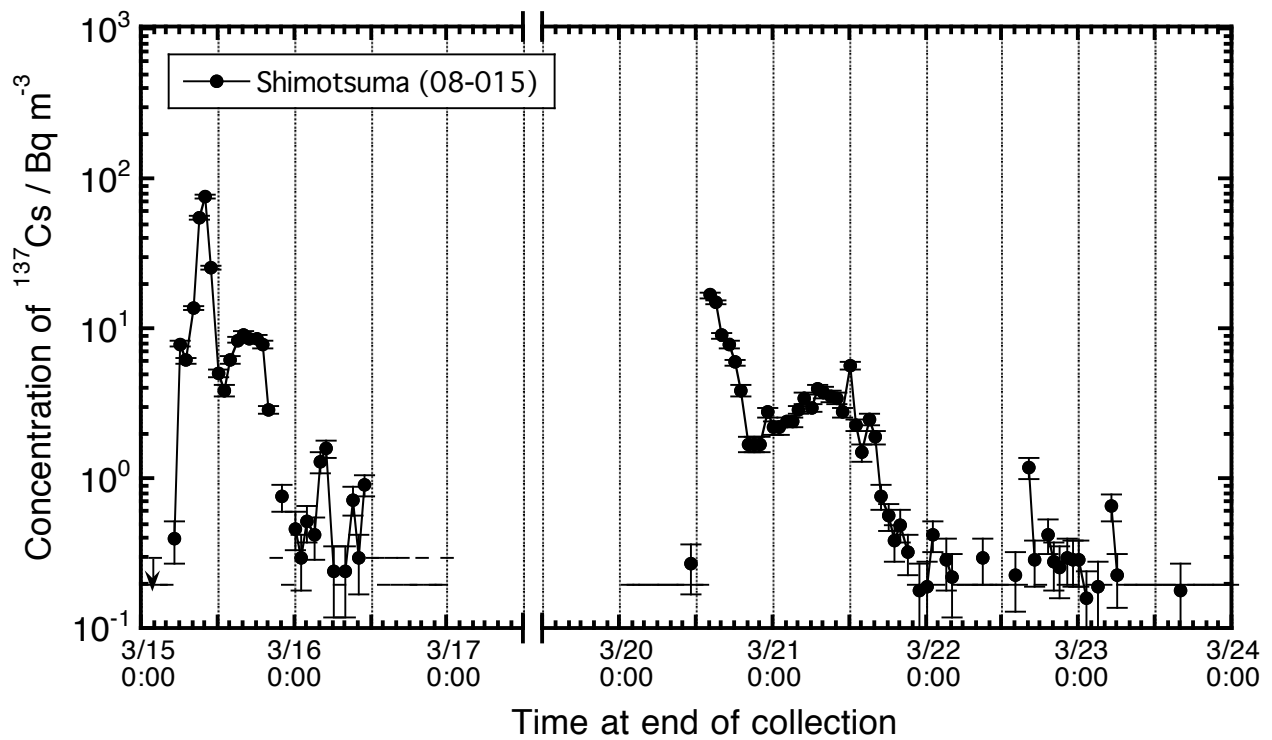


Figure B35. Time series variation of atmospheric  $^{137}\text{Cs}$  concentration observed at Shimotsuma station (08-015) in Shimotsuma-shi, Ibaraki.

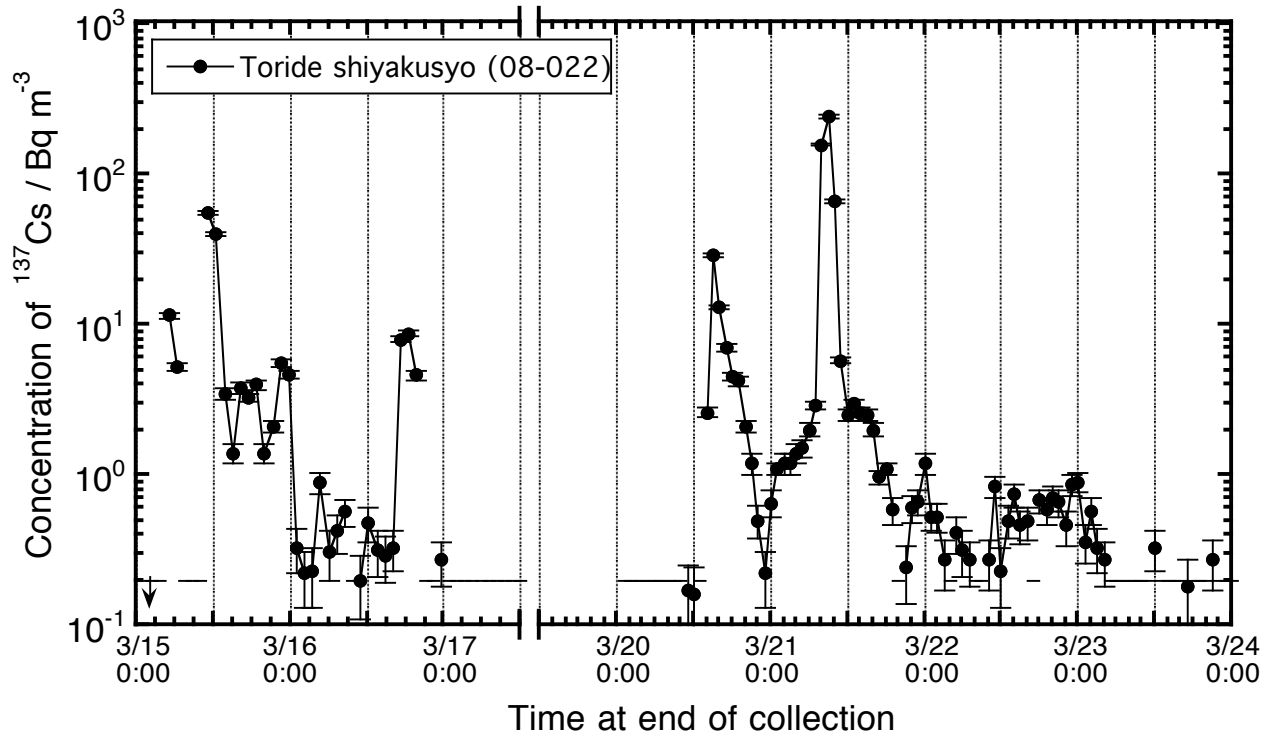


Figure B36. Time series variation of atmospheric  $^{137}\text{Cs}$  concentration observed at Toride shiyakusho station (08-022) in Toride-shi, Ibaraki.

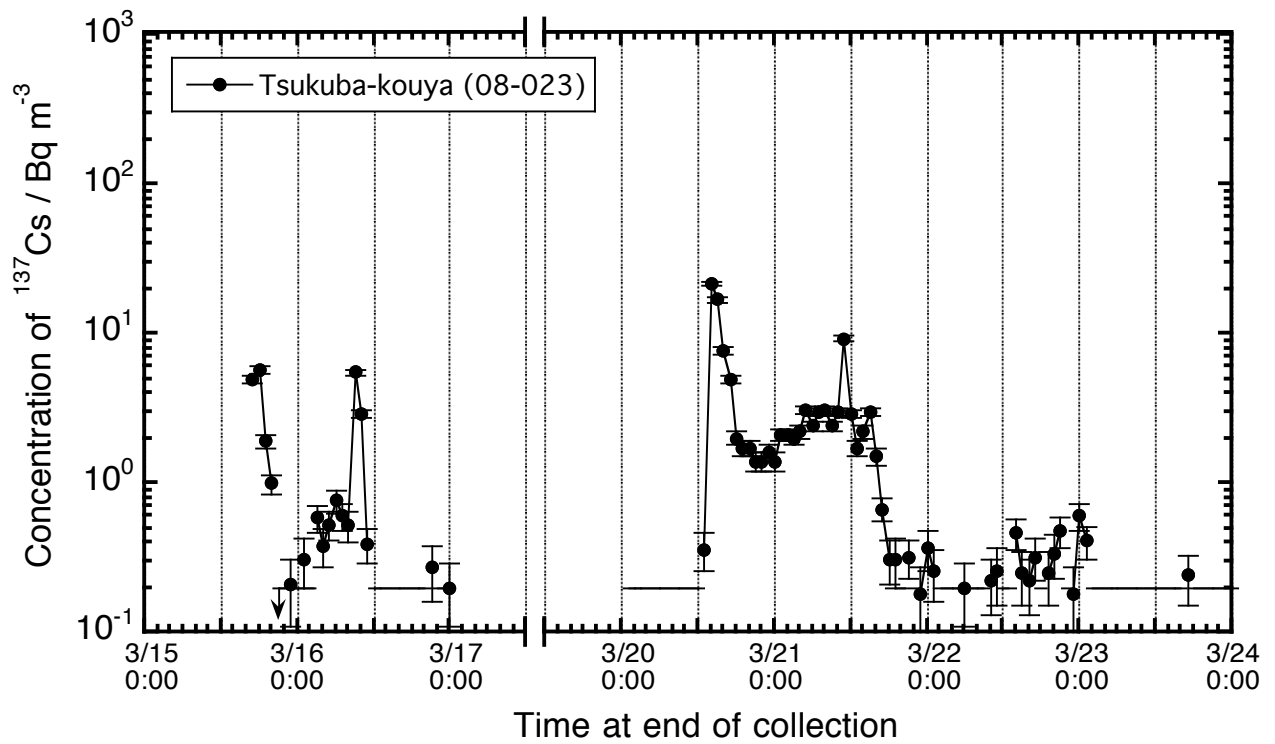


Figure B37. Time series variation of atmospheric  $^{137}\text{Cs}$  concentration observed at Tsukuba-kouya (08-023) in Tsukuba-shi, Ibaraki.

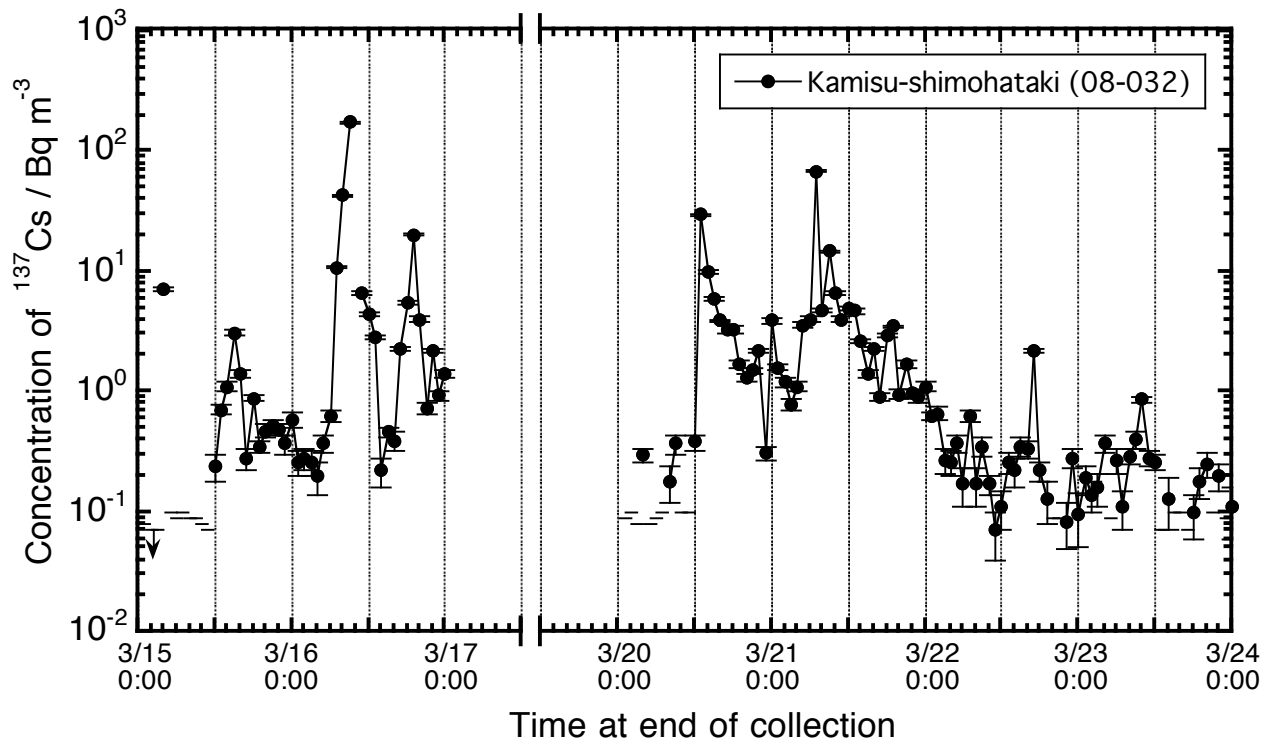


Figure B38. Time series variation of atmospheric  $^{137}\text{Cs}$  concentration observed at Kamisu-shimohataki (08-032) in Kamisu-shi, Ibaraki.

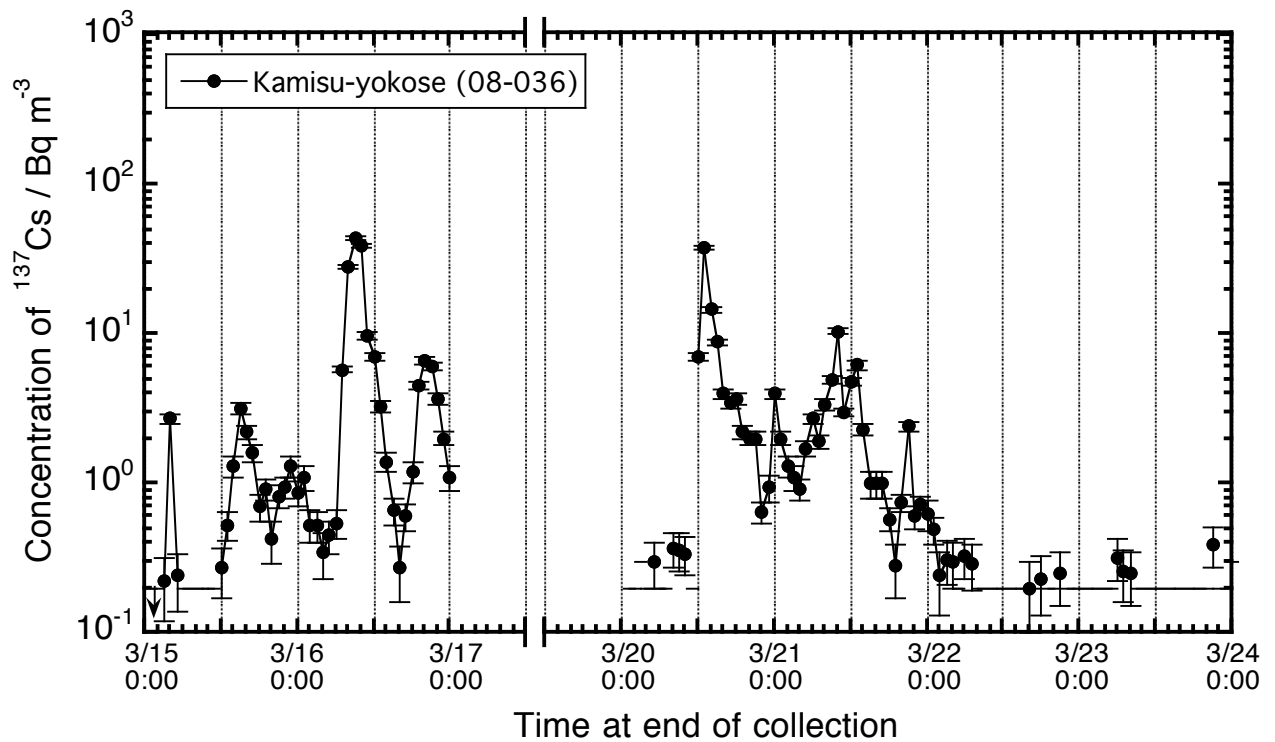


Figure B39. Time series variation of atmospheric  $^{137}\text{Cs}$  concentration observed at Kamisu-yokose station (08-036) in Kamisu-shi, Ibaraki.

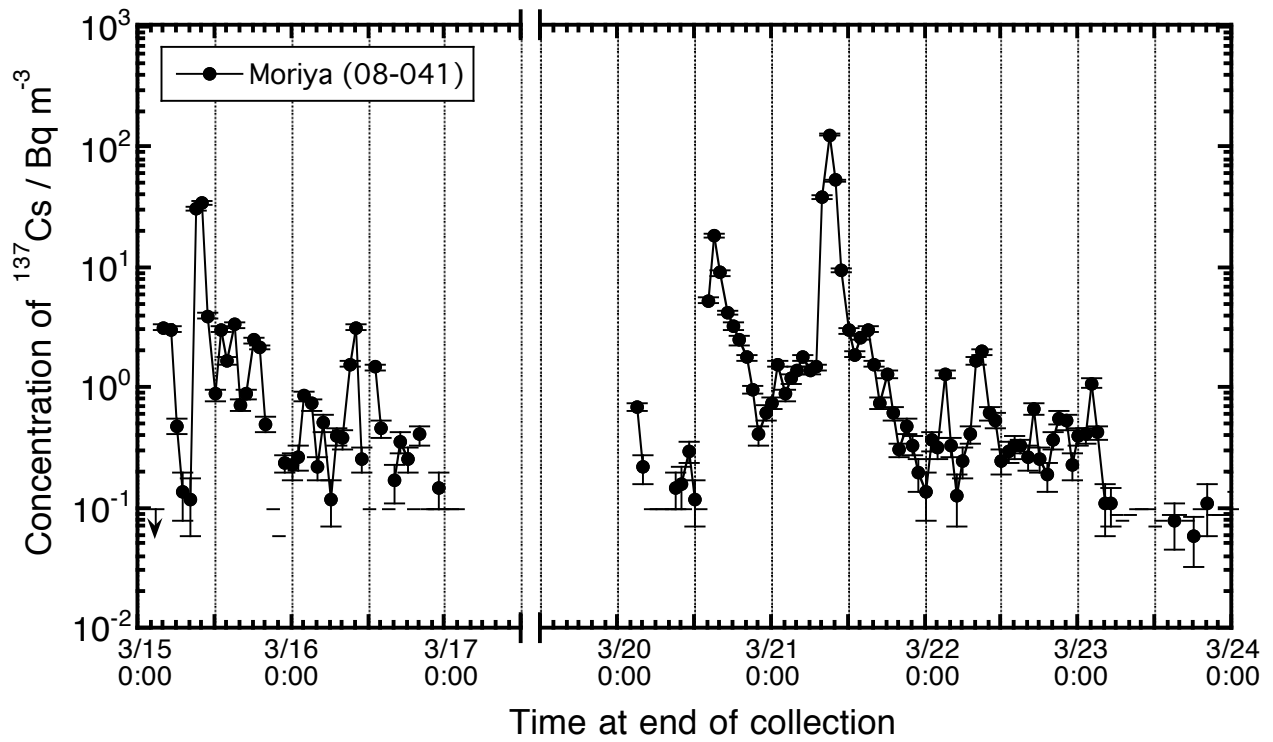


Figure B40. Time series variation of atmospheric  $^{137}\text{Cs}$  concentration observed at Moriya station (08-041) in Moriya-shi, Ibaraki.

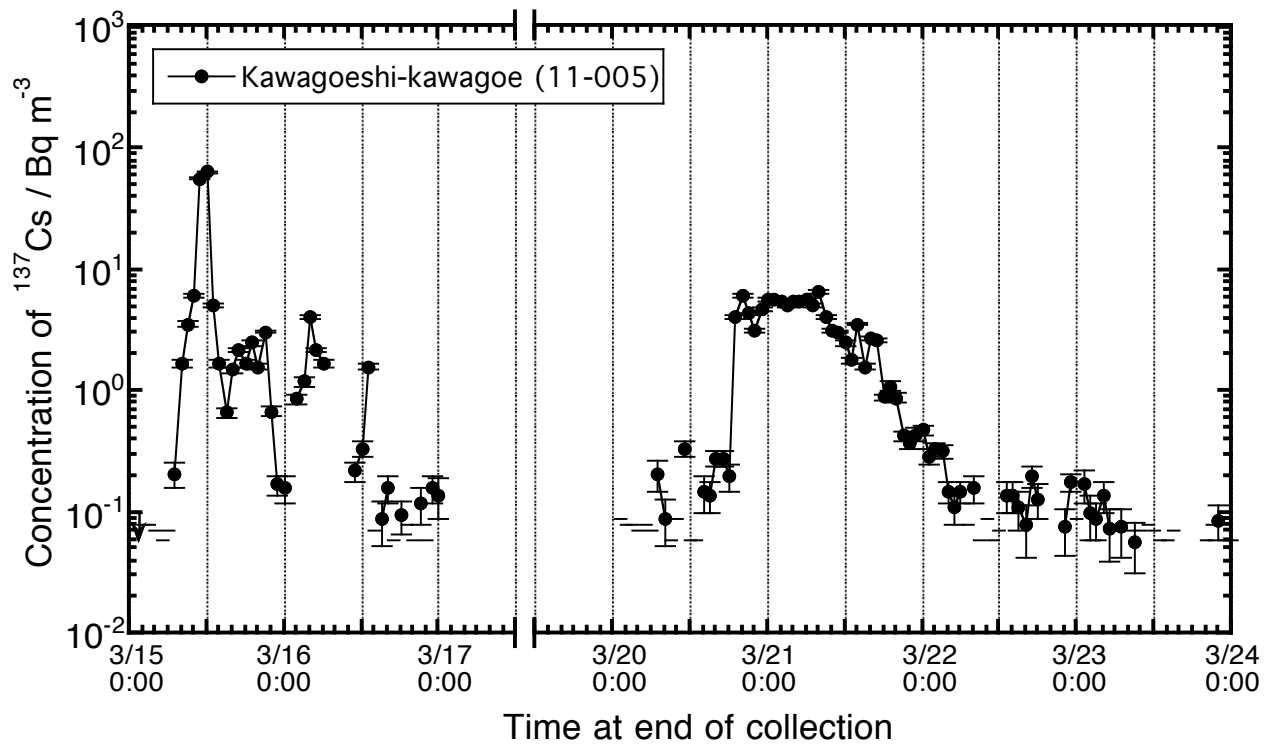


Figure B41. Time series variation of atmospheric  $^{137}\text{Cs}$  concentration observed at Kawagoeshi-kawagoe station (11-005) in Kawagoe-shi, Saitama.

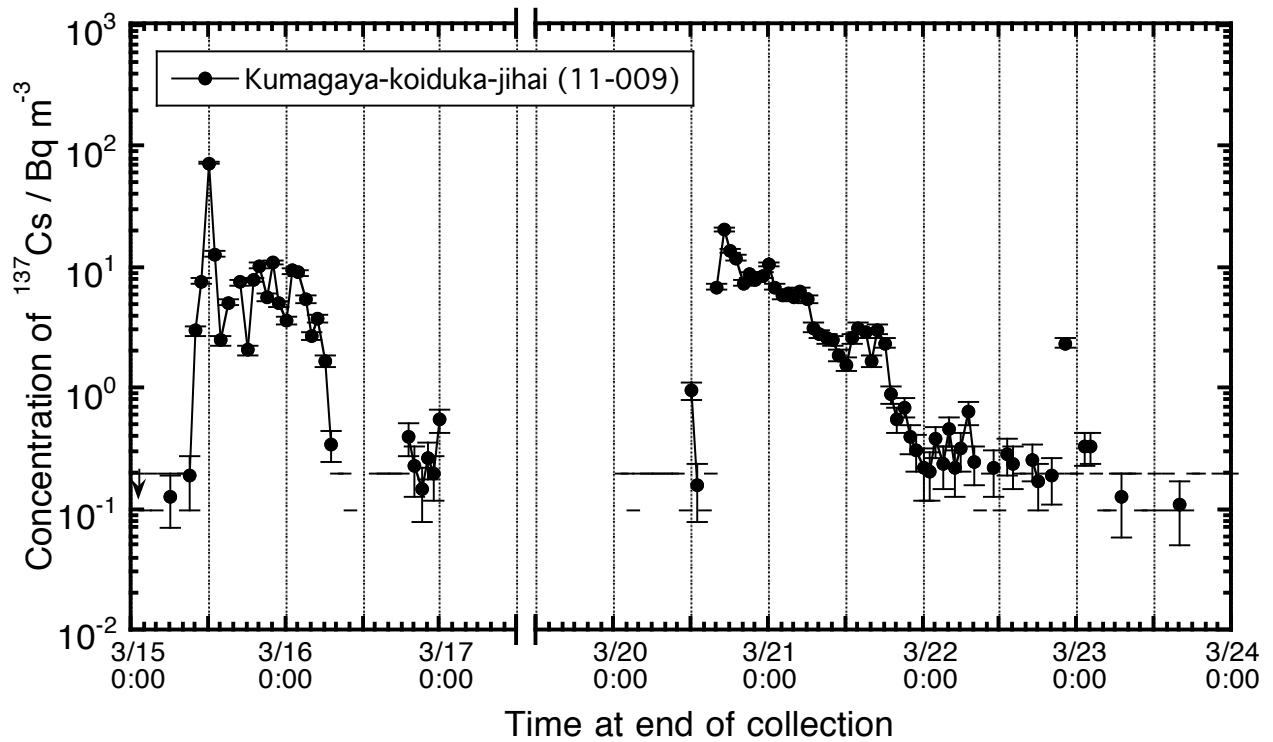


Figure B42. Time series variation of atmospheric  $^{137}\text{Cs}$  concentration observed at Kumagaya-koiduka-jihai station (11-009) in Kumagaya-shi, Saitama.

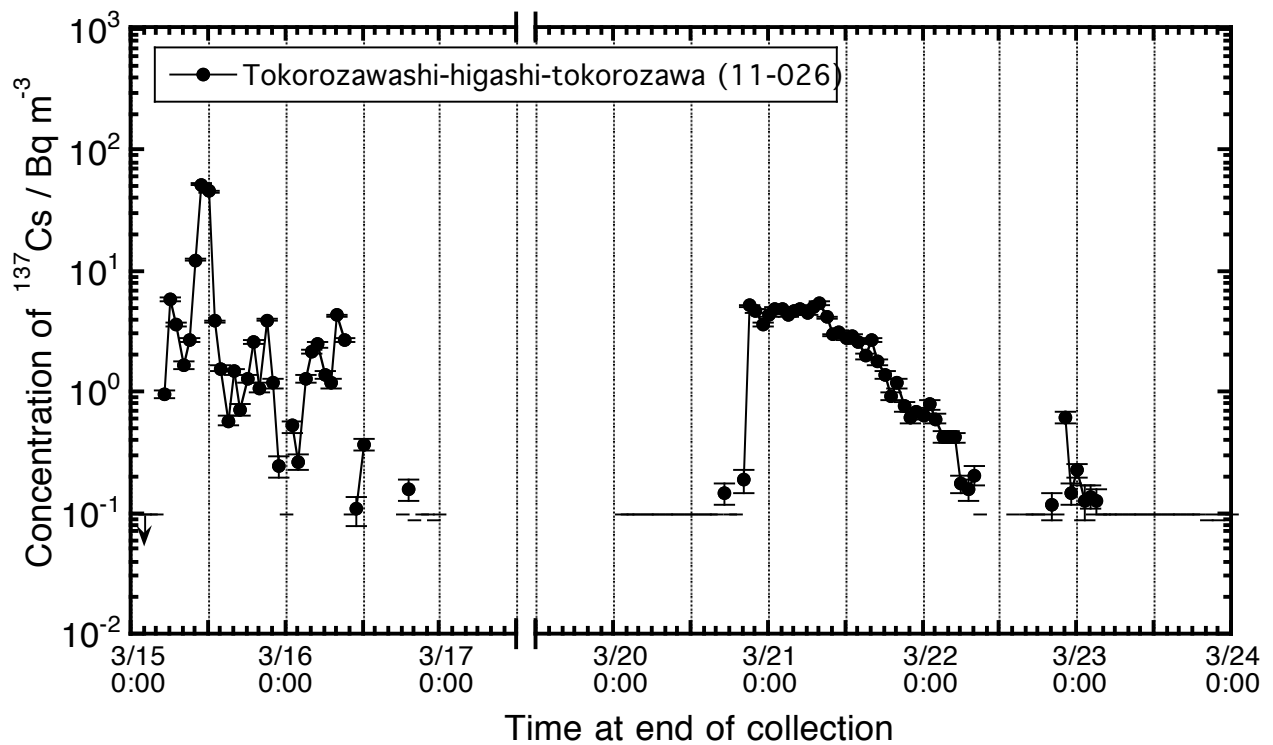


Figure B43. Time series variation of atmospheric  $^{137}\text{Cs}$  concentration observed at Tokorozawashi-higashi-tokorozawa station (11-026) in Tokorozawa-shi, Saitama.

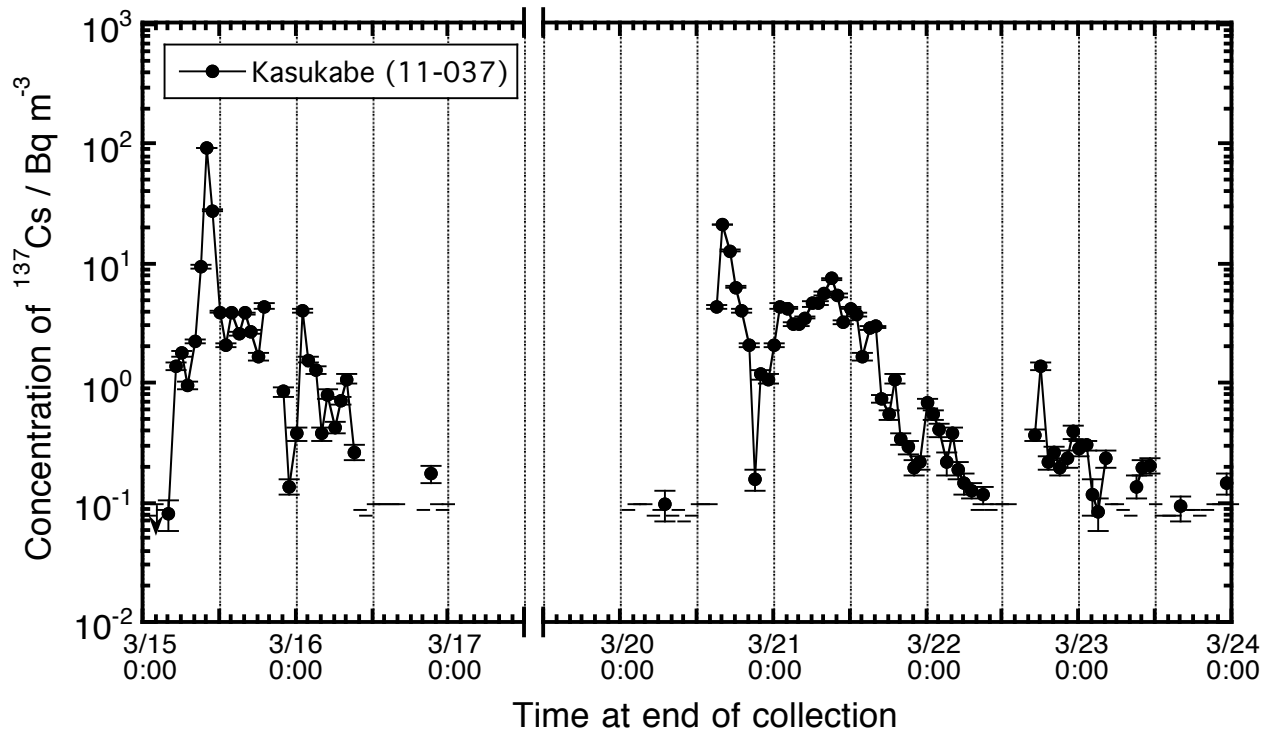


Figure B44. Time series variation of atmospheric  $^{137}\text{Cs}$  concentration observed at Kasukabe station (11-037) in Kasukabe-shi, Saitama.

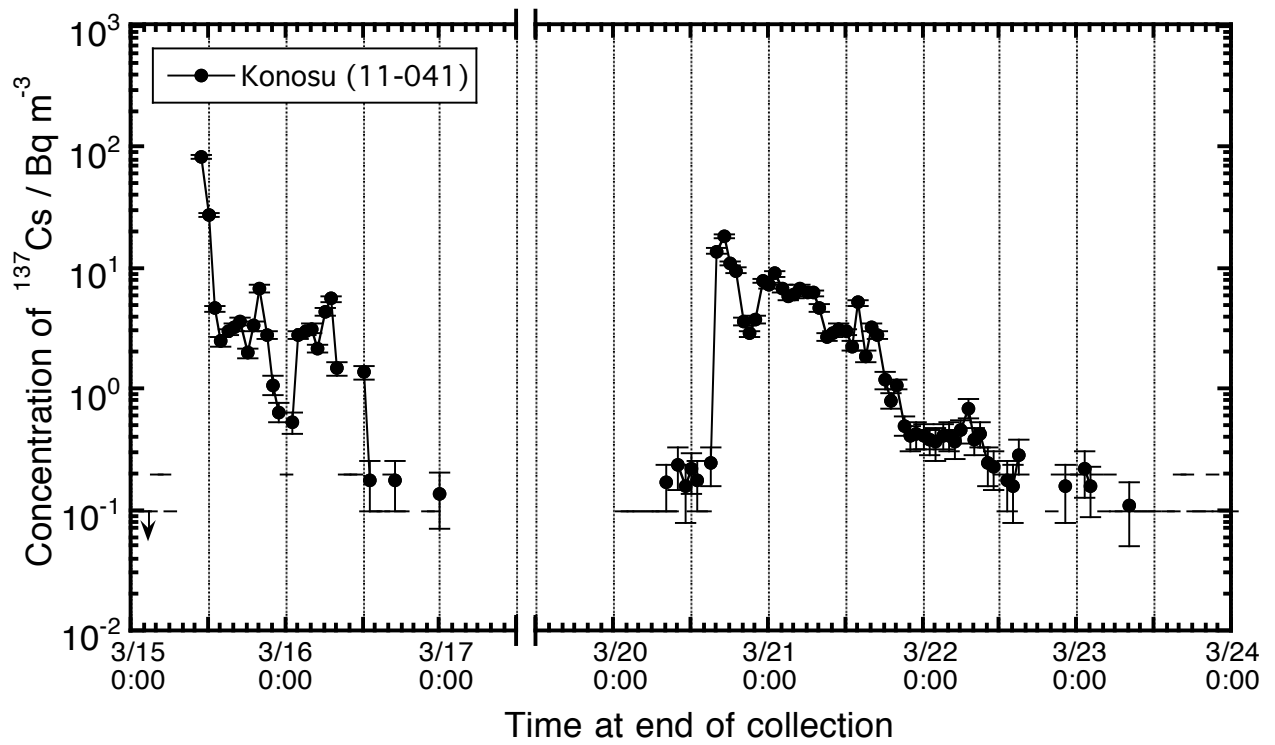


Figure B45. Time series variation of atmospheric  $^{137}\text{Cs}$  concentration observed at Konosu station (11-041) in Konosu-shi, Saitama.

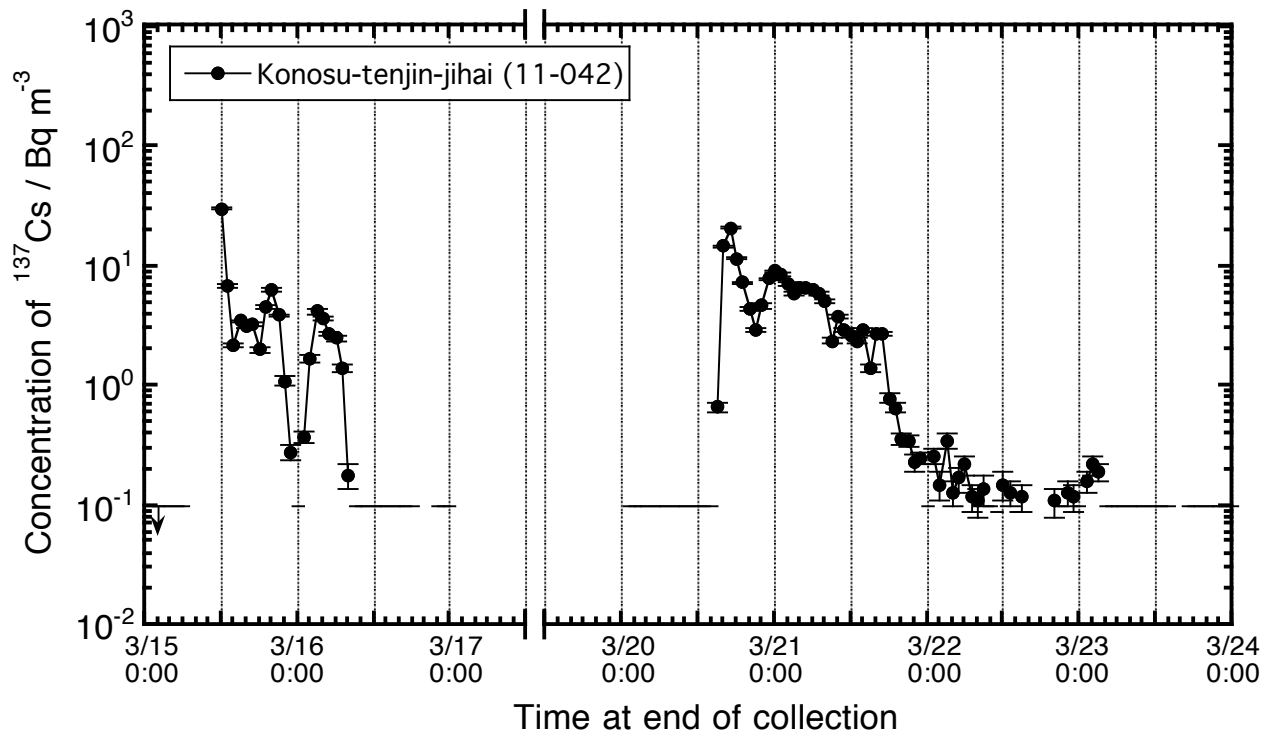


Figure B46. Time series variation of atmospheric  $^{137}\text{Cs}$  concentration observed at Konosu-tenjin-jihai station (11-042) in Konosu-shi, Saitama.

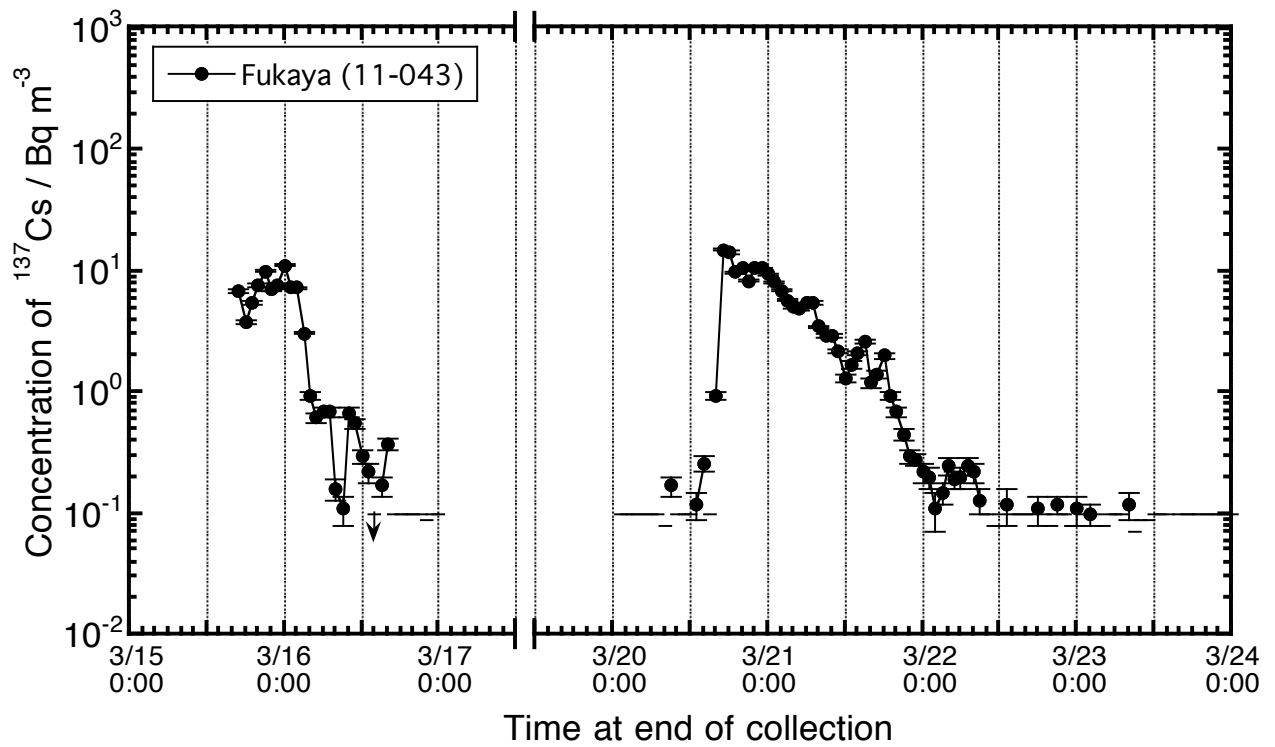


Figure B47. Time series variation of atmospheric  $^{137}\text{Cs}$  concentration observed at Fukaya station (11-043) in Fukaya-shi, Saitama.



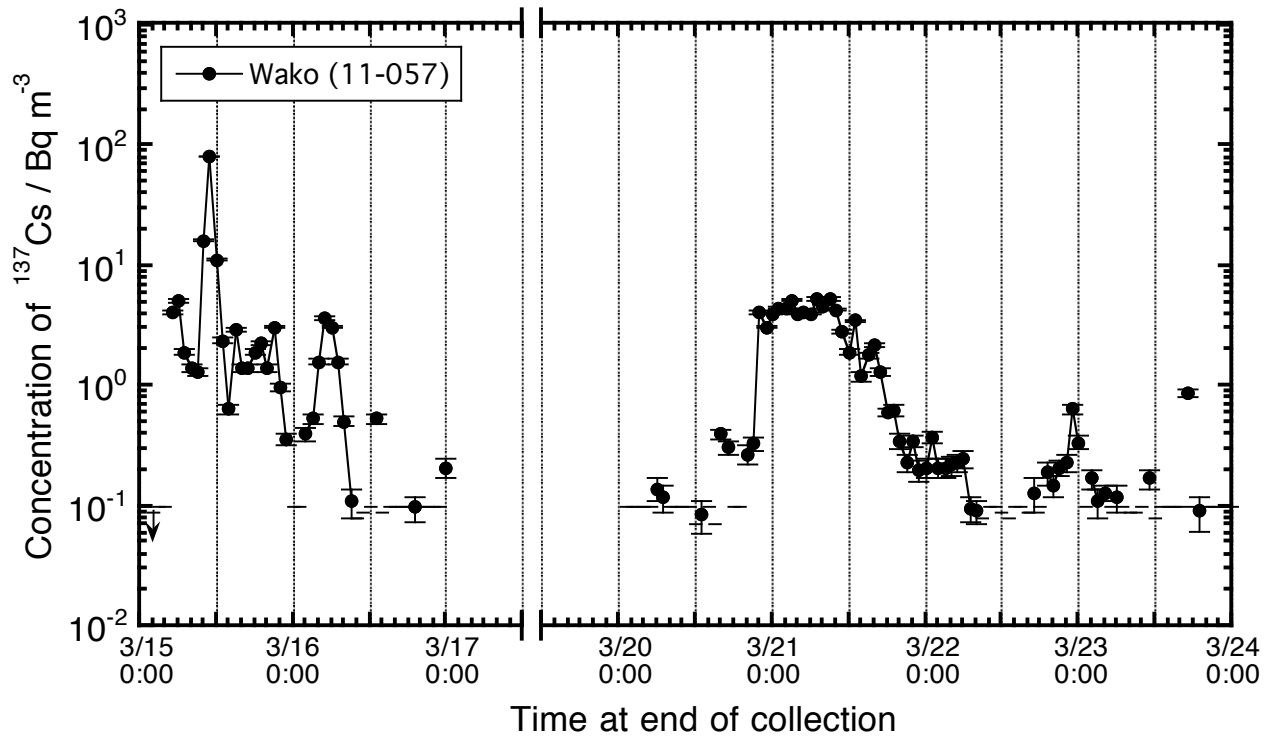


Figure B48. Time series variation of atmospheric  $^{137}\text{Cs}$  concentration observed at Wako station (11-057) in Wako-shi, Saitama.

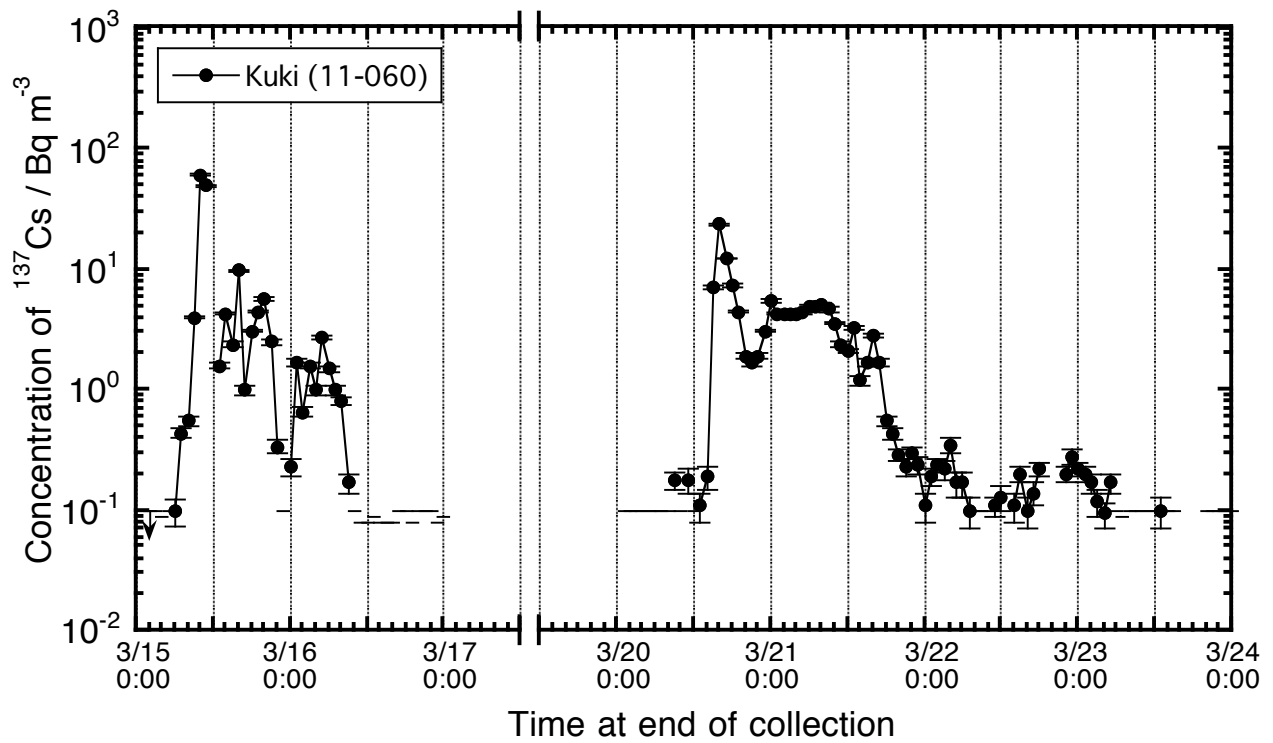


Figure B49. Time series variation of atmospheric  $^{137}\text{Cs}$  concentration observed at Kuki station (11-060) in Kuki-shi, Saitama.

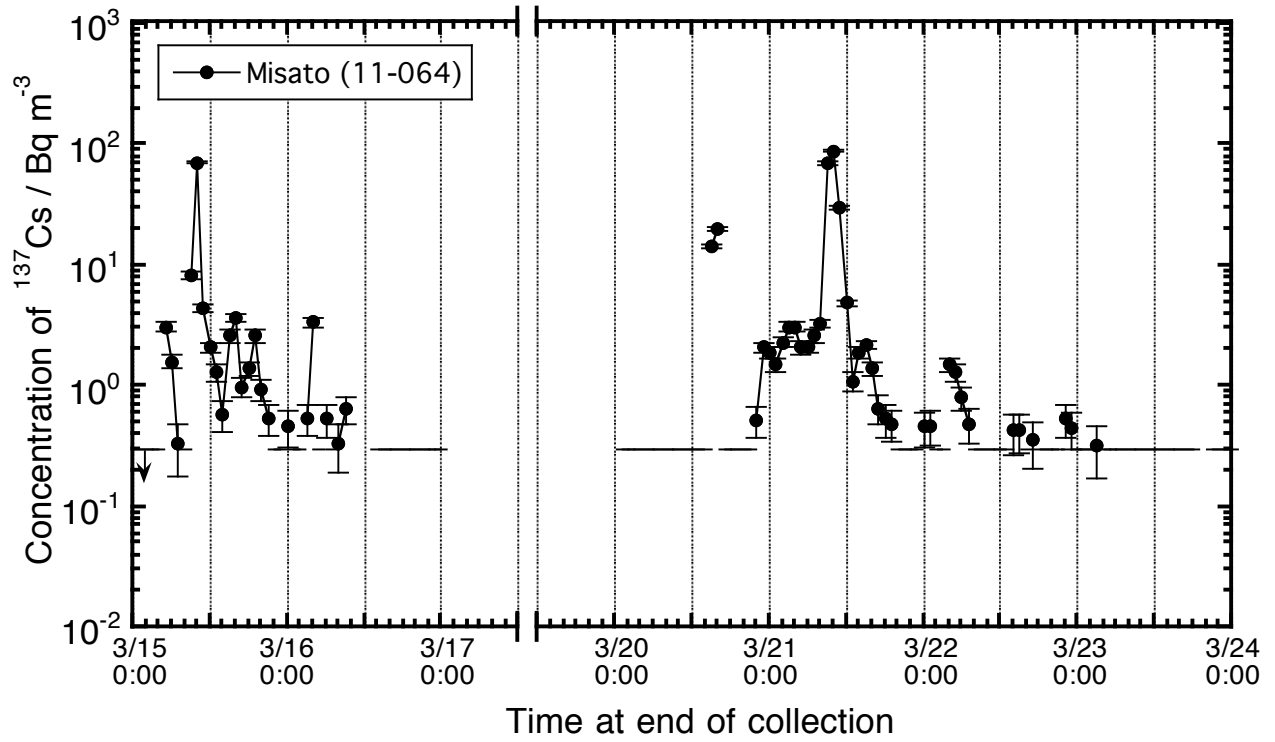


Figure B50. Time series variation of atmospheric  $^{137}\text{Cs}$  concentration observed at Misato station (11-064) in Misato-shi, Saitama.

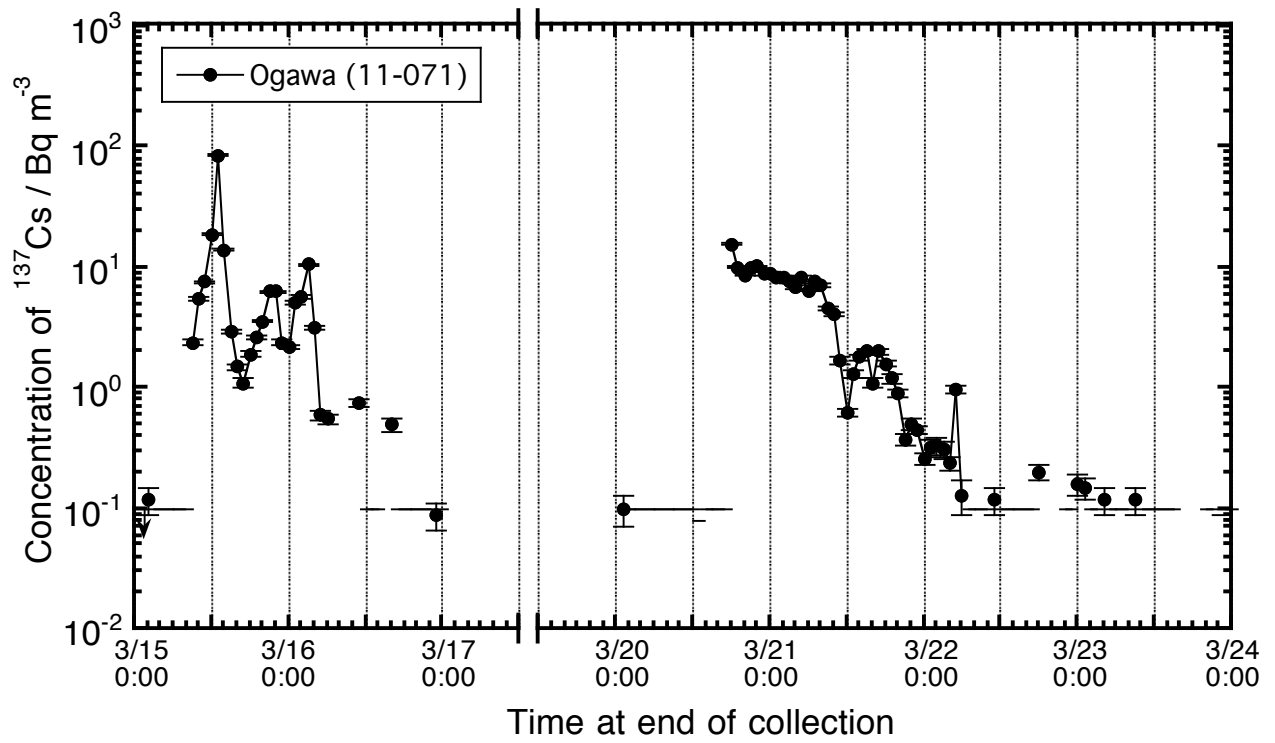


Figure B51. Time series variation of atmospheric  $^{137}\text{Cs}$  concentration observed at Ogawa station (11-071) in Ogawa-machi,

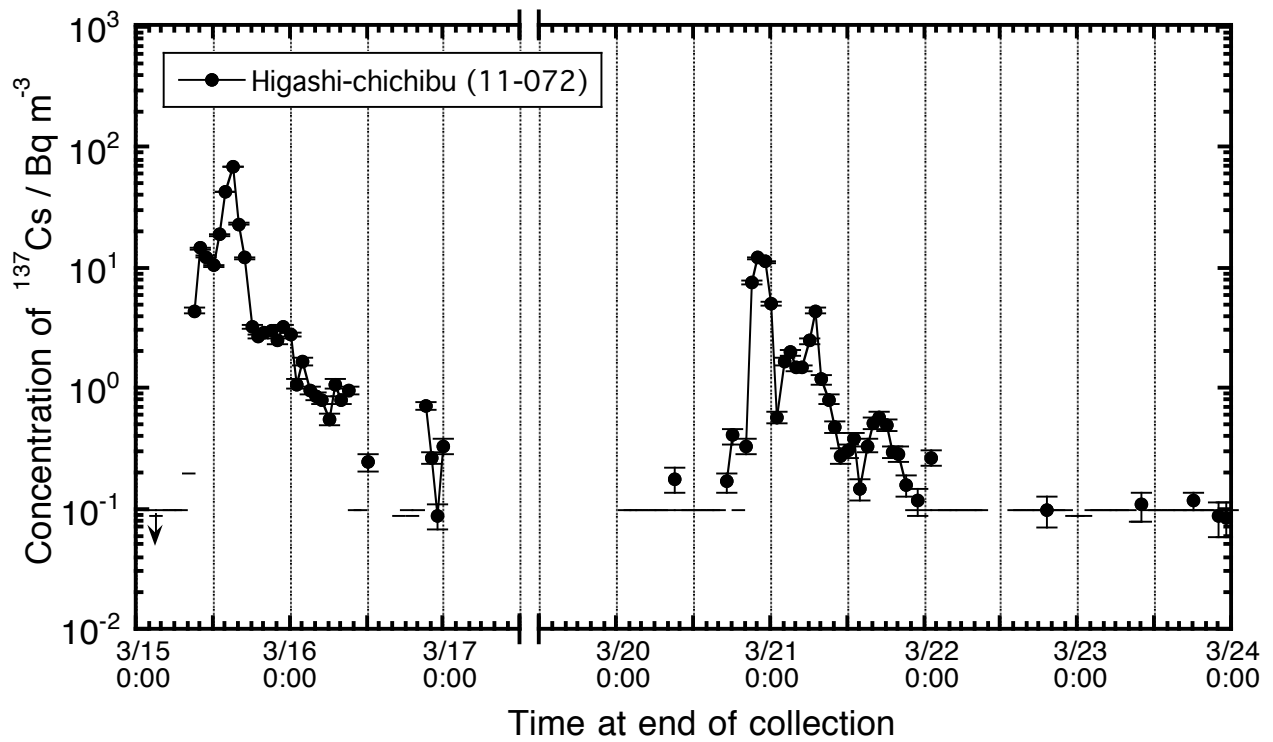


Figure B52. Time series variation of atmospheric  $^{137}\text{Cs}$  concentration observed at Higashi-chichibu station (11-072) in Higashichichibu-mura, Saitama.

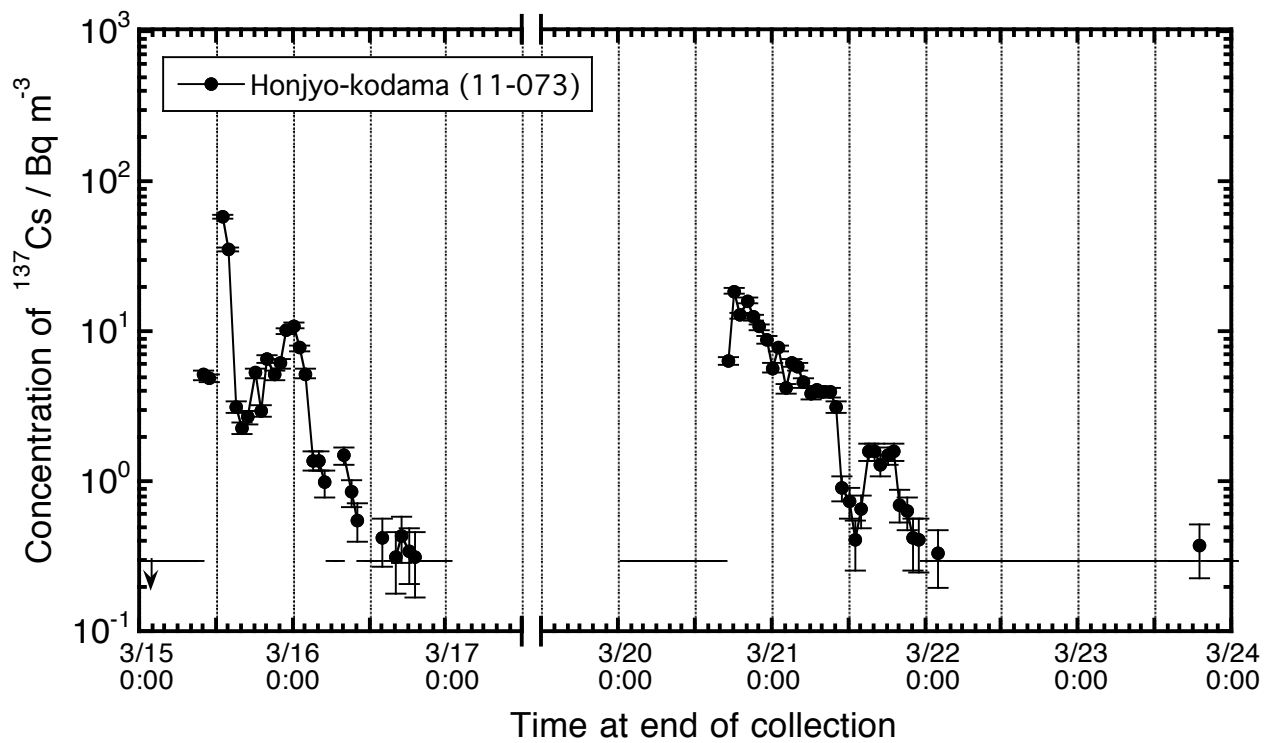


Figure B53. Time series variation of atmospheric  $^{137}\text{Cs}$  concentration observed at Honjyo-kodama station (11-073) in Honjyo-shi, Saitama.

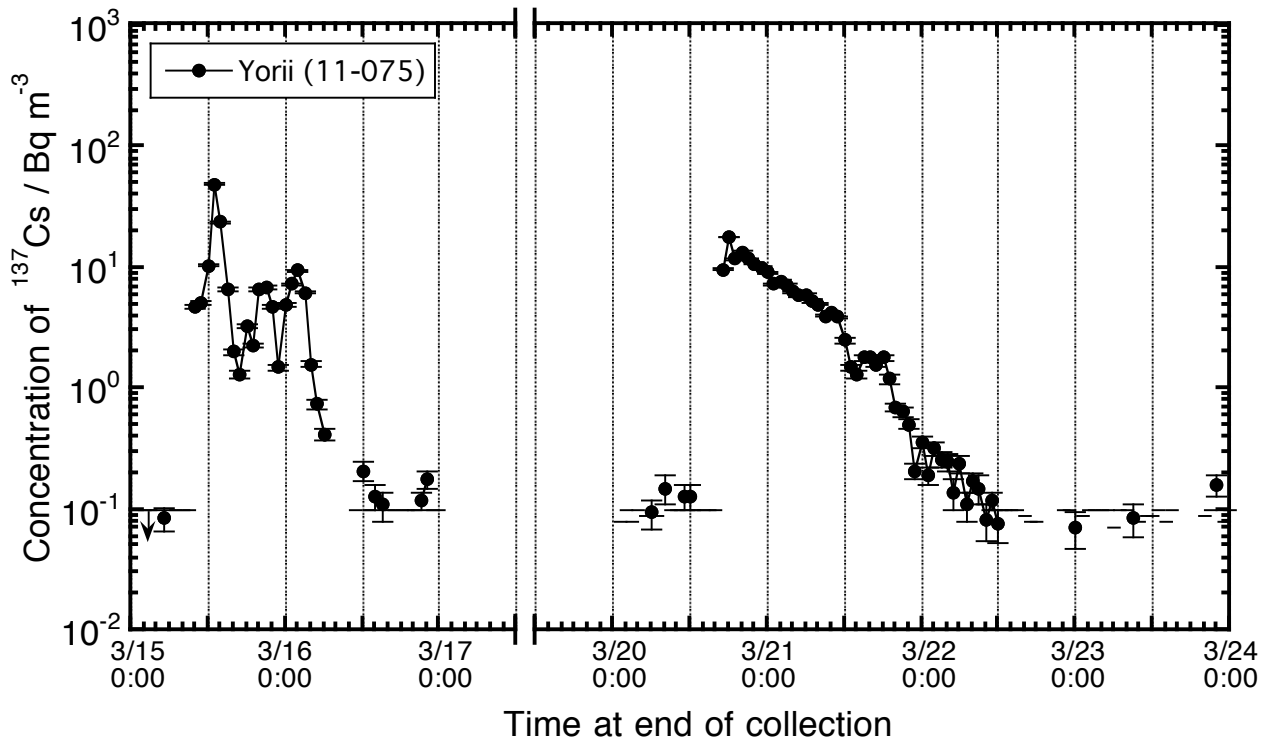


Figure B54. Time series variation of atmospheric  $^{137}\text{Cs}$  concentration observed at Yorii station (11-075) in Yorii-machi, Saitama.

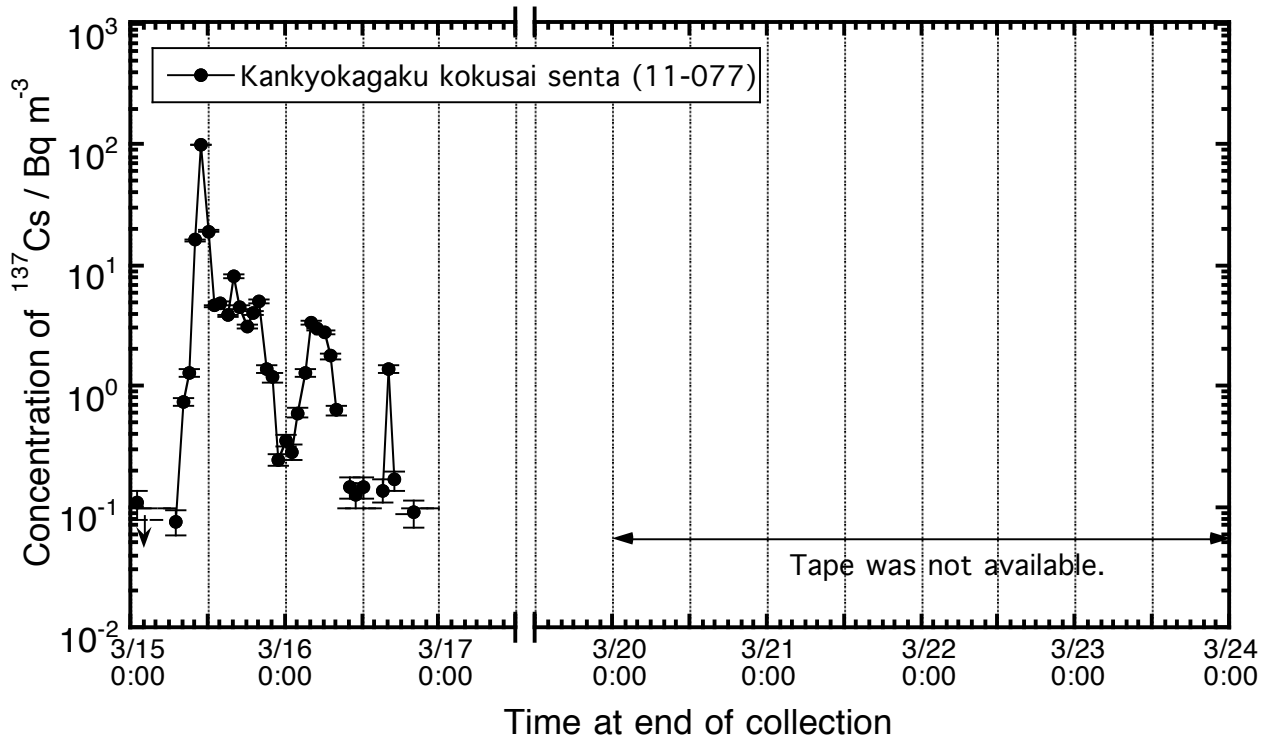


Figure B55. Time series variation of atmospheric  $^{137}\text{Cs}$  concentration observed at Kankyokagaku kokusai senta (11-077) in Kazo-shi, Saitama. The collection time of March 16 is tentatively identified because the day has only 23 spots.

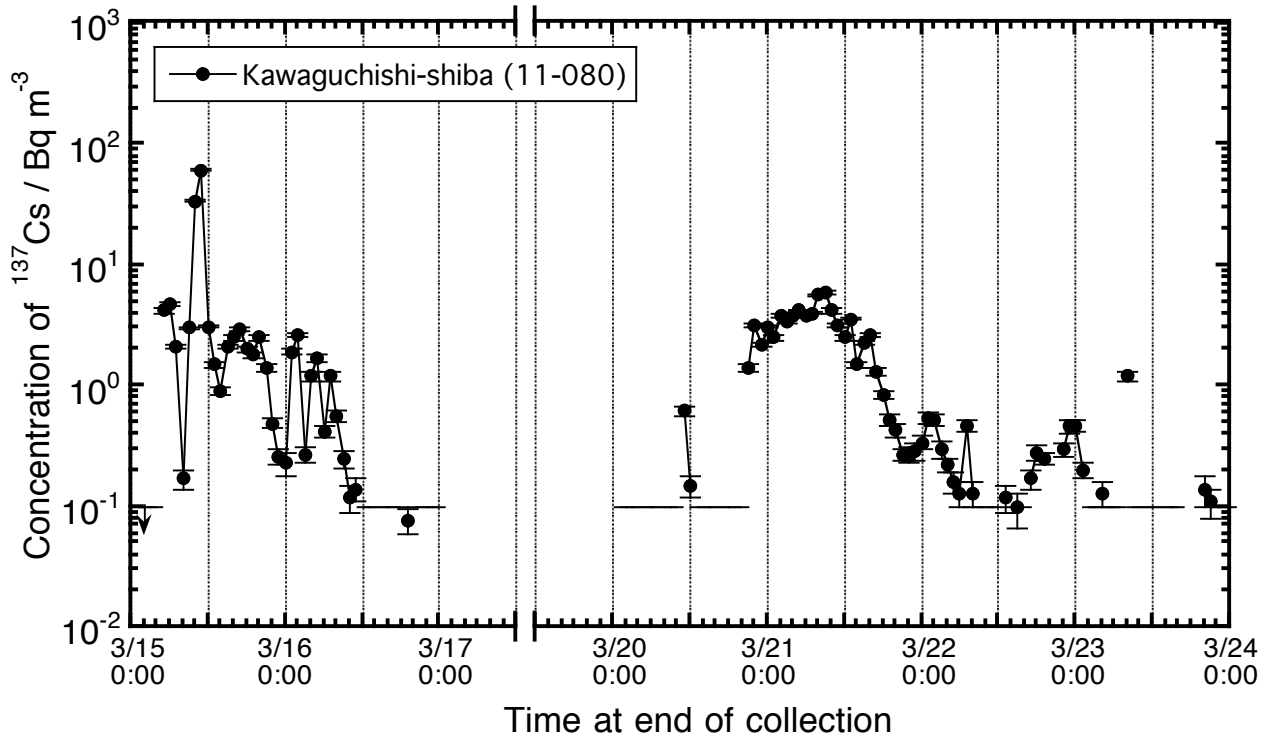


Figure B56. Time series variation of atmospheric  $^{137}\text{Cs}$  concentration observed at Kawaguchishi-shiba station (11-080) in Kawaguchi-shi, Saitama.

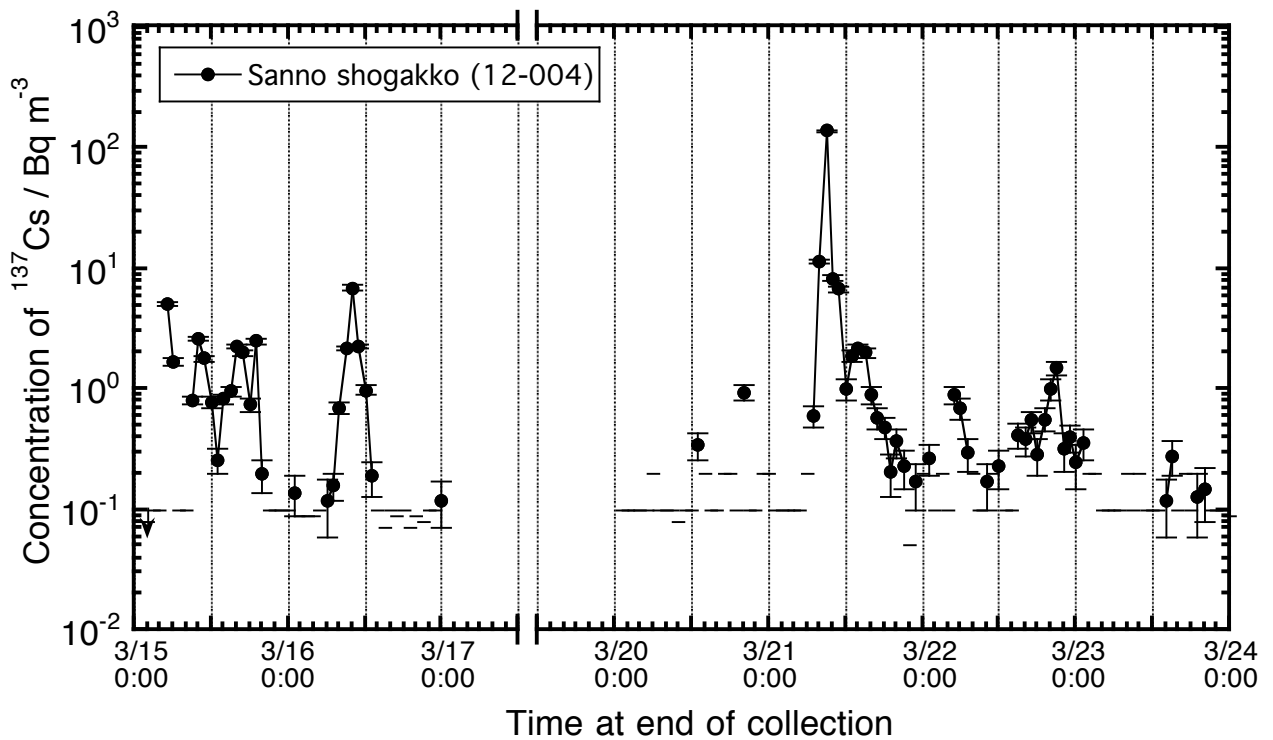


Figure B57. Time series variation of atmospheric  $^{137}\text{Cs}$  concentration observed at Sanno shogakko station (12-004) in Chiba-shi, Chiba.



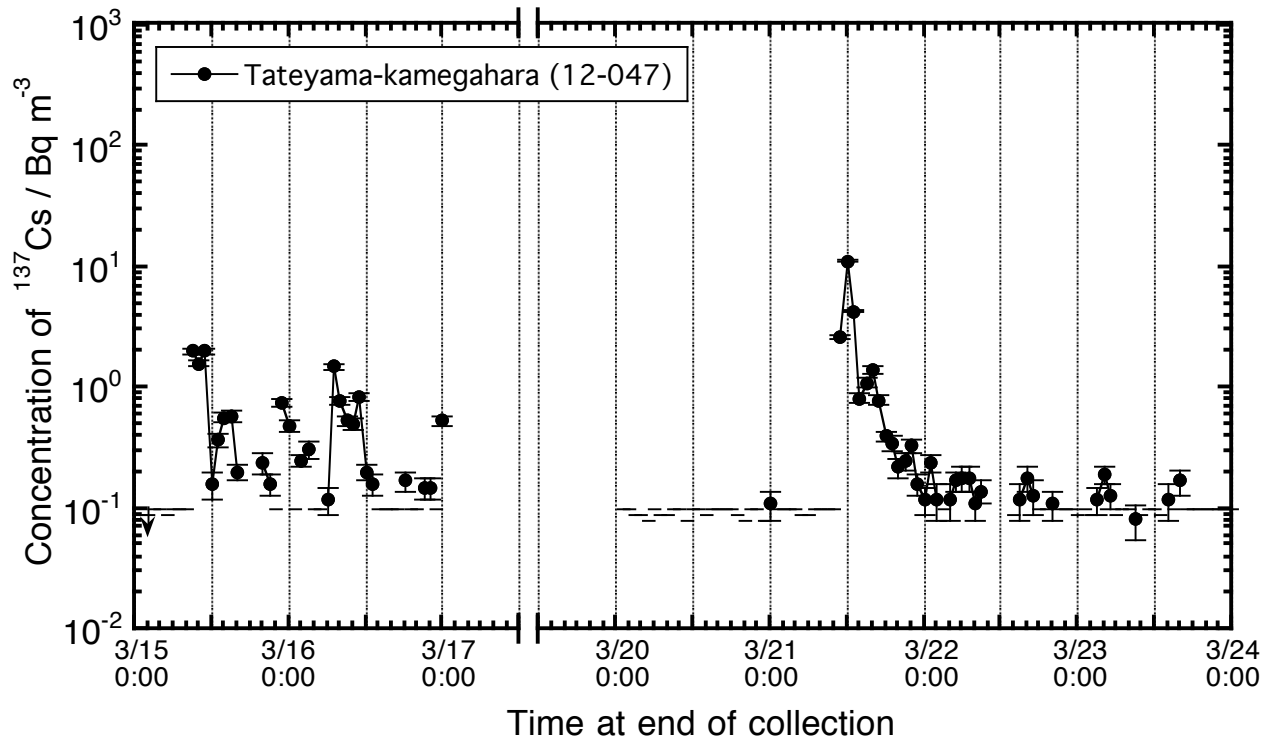


Figure B60. Time series variation of atmospheric  $^{137}\text{Cs}$  concentration observed at Tateyama-kamegahara station (12-047) in Tateyama-shi, Chiba.

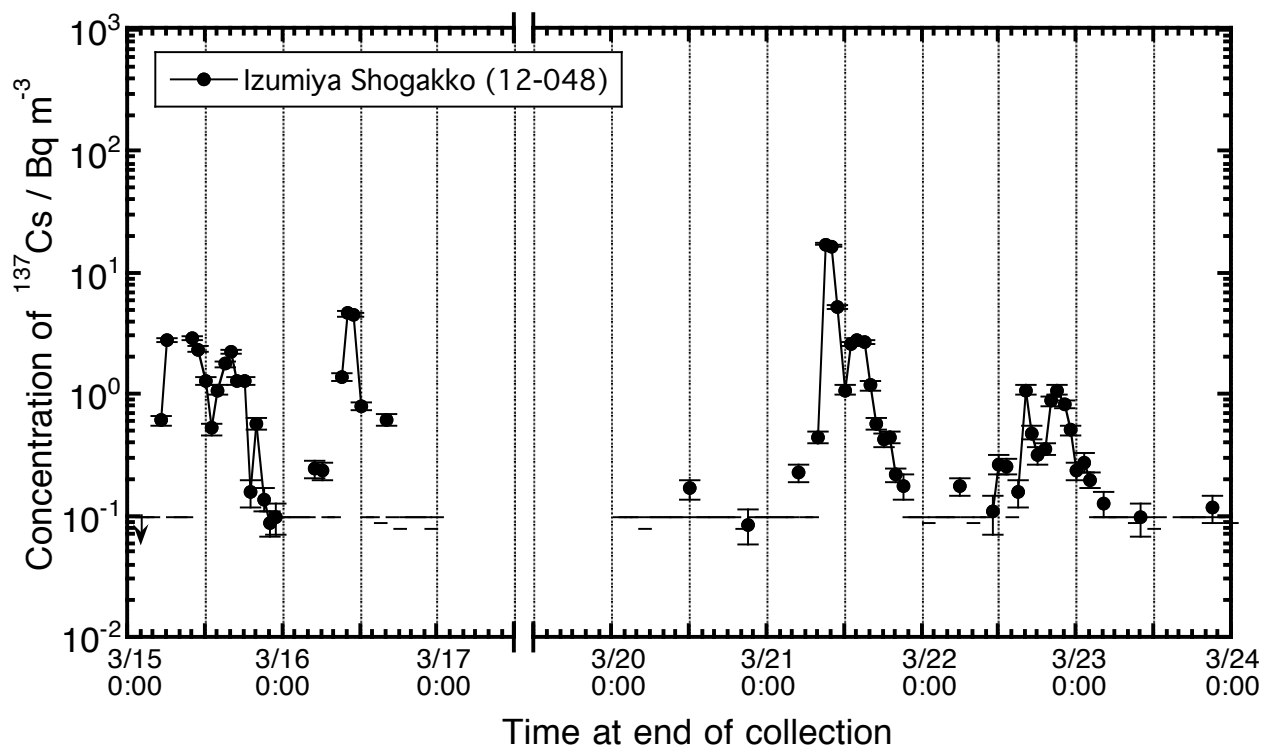


Figure B61. Time series variation of atmospheric  $^{137}\text{Cs}$  concentration observed at Izumiya shogakko station (12-048) in Chiba-shi, Chiba.

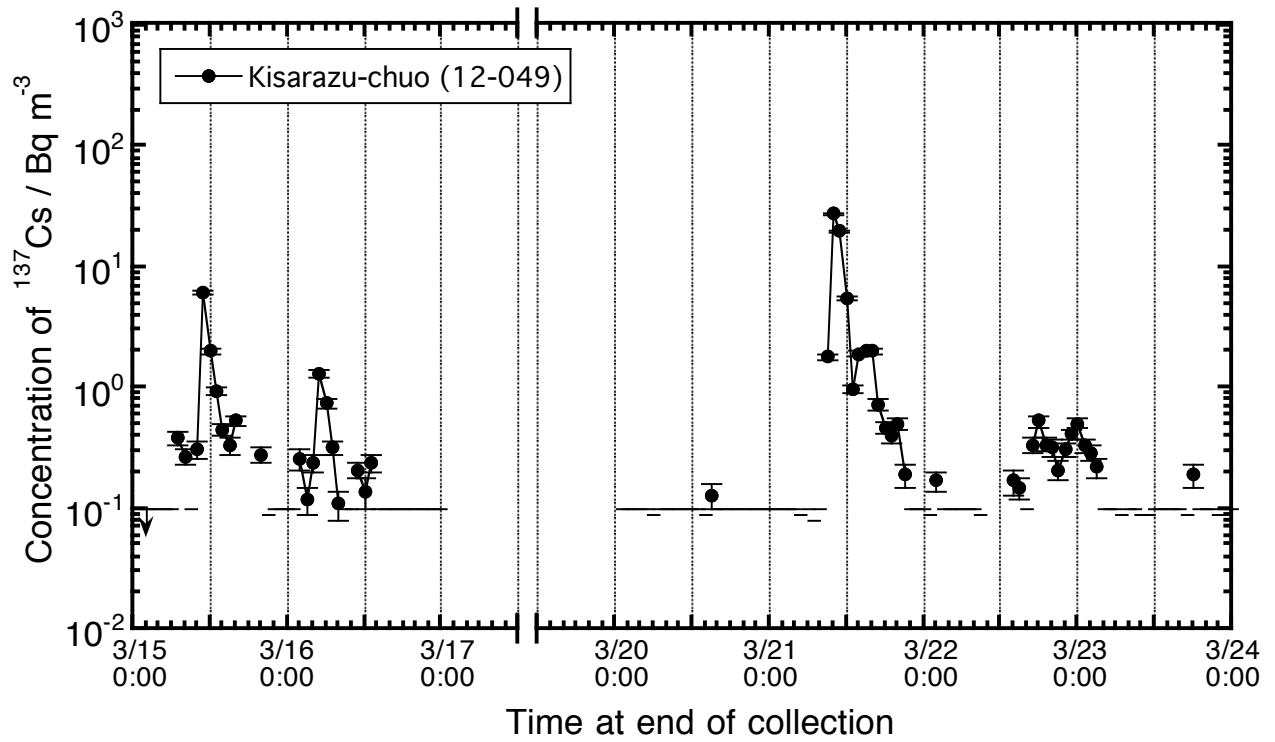


Figure B62. Time series variation of atmospheric  $^{137}\text{Cs}$  concentration observed at Kisarazu-chuo station (12-049) in Kisarazu-shi, Chiba.

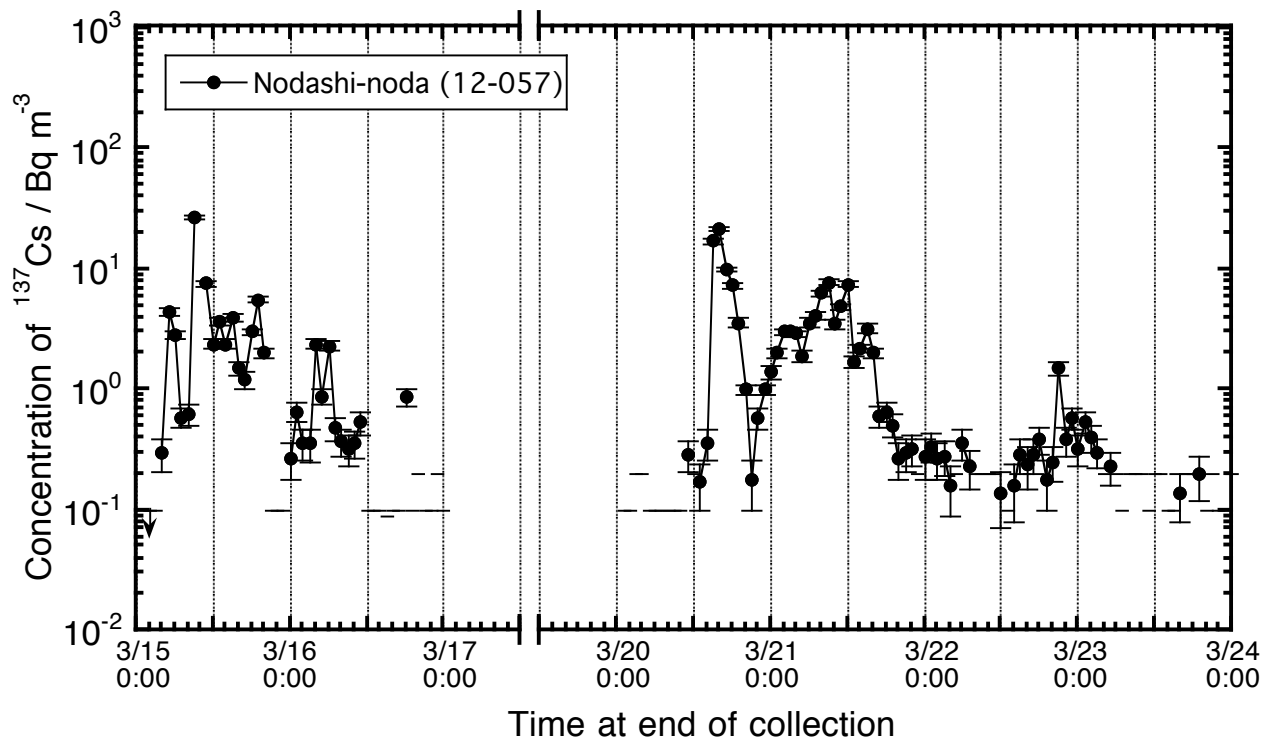


Figure B63. Time series variation of atmospheric  $^{137}\text{Cs}$  concentration observed at Nodashi-noda station (12-057) in Noda-shi, Chiba.



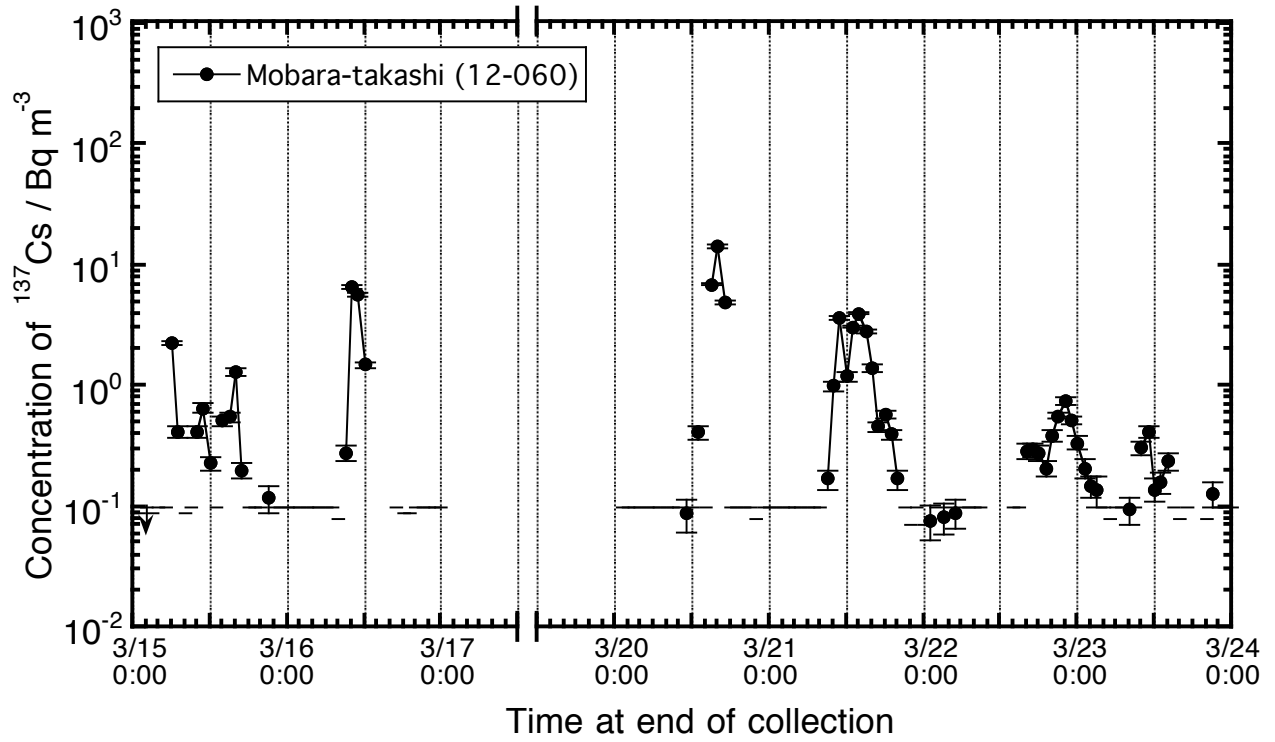


Figure B64. Time series variation of atmospheric  $^{137}\text{Cs}$  concentration observed at Mobaratakasashi station (12-060) in Mobaratakasashi, Chiba.

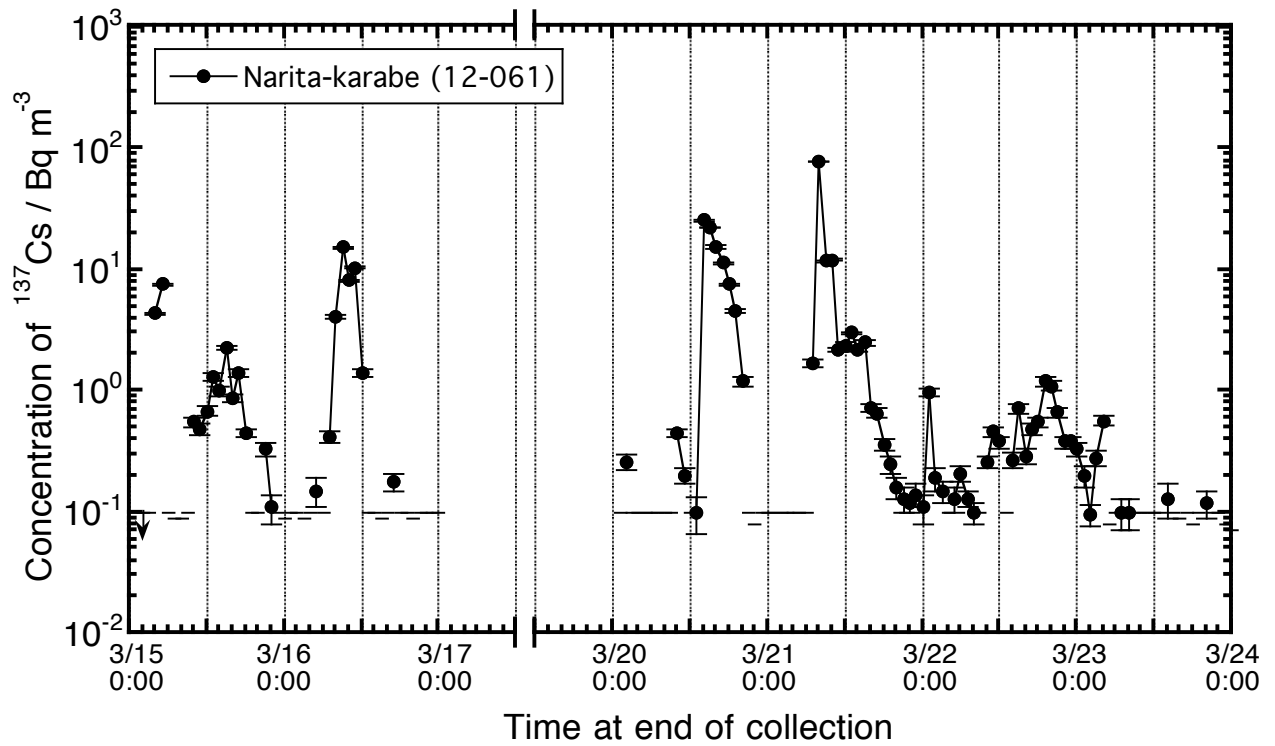


Figure B65. Time series variation of atmospheric  $^{137}\text{Cs}$  concentration observed at Naritakarabe station (12-061) in Naritakarabe, Chiba.

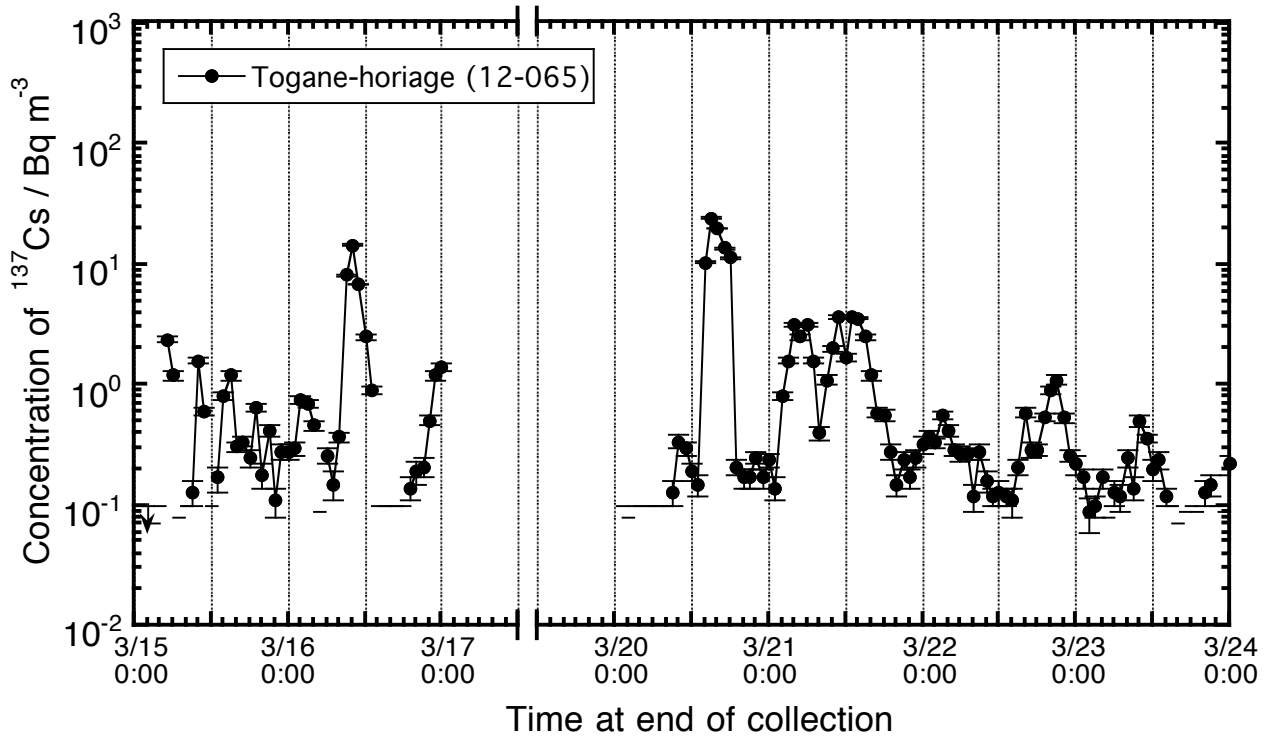


Figure B66. Time series variation of atmospheric  $^{137}\text{Cs}$  concentration observed at Togane-horiage station (12-065) in Togane-shi, Chiba.

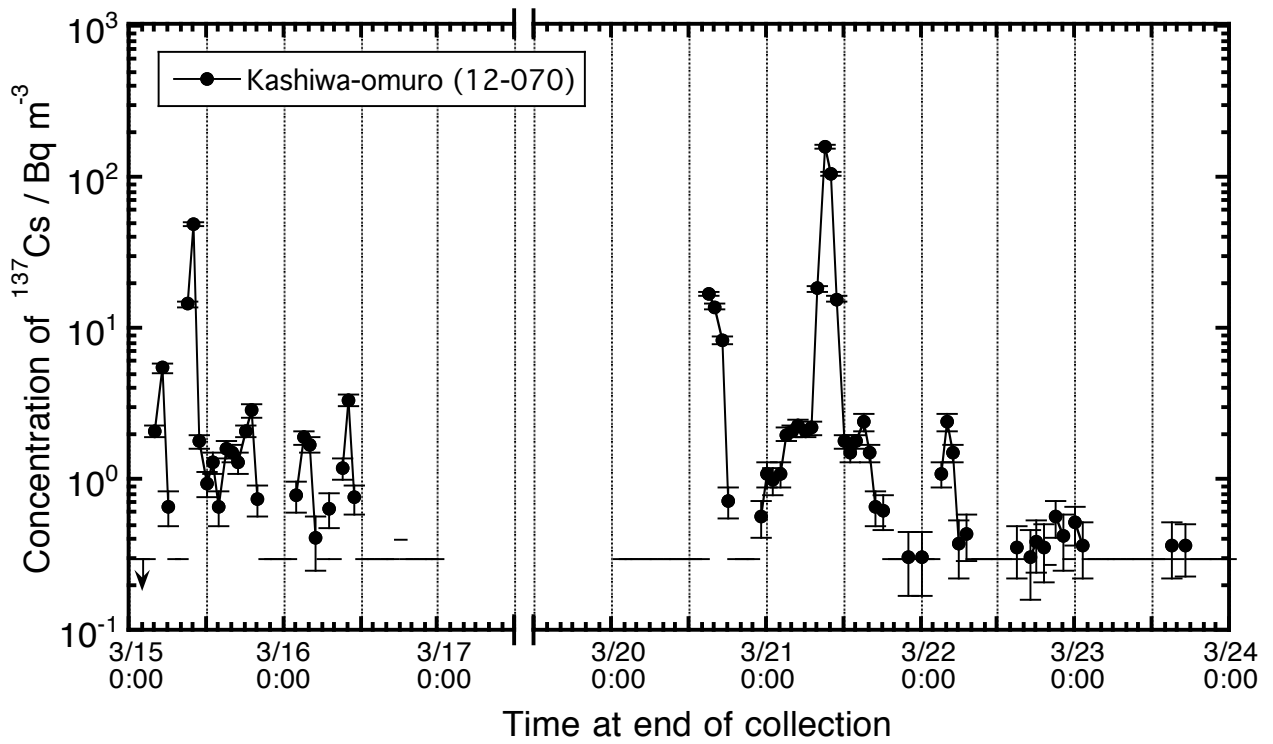


Figure B67. Time series variation of atmospheric  $^{137}\text{Cs}$  concentration observed at Kashiwa-omuro station (12-070) in Kashiwa-shi, Chiba.

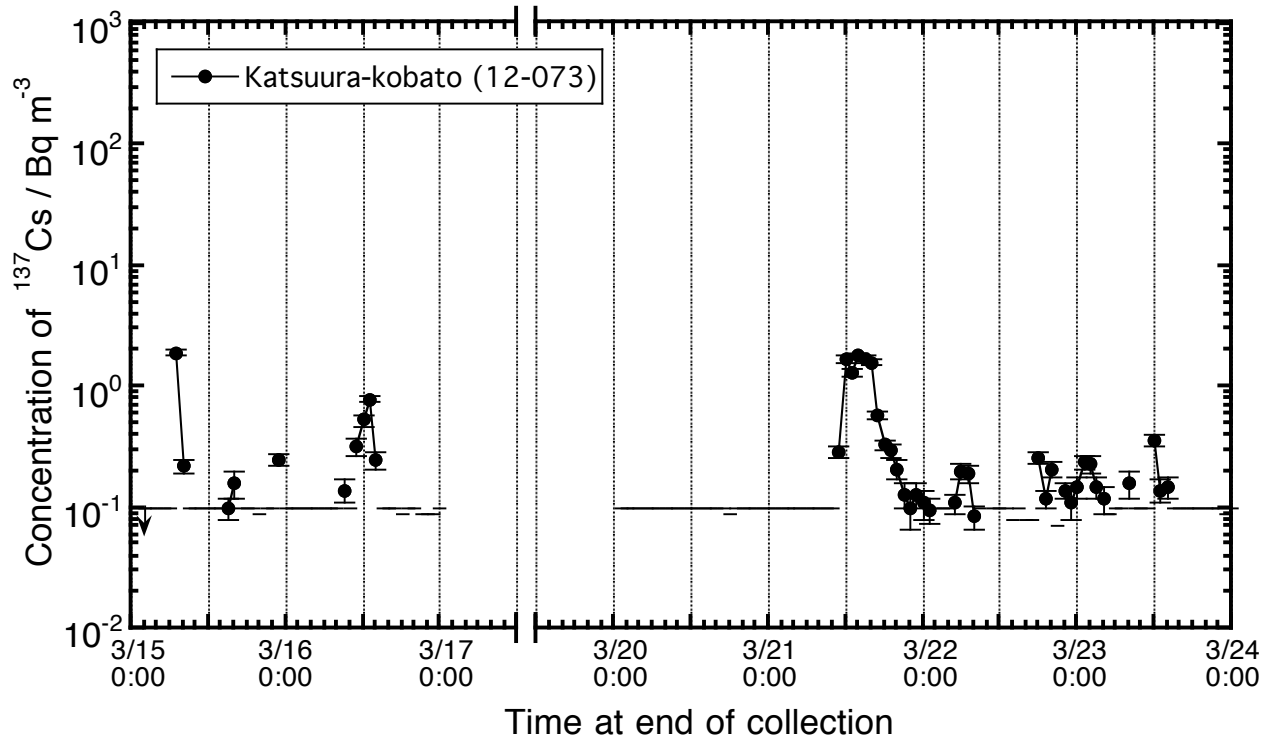


Figure B68. Time series variation of atmospheric  $^{137}\text{Cs}$  concentration observed at Katsuura-kobato station (12-073) in Katsuura-shi, Chiba.

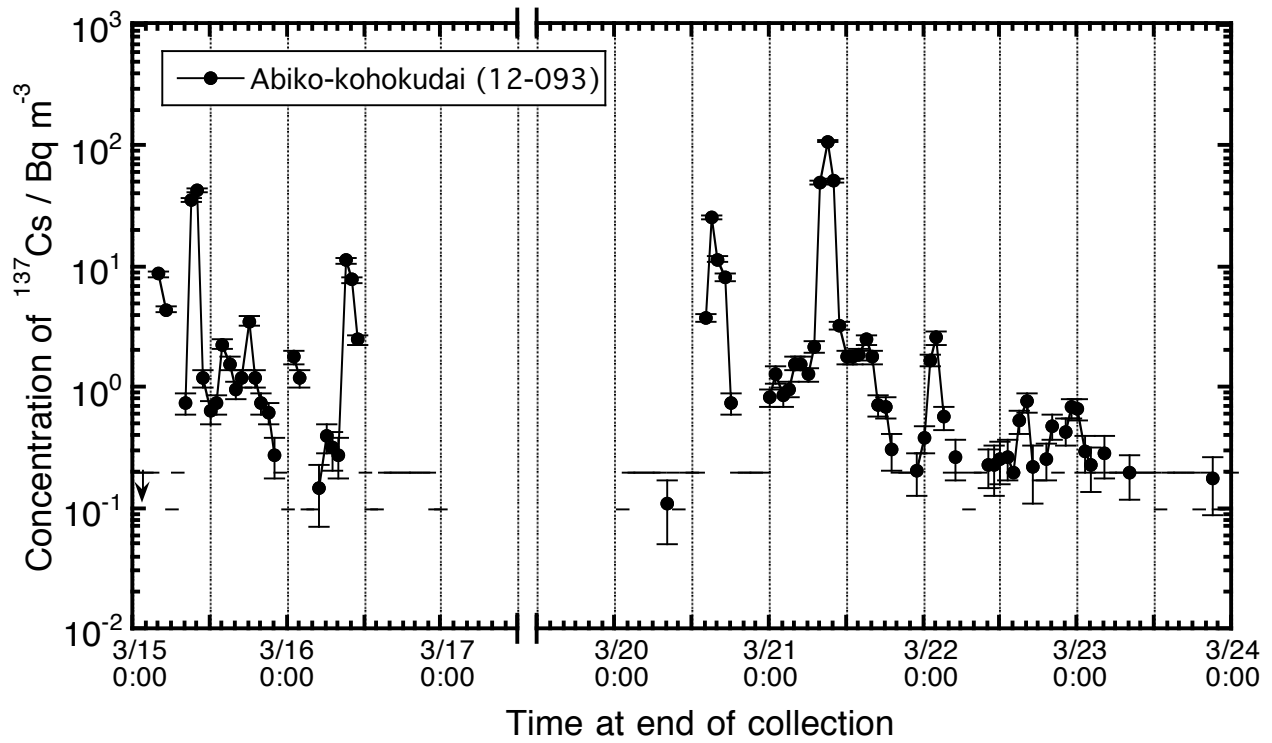


Figure B69. Time series variation of atmospheric  $^{137}\text{Cs}$  concentration observed at Abiko-kohokudai station (12-093) in Abiko-shi, Chiba.

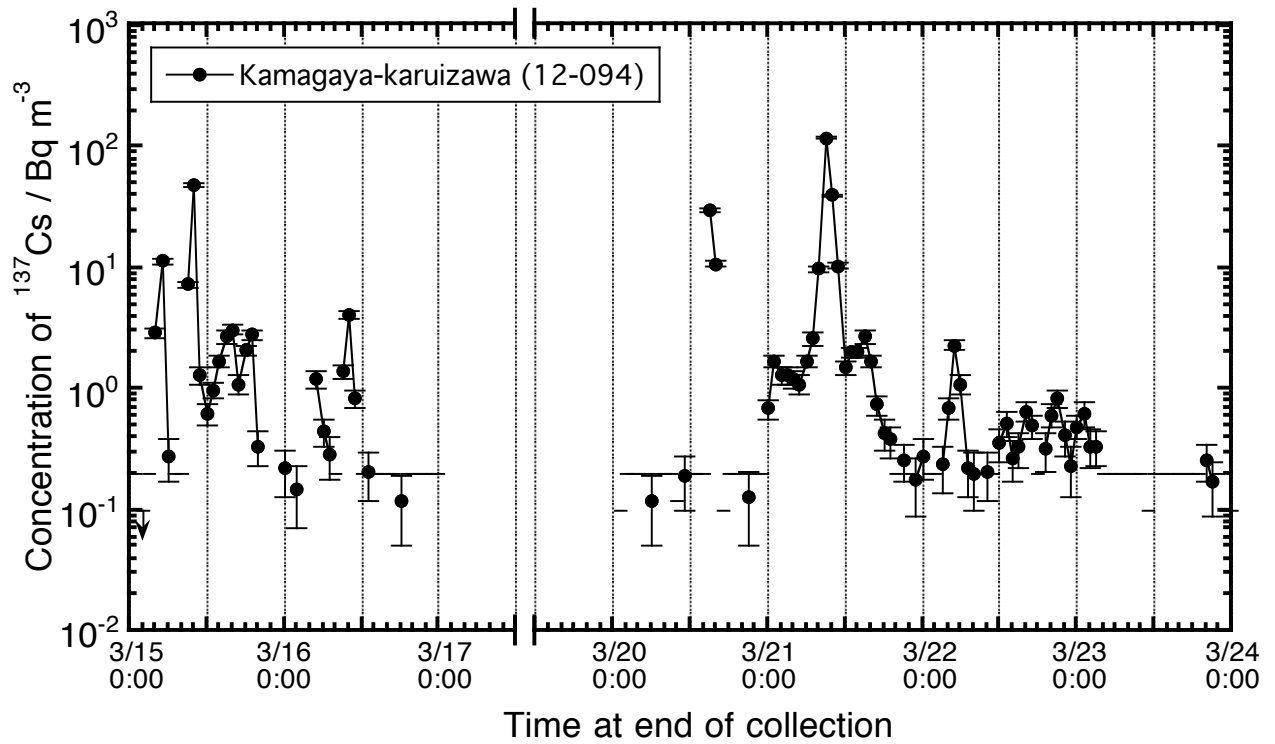


Figure B70. Time series variation of atmospheric  $^{137}\text{Cs}$  concentration observed at Kamagaya-karuizawa station (12-094) in Kamagaya-shi, Chiba.

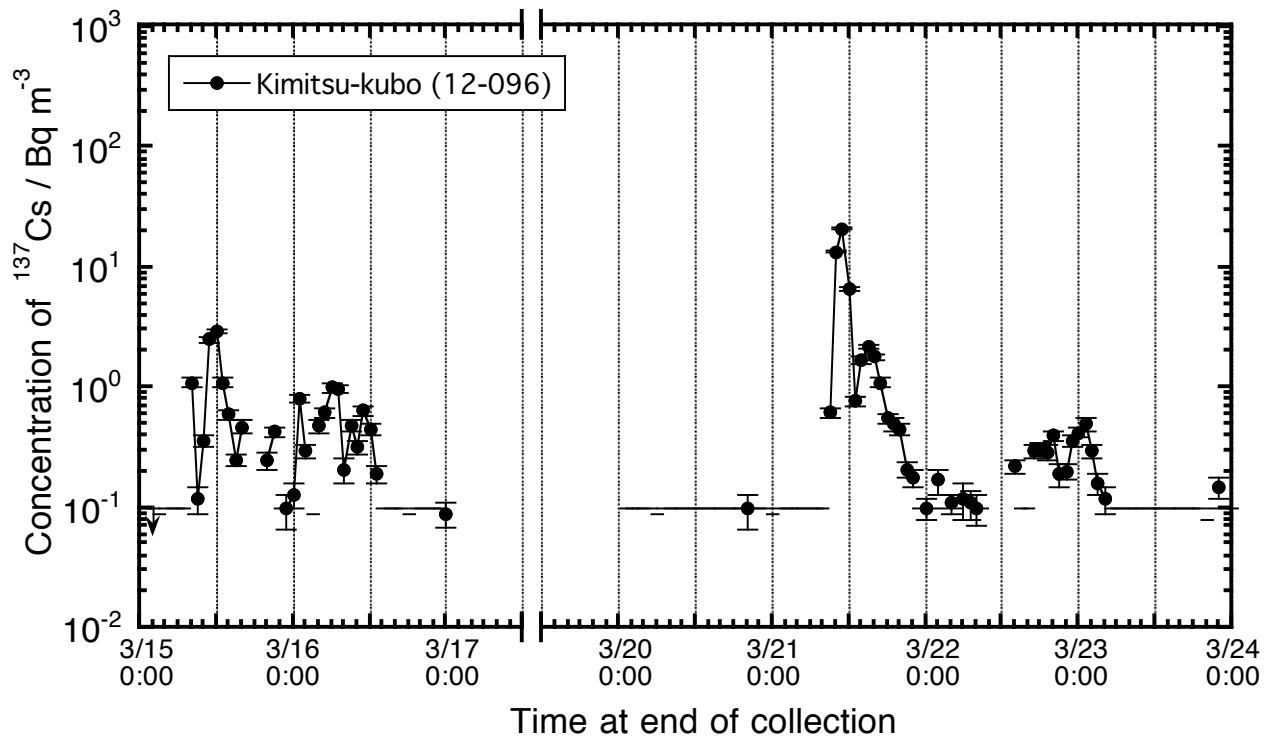


Figure B71. Time series variation of atmospheric  $^{137}\text{Cs}$  concentration observed at Kimitsu-kubo station (12-096) in Kimitsu-shi, Chiba.

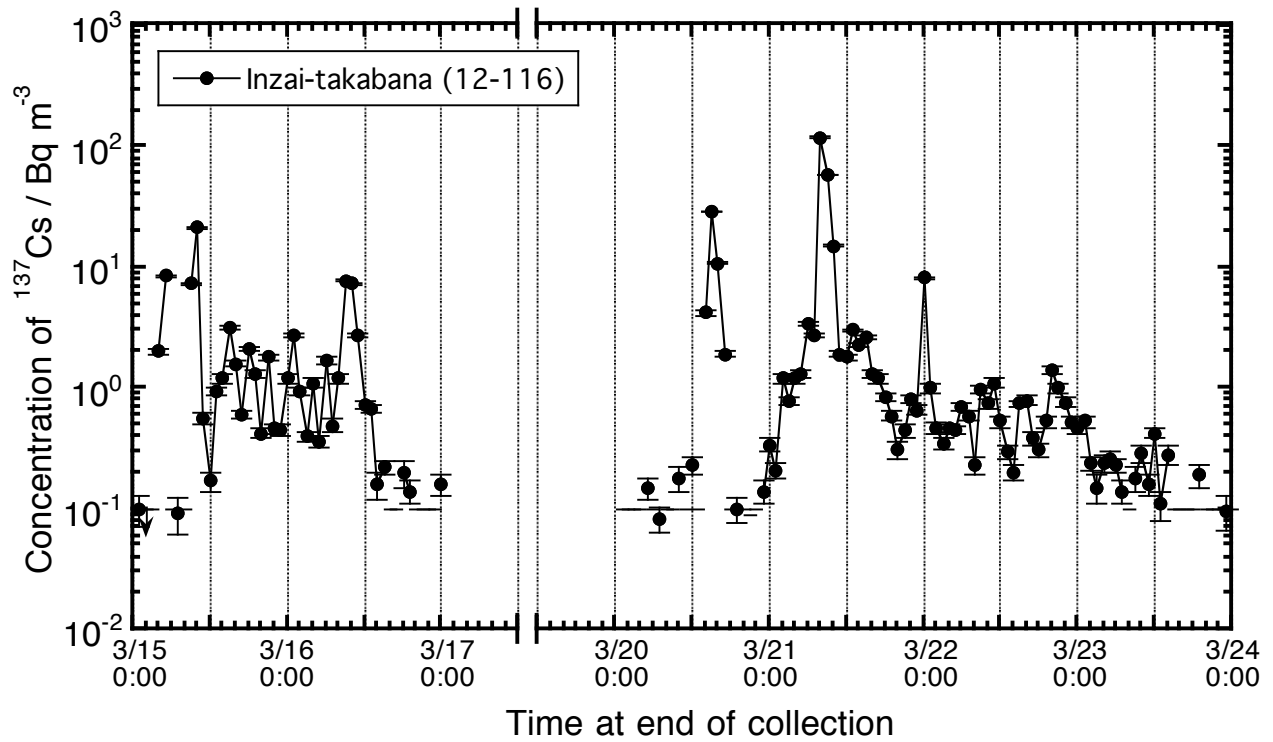


Figure B72. Time series variation of atmospheric  $^{137}\text{Cs}$  concentration observed at Inzai-takabana station (12-116) in Inzai-shi, Chiba.

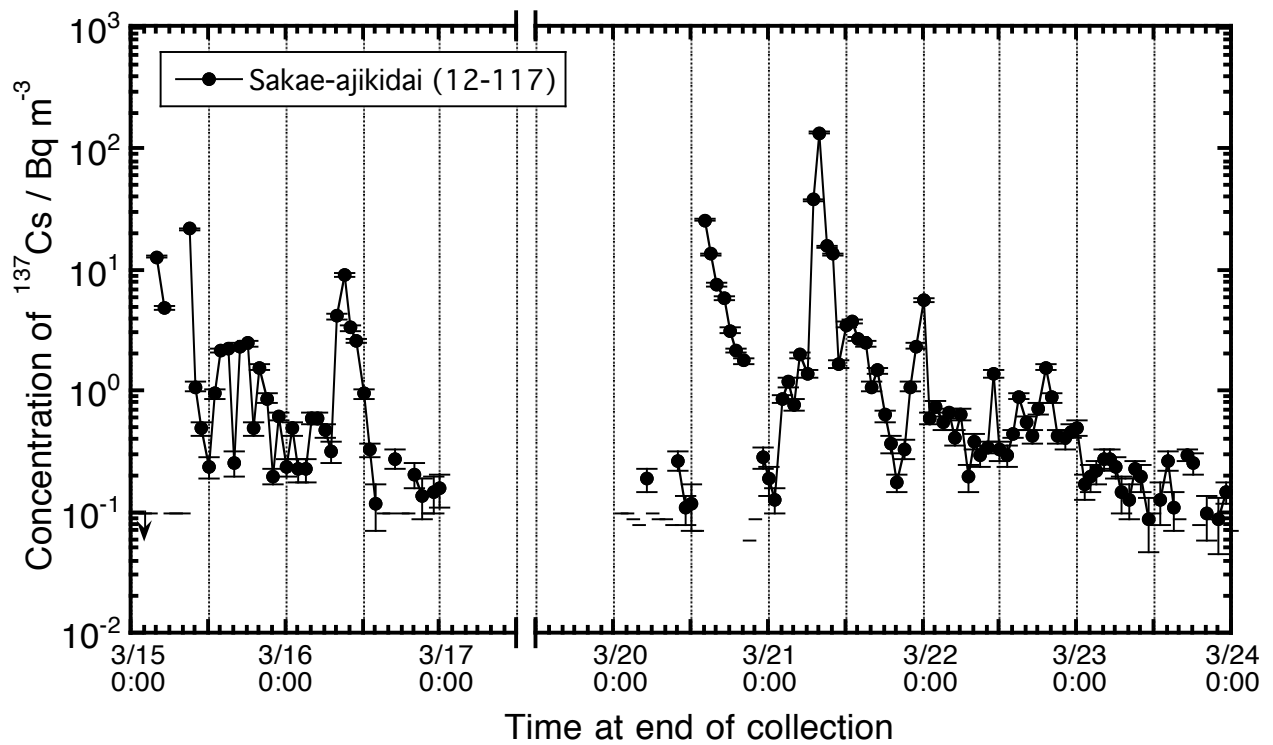


Figure B73. Time series variation of atmospheric  $^{137}\text{Cs}$  concentration observed at Sakae-ajikidai station (12-117) in Sakae-machi, Chiba.

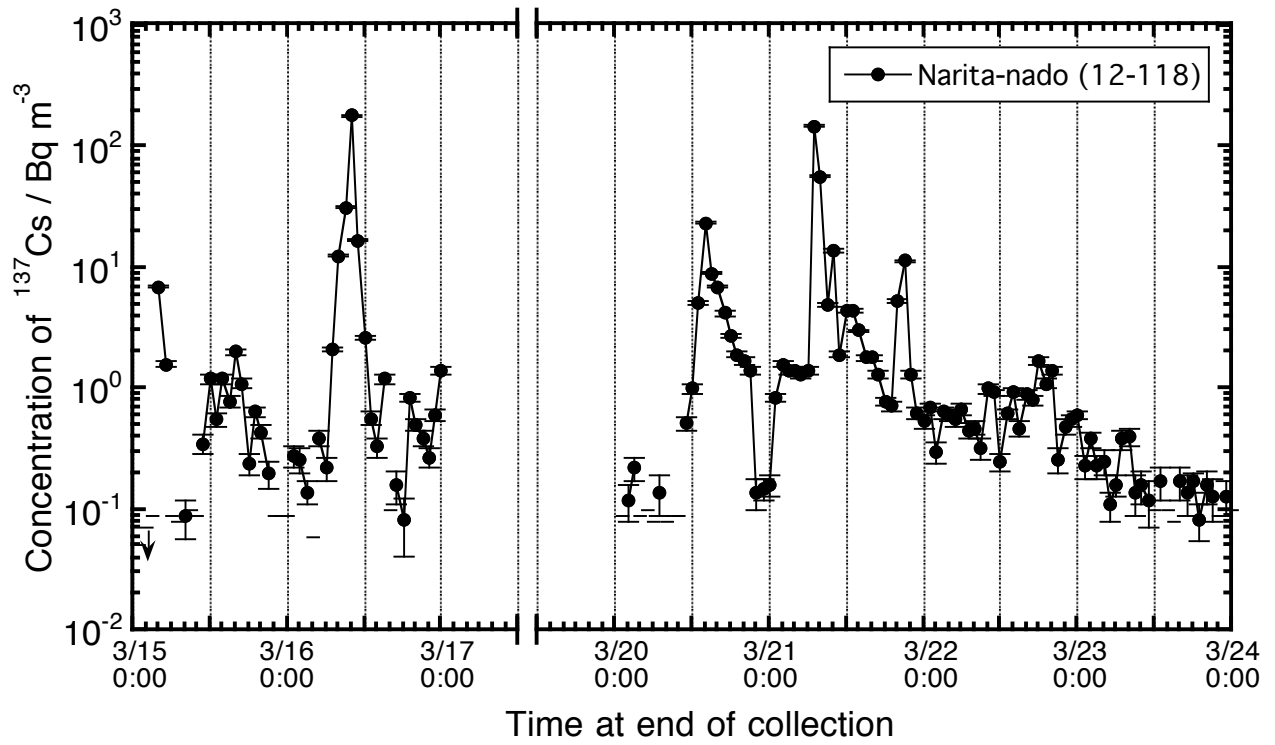


Figure B74. Time series variation of atmospheric  $^{137}\text{Cs}$  concentration observed at Narita-nado station (12-118) in Narita-shi, Chiba.

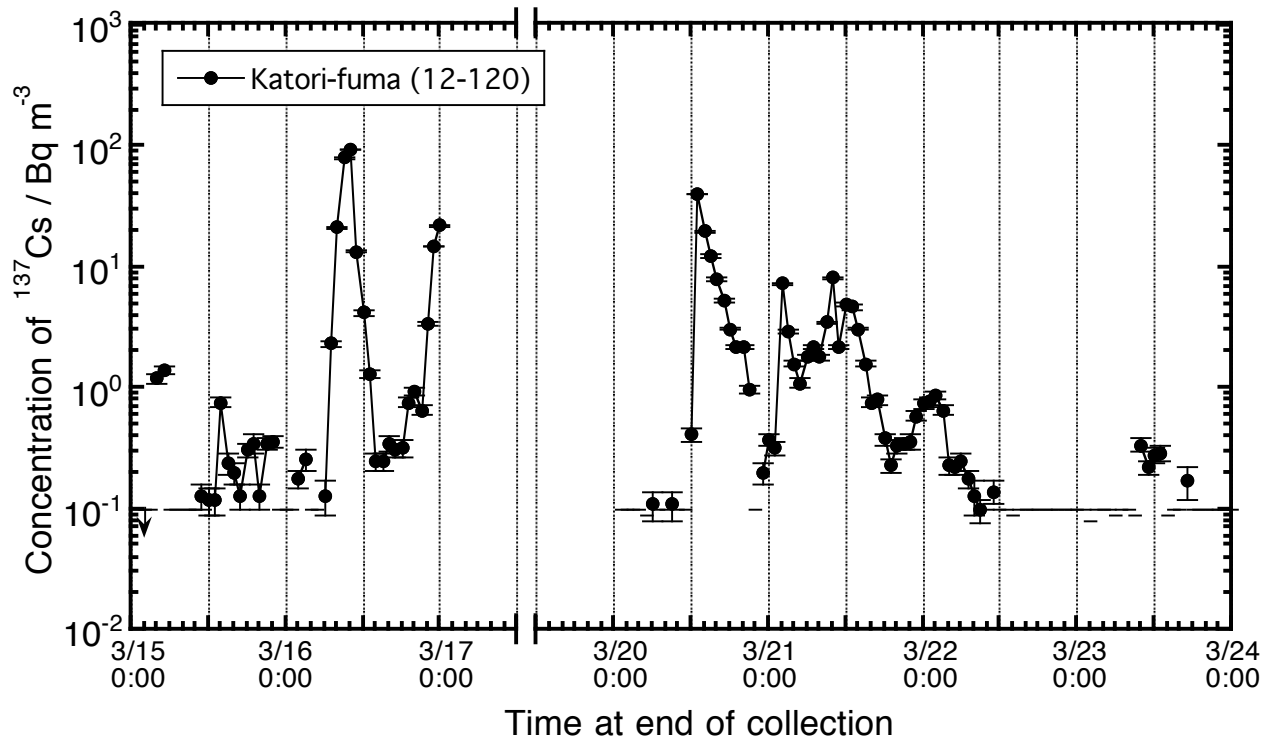


Figure B75. Time series variation of atmospheric  $^{137}\text{Cs}$  concentration observed at Katori-fuma station (12-120) in Katori-shi, Chiba.

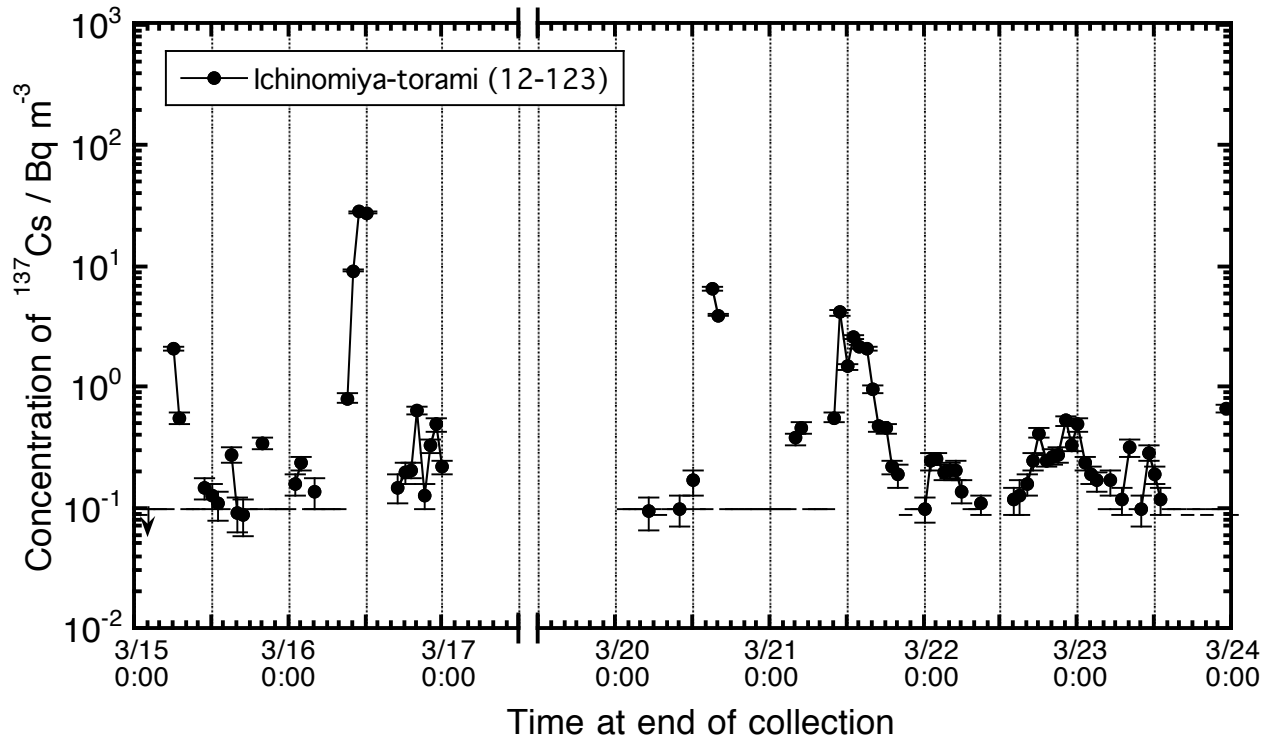


Figure B76. Time series variation of atmospheric  $^{137}\text{Cs}$  concentration observed at Ichinomiya-torami station (12-123) in Ichinomiya-machi, Chiba.

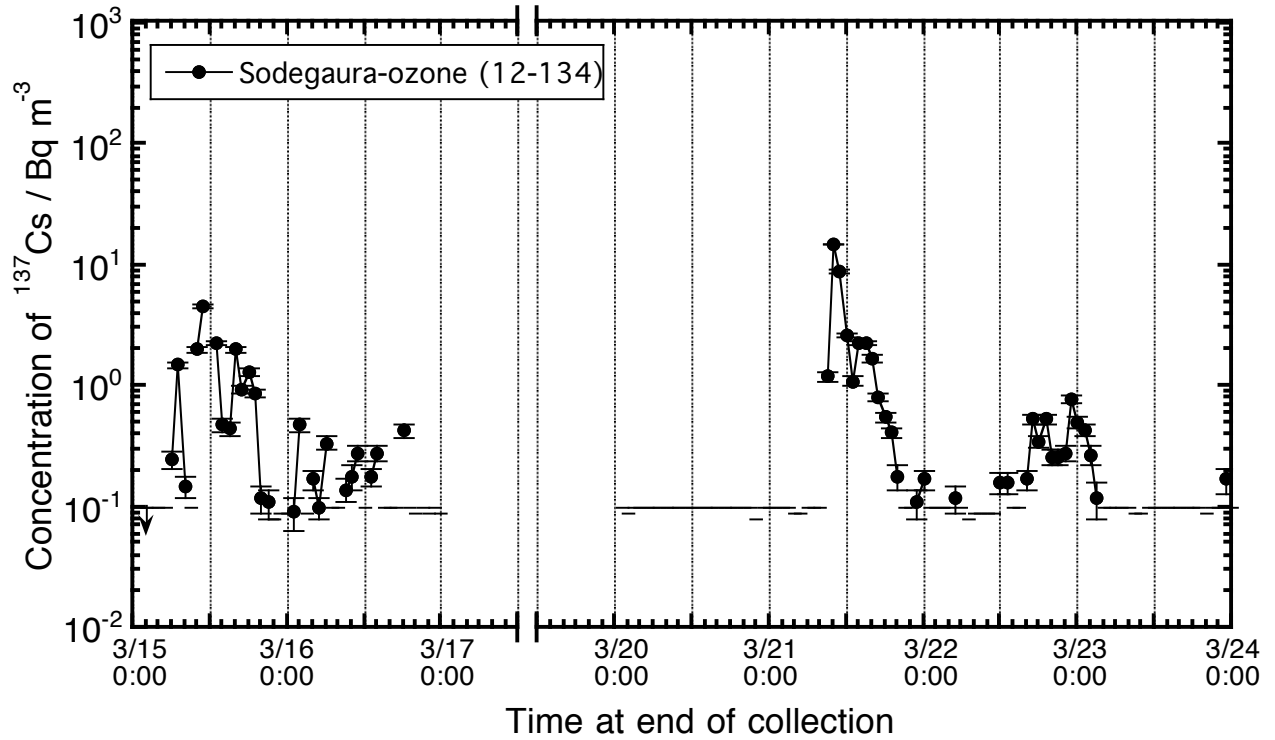


Figure B77. Time series variation of atmospheric  $^{137}\text{Cs}$  concentration observed at Sodegaura-ozone station (12-134) in Sodegaura-shi, Chiba.

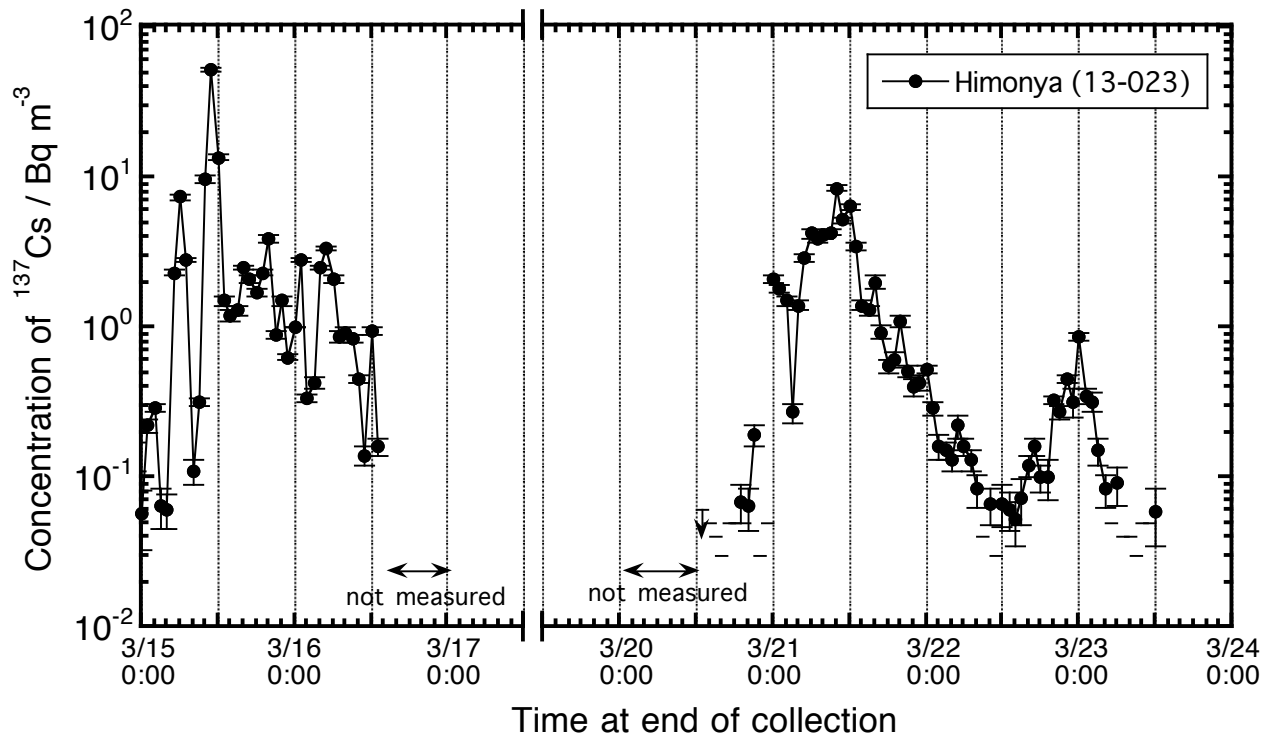


Figure B78. Time series variation of atmospheric  $^{137}\text{Cs}$  concentration observed at Himonya station (13-023) in Meguro-ku, Tokyo.

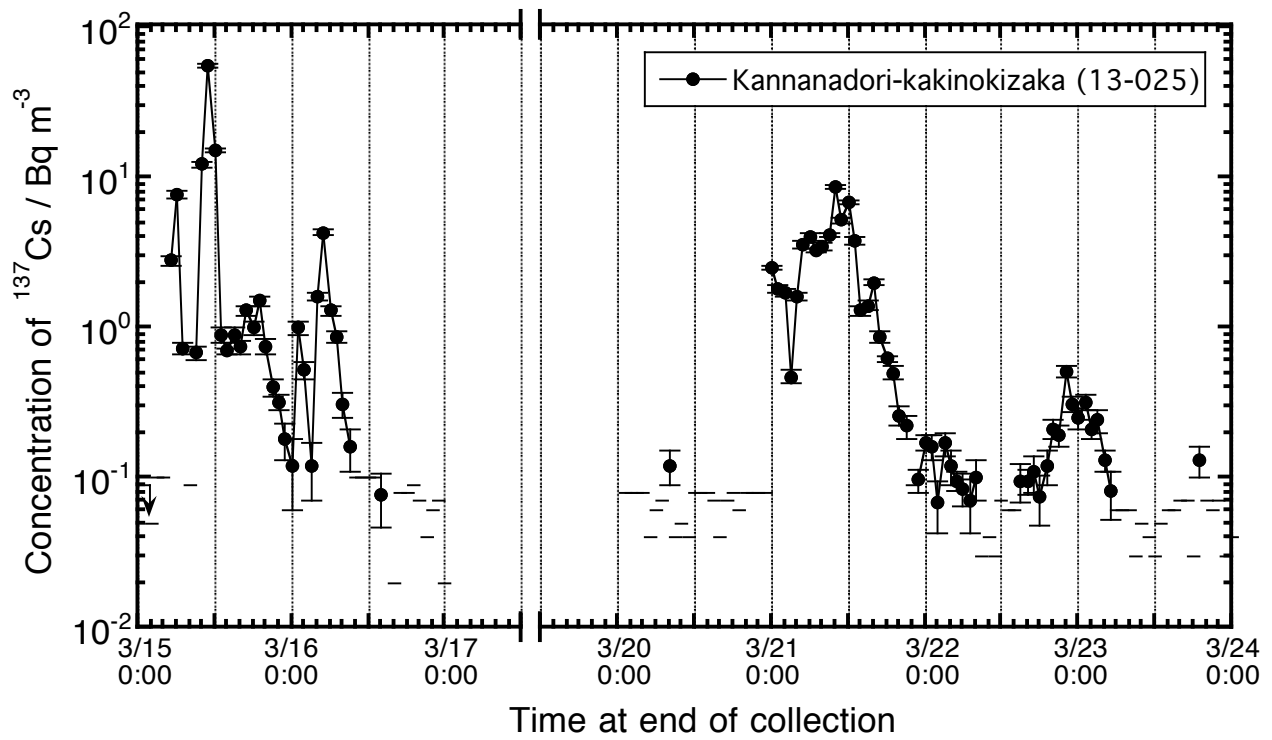


Figure B79. Time series variation of atmospheric  $^{137}\text{Cs}$  concentration observed at Kannanadori-kakinokizaka station (13-025) in Meguro-ku, Tokyo.



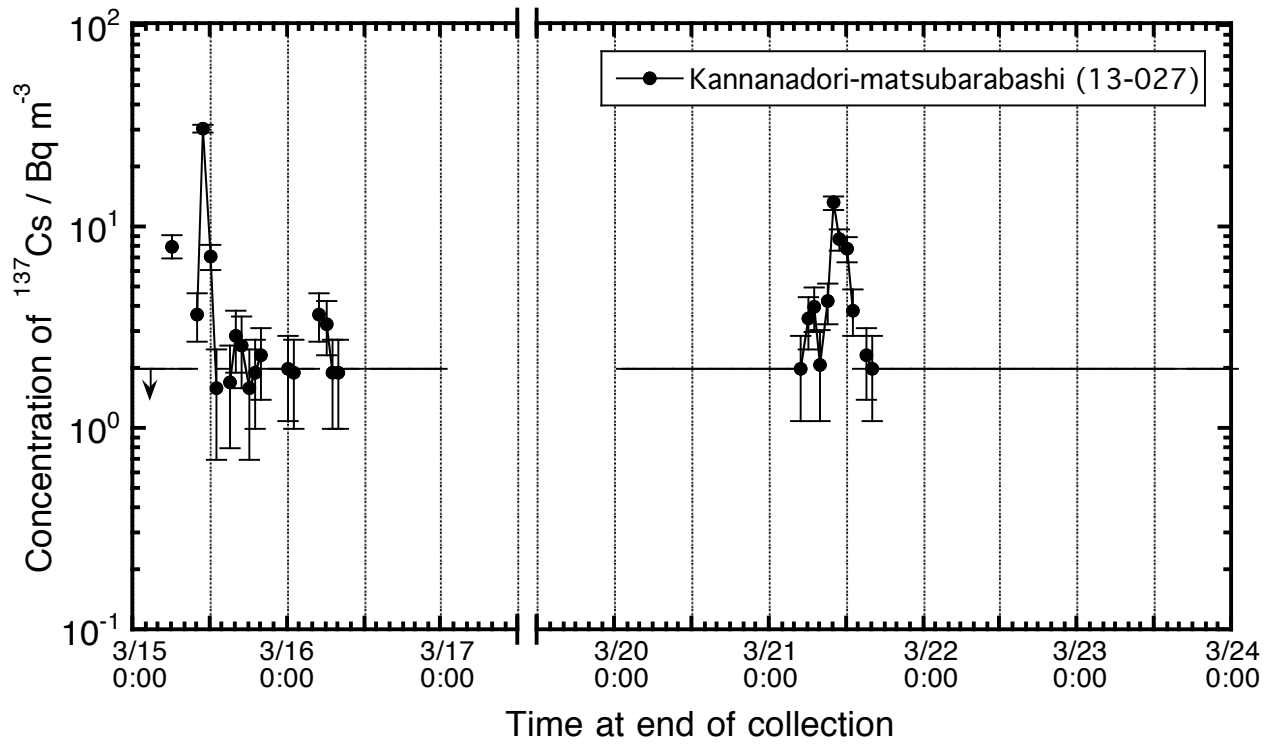


Figure B80. Time series variation of atmospheric  $^{137}\text{Cs}$  concentration observed at Kannadori-matsubarabashi (13-027) in Ota-ku, Tokyo.

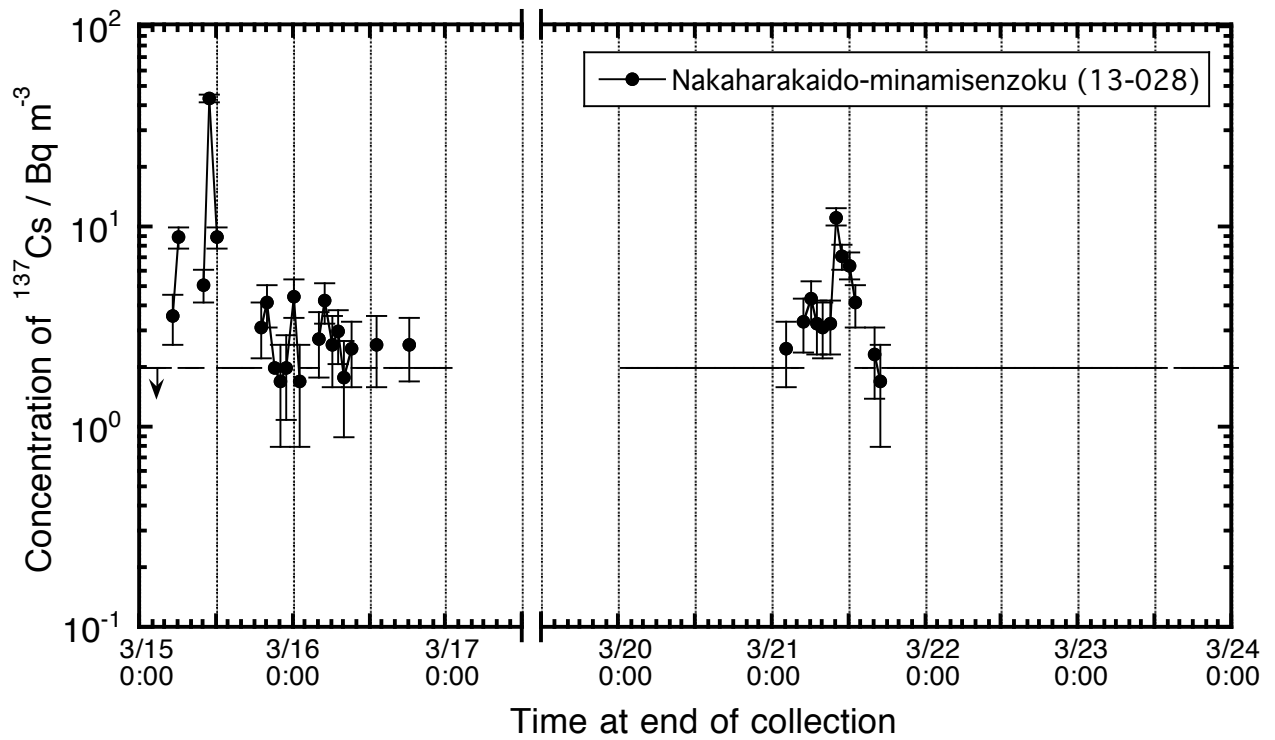


Figure B81. Time series variation of atmospheric  $^{137}\text{Cs}$  concentration observed at Nakaharakaido-minamisenzoku (13-028) in Ota-ku, Tokyo.

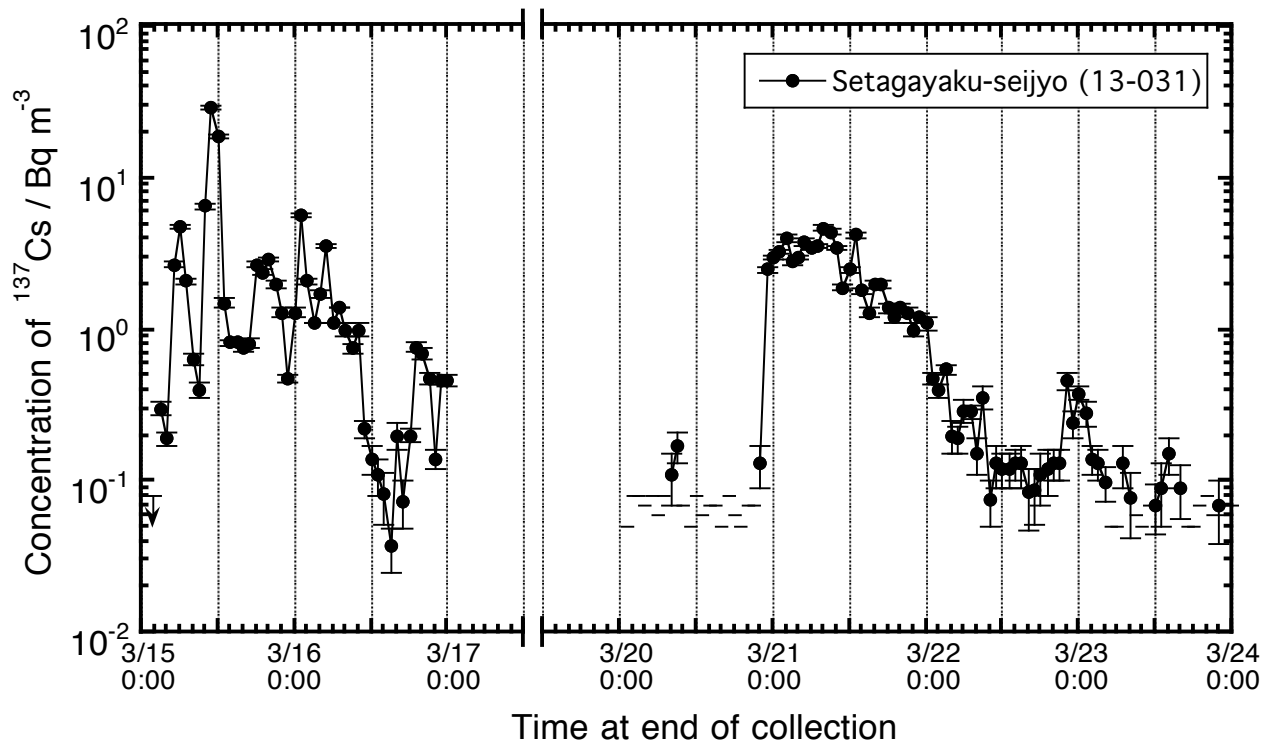


Figure B82. Time series variation of atmospheric  $^{137}\text{Cs}$  concentration observed at Setagayaku-seijyo (13-031) in Setagaya-ku, Tokyo.

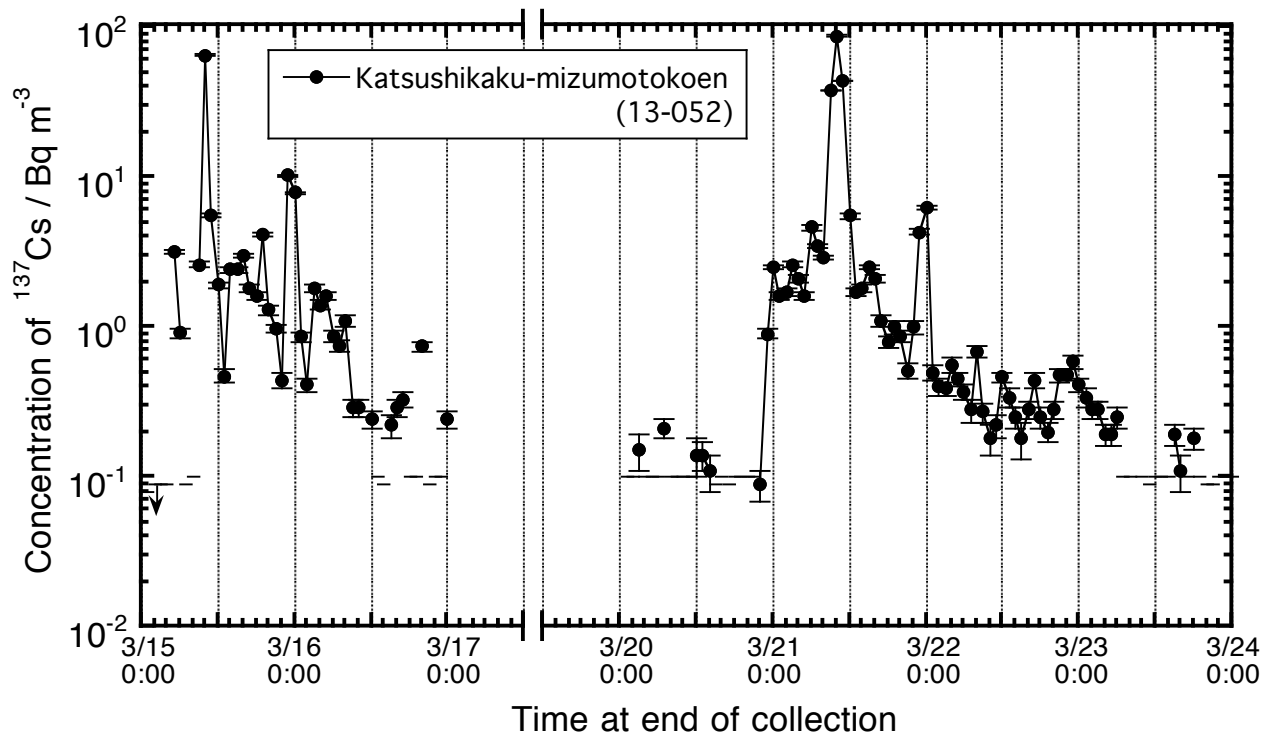


Figure B83. Time series variation of atmospheric  $^{137}\text{Cs}$  concentration observed at Katsushikaku-mizumotoken (13-052) in Katsushika-ku, Tokyo.

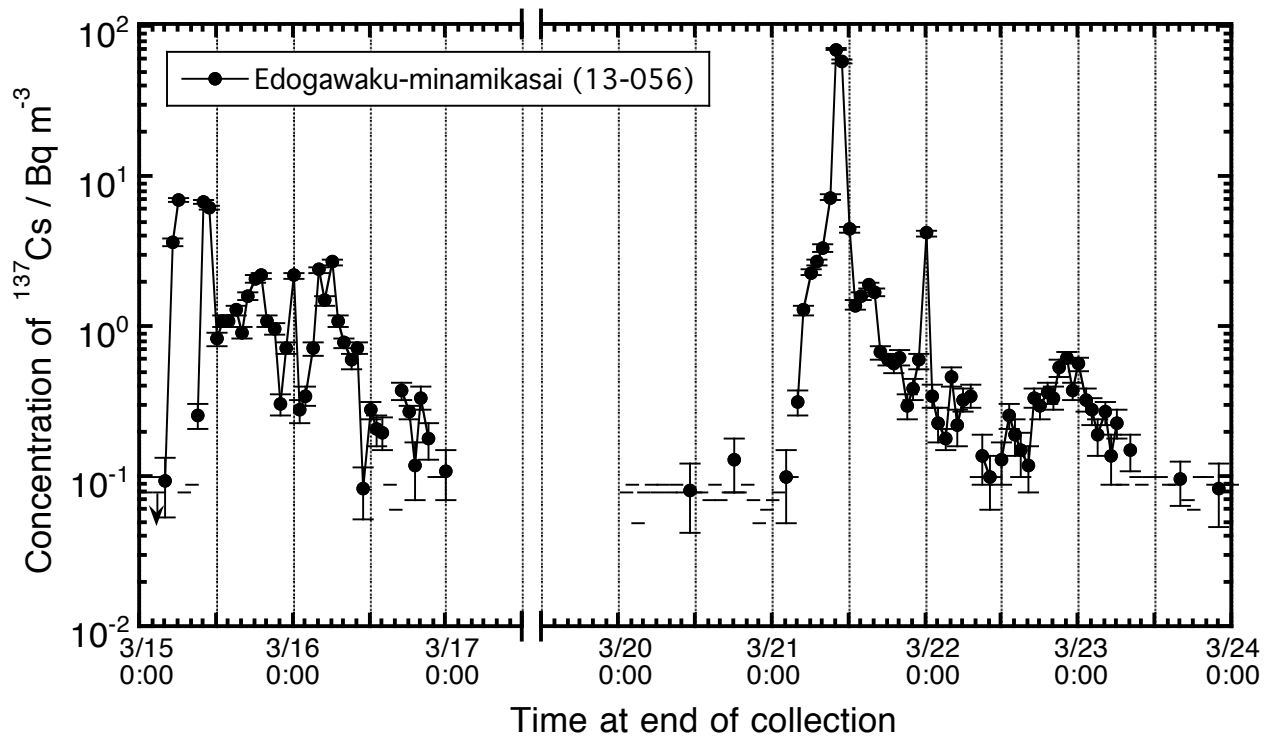


Figure B84. Time series variation of atmospheric  $^{137}\text{Cs}$  concentration observed at Edogawaku-minamikasai (13-056) in Edogawa-ku, Tokyo.

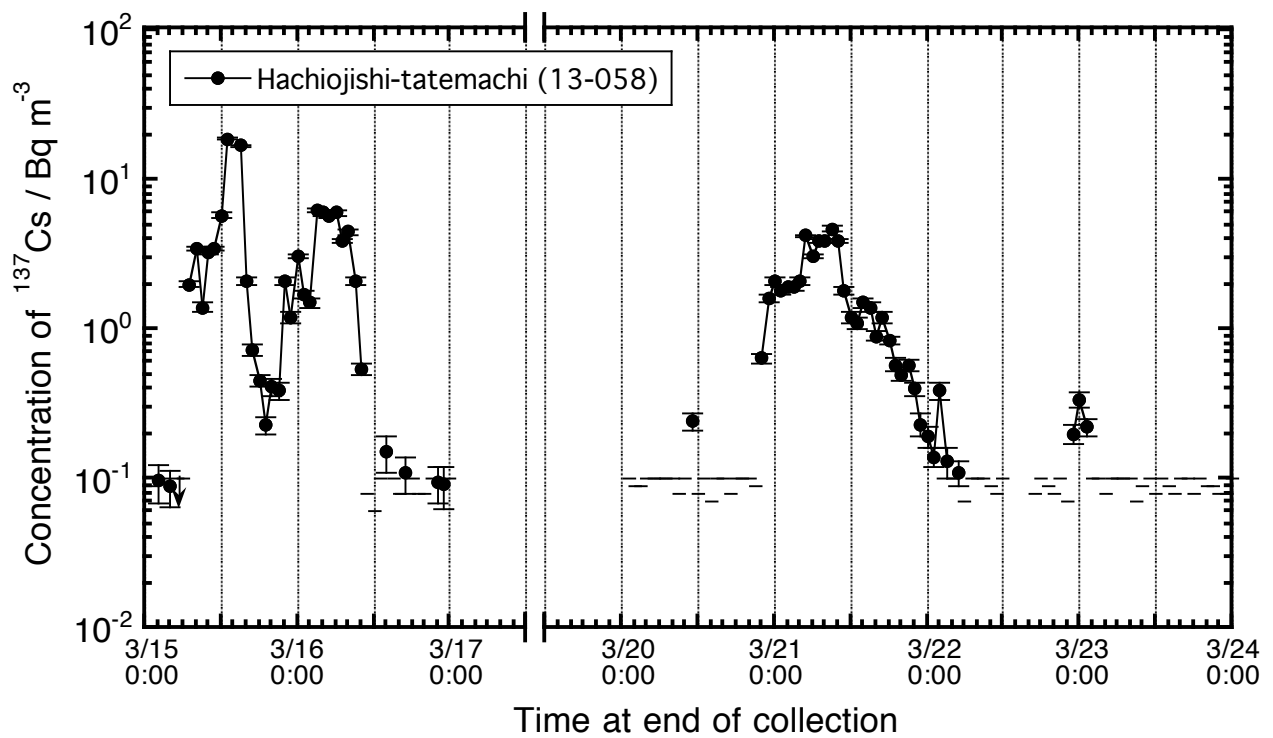


Figure B85. Time series variation of atmospheric  $^{137}\text{Cs}$  concentration observed at Hachiojishi-tatemachi (13-058) in Hachioji-shi, Tokyo.

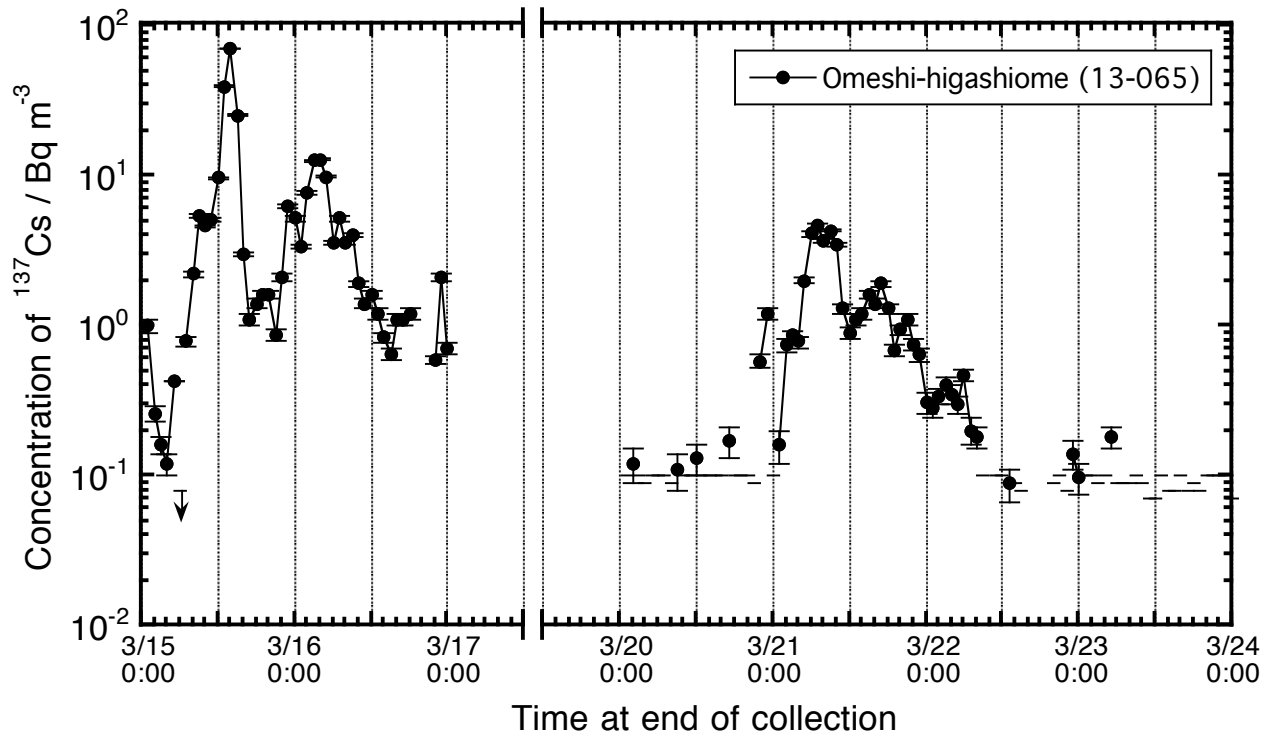


Figure B86. Time series variation of atmospheric  $^{137}\text{Cs}$  concentration observed at Omeshi-higashiome (13-065) in Ome-shi, Tokyo.

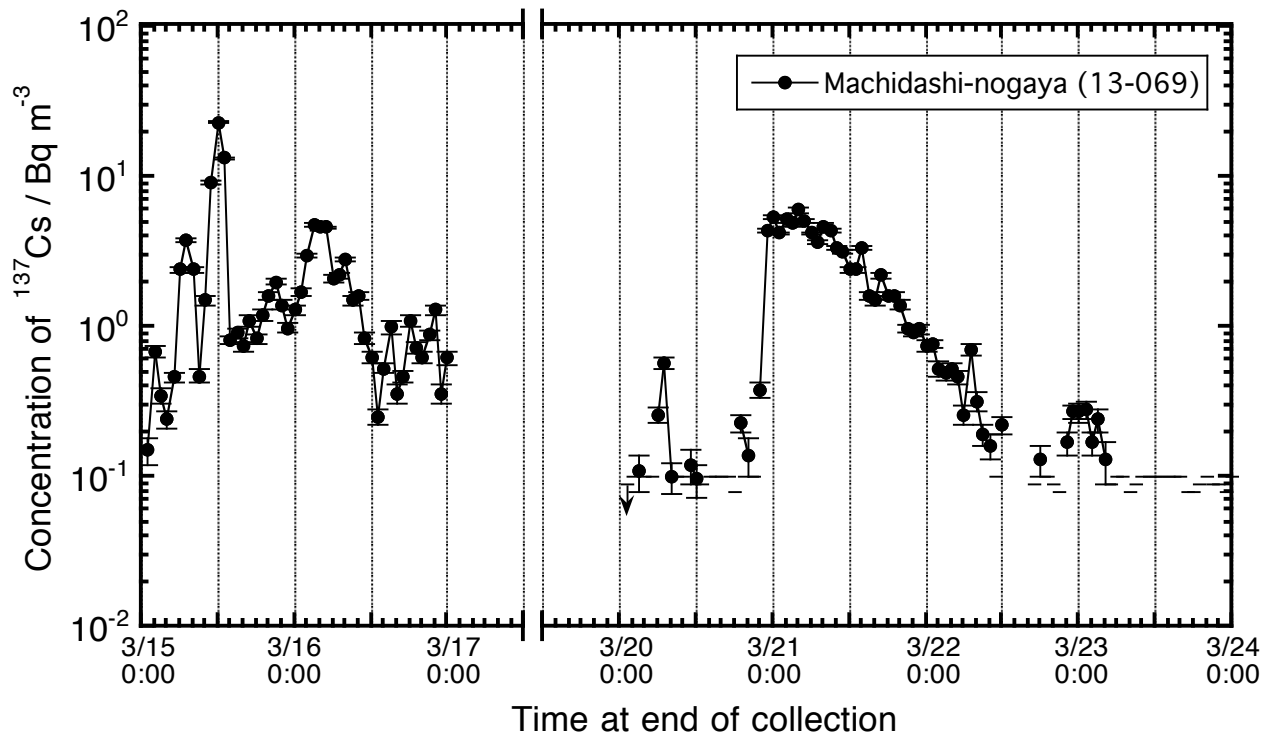


Figure B87. Time series variation of atmospheric  $^{137}\text{Cs}$  concentration observed at Machidashi-nogaya (13-069) in Machida-shi, Tokyo.

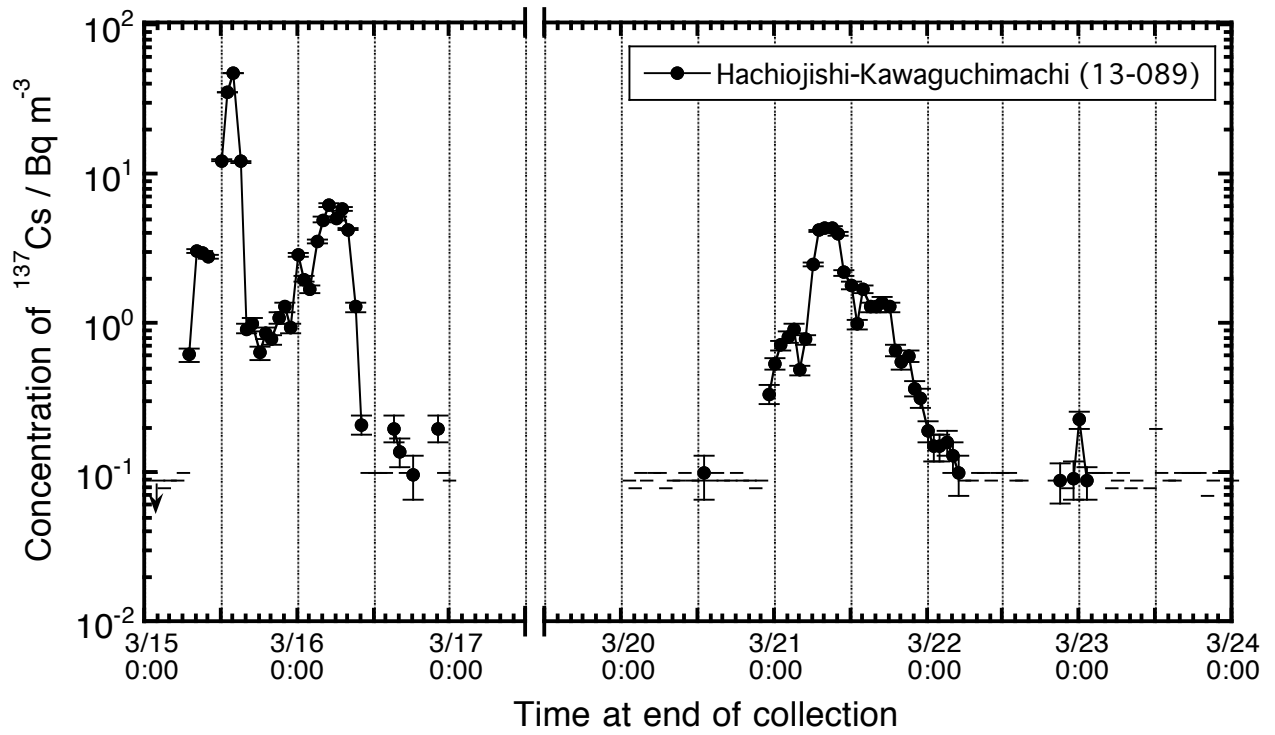


Figure B88. Time series variation of atmospheric  $^{137}\text{Cs}$  concentration observed at Hachiojishi-Kawaguchimachi (13-089) in Hachioji-shi, Tokyo.

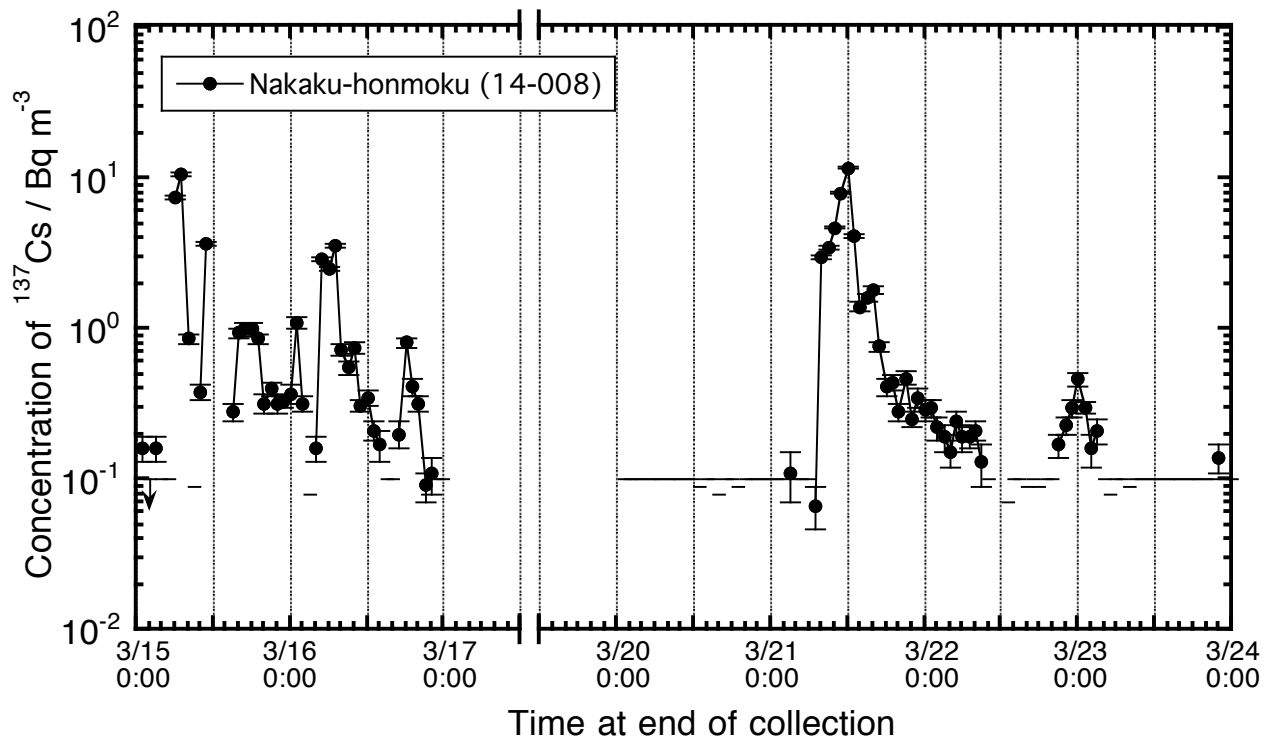


Figure B89. Time series variation of atmospheric  $^{137}\text{Cs}$  concentration observed at Nakaku-honmoku station (14-008) in Yokohama-shi, Kanagawa.

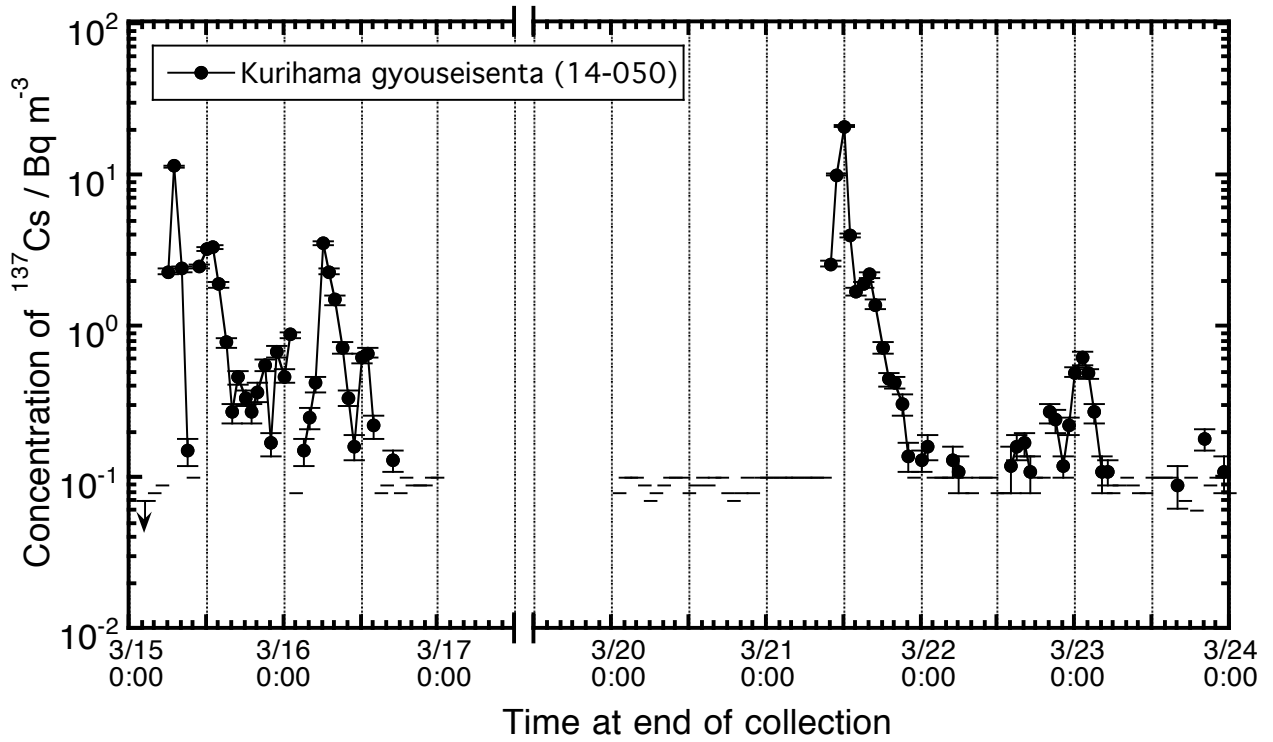


Figure B90. Time series variation of atmospheric  $^{137}\text{Cs}$  concentration observed at Kurihama gyouseisenta station (14-050) in Yokosuka-shi, Kanagawa.

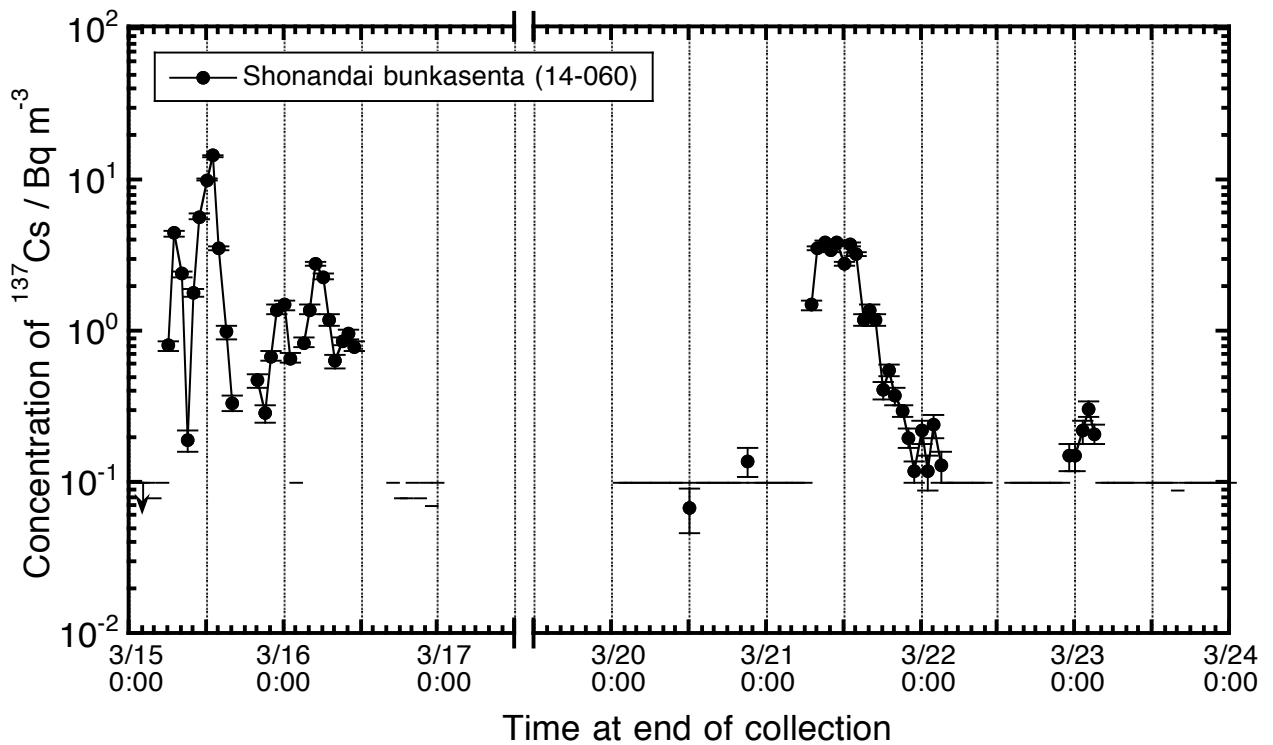


Figure B91. Time series variation of atmospheric  $^{137}\text{Cs}$  concentration observed at Shonandai bunkasenta station (14-060) in Fujisawa-shi, Kanagawa.

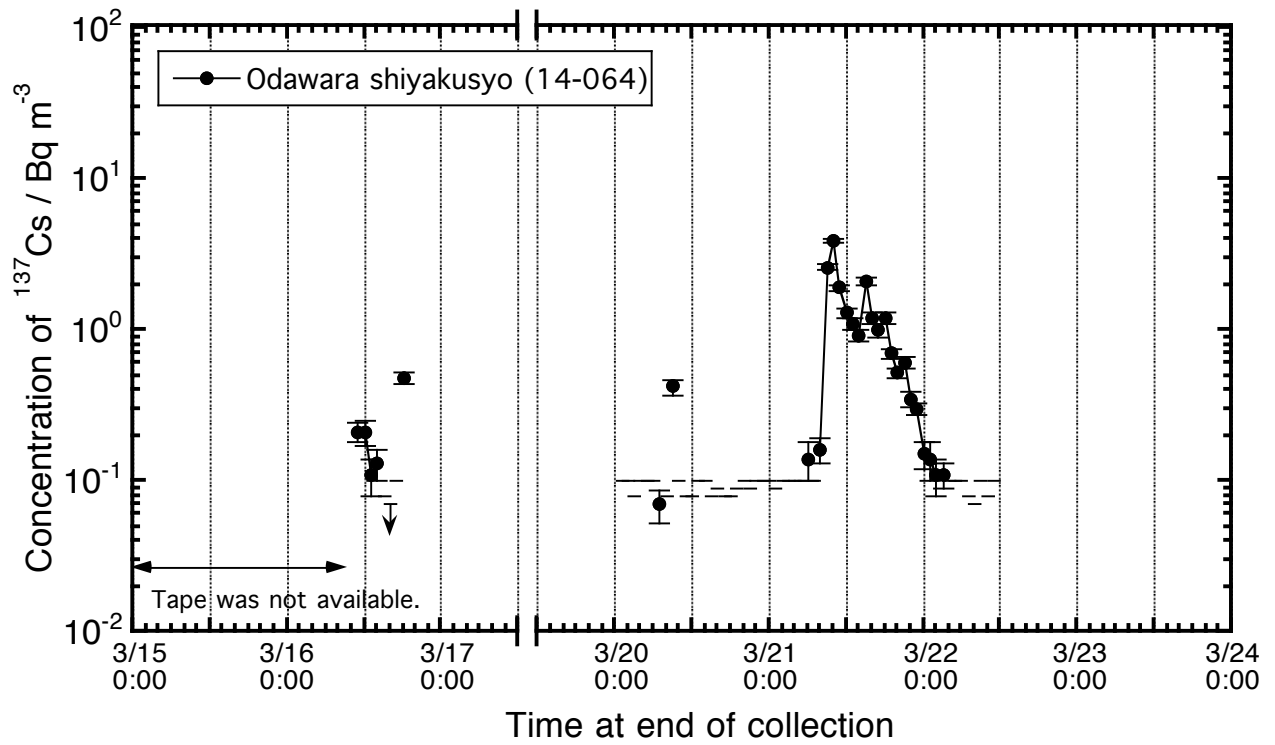


Figure B92. Time series variation of atmospheric  $^{137}\text{Cs}$  concentration observed at Odawara shiyakusyo station (14-064) in Odawara-shi, Kanagawa.

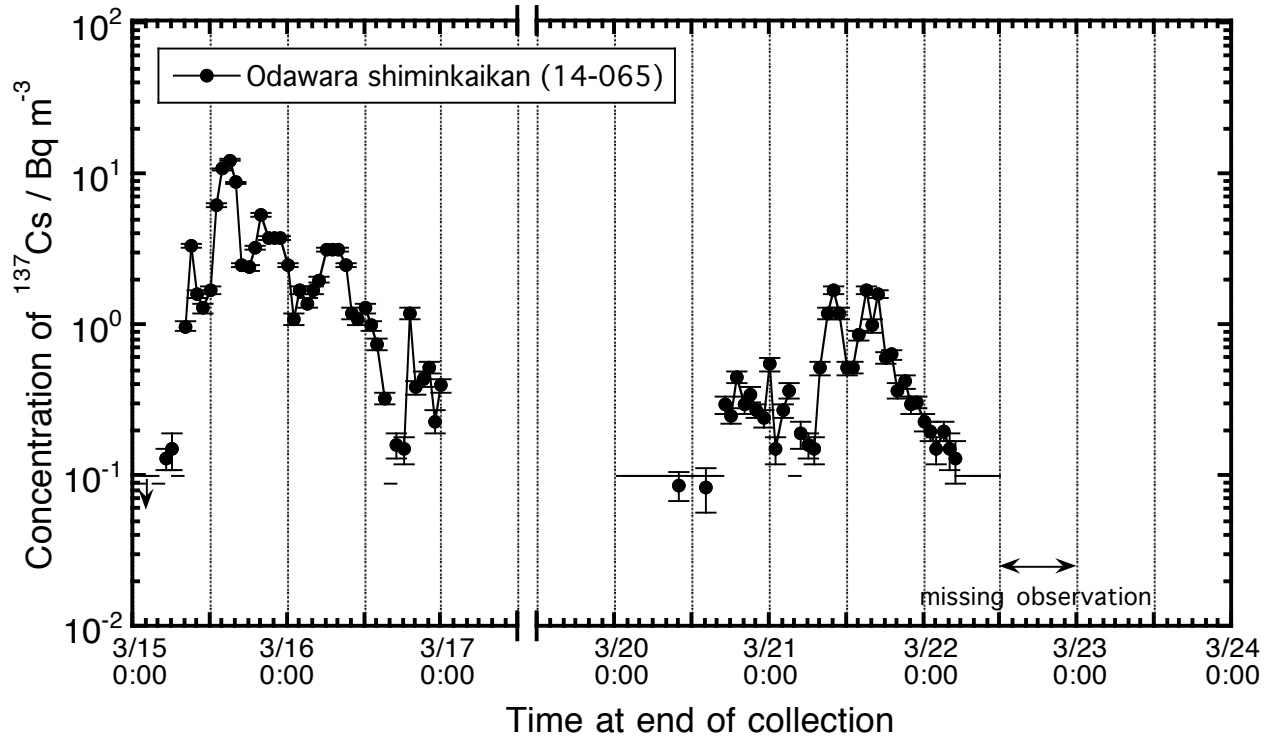


Figure B93. Time series variation of atmospheric  $^{137}\text{Cs}$  concentration observed at Odawara shiminkaikan station (14-065) in Odawara-shi, Kanagawa.

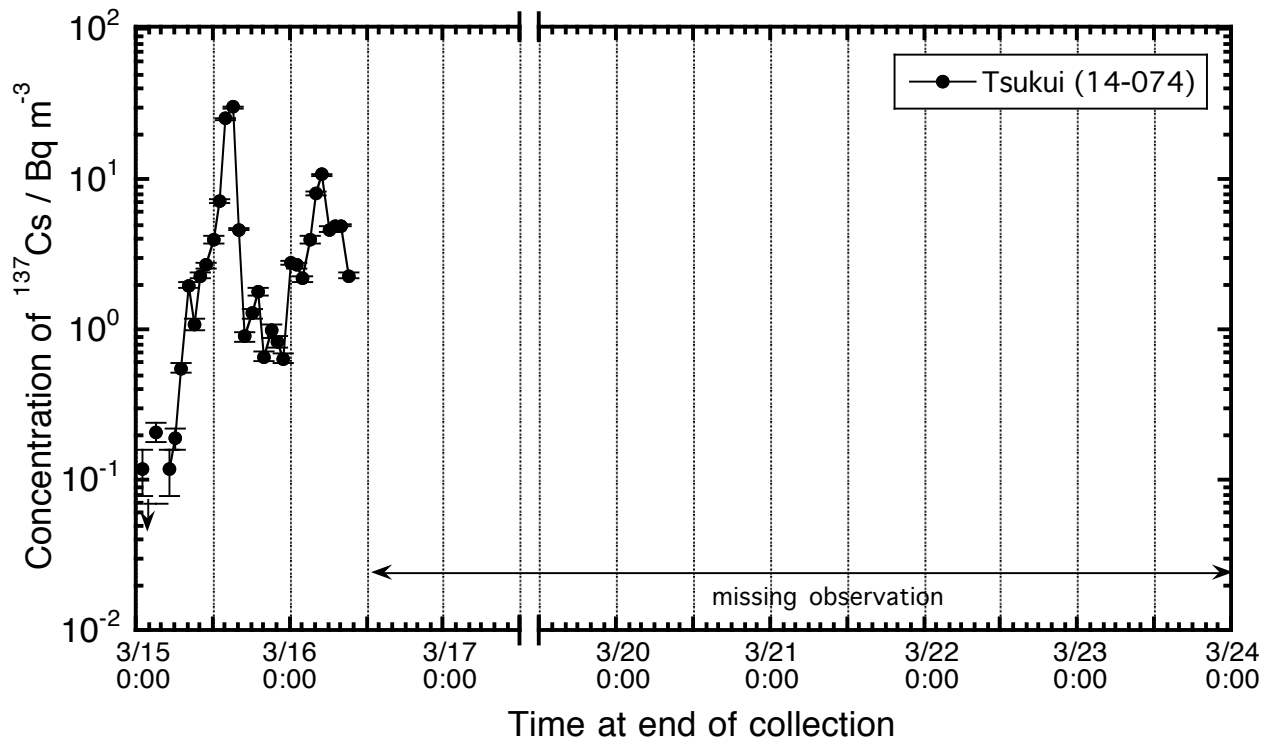


Figure B94. Time series variation of atmospheric  $^{137}\text{Cs}$  concentration observed at Tsukui station (14-074) in Sagami-hara-shi, Kanagawa.

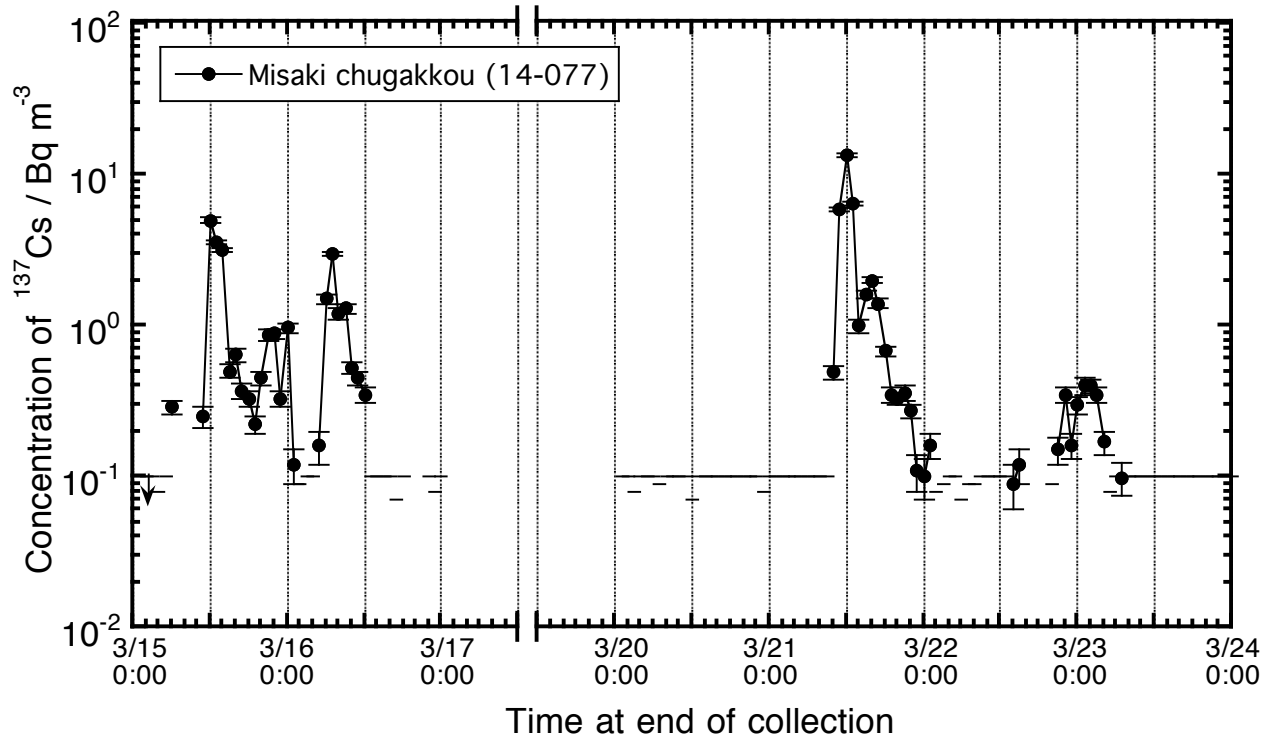


Figure B95. Time series variation of atmospheric  $^{137}\text{Cs}$  concentration observed at Misaki chugakkou station (14-077) in Miura-shi, Kanagawa.



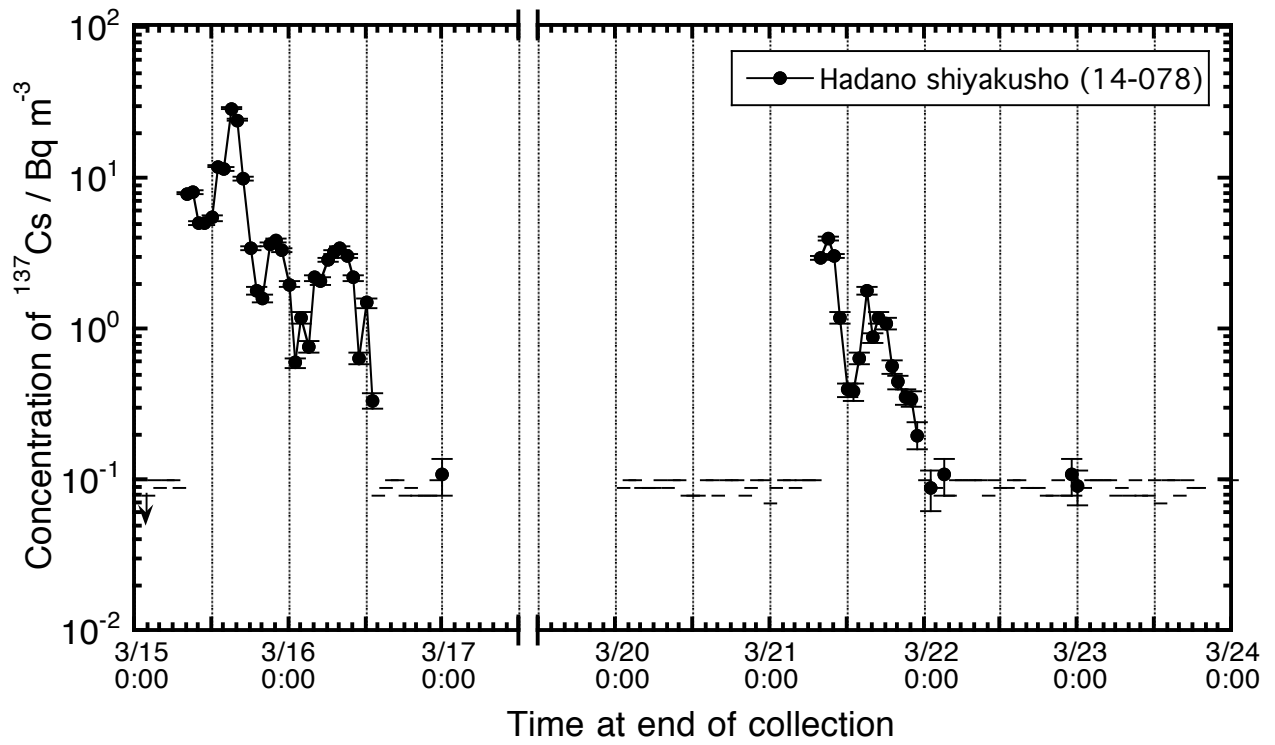


Figure B96. Time series variation of atmospheric  $^{137}\text{Cs}$  concentration observed at Hadano shiyakusho station (14-078) in Hadano-shi, Kanagawa.

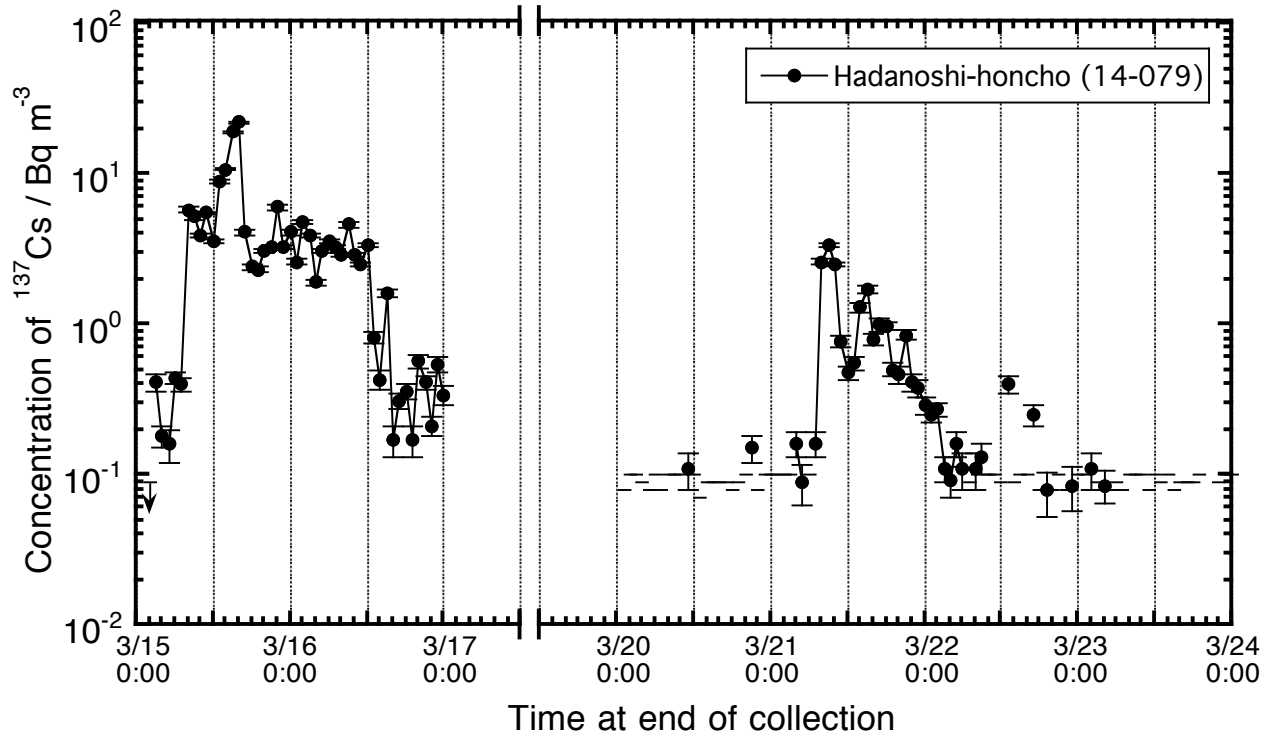


Figure B97. Time series variation of atmospheric  $^{137}\text{Cs}$  concentration observed at Hadanoshi-honcho station (14-079) in Hadano-shi, Kanagawa.

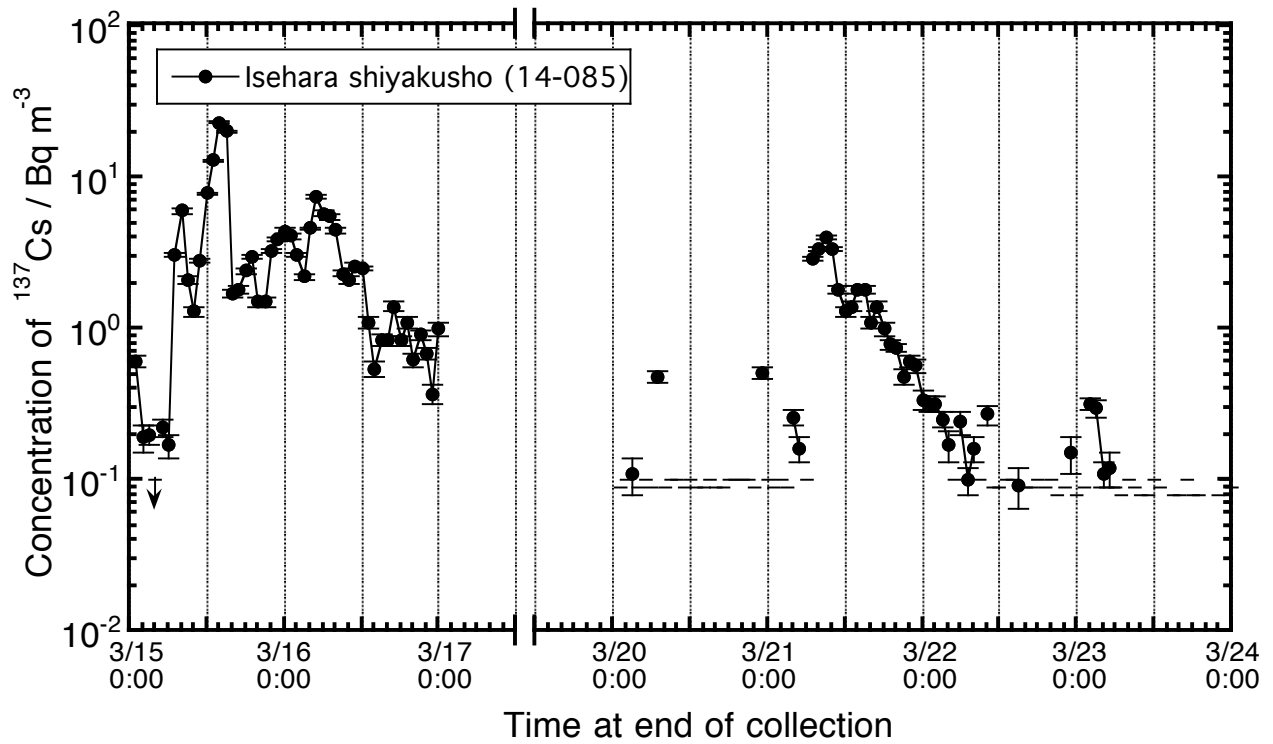


Figure B98. Time series variation of atmospheric  $^{137}\text{Cs}$  concentration observed at Isehara shiyakusho station (14-085) in Isehara-shi, Kanagawa.

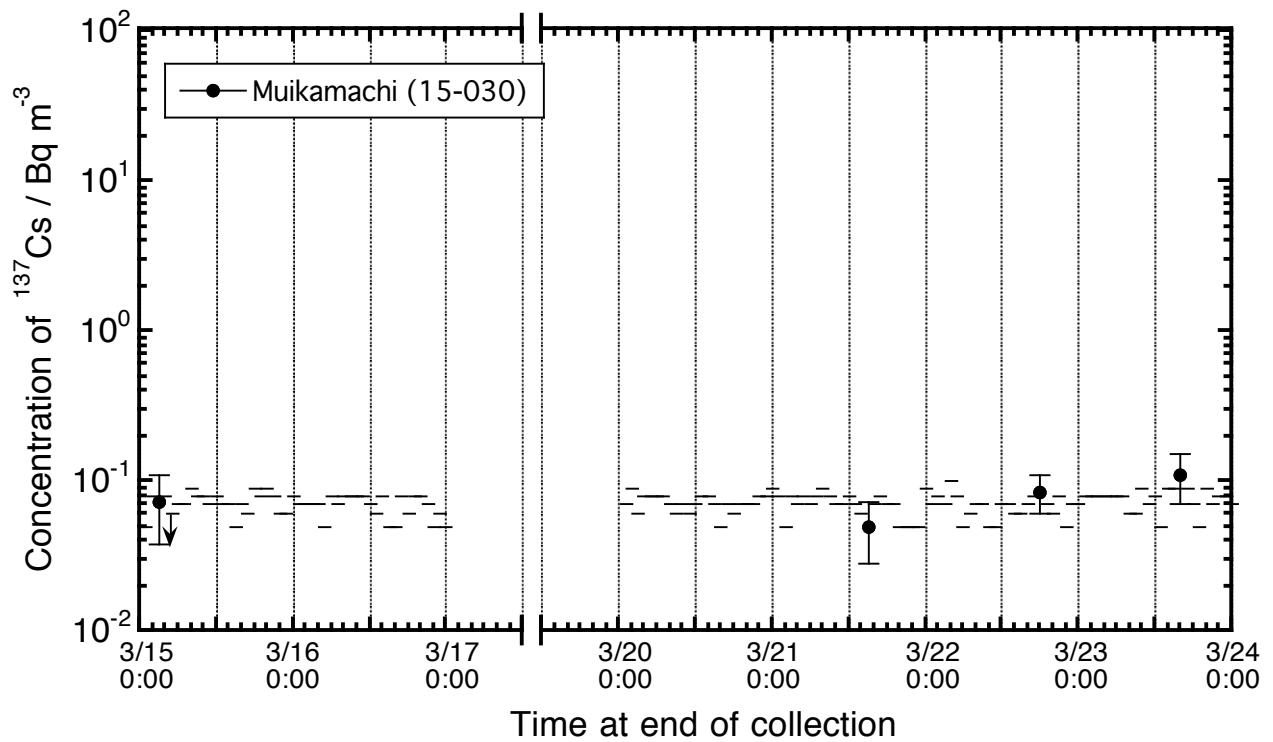


Figure B99. Time series variation of atmospheric  $^{137}\text{Cs}$  concentration observed at Muikamachi station (15-030) in Minamiuonuma-shi, Niigata.